The role of heat shock protein-60 in vascular smooth muscle cell proliferation and atherosclerotic development

By

Thomas Elliot Hedley

A thesis submitted to the Faculty of Graduate Studies of

The University of Manitoba

in partial fulfillment of the requirements of the degree of

MASTER OF SCIENCE

2017

Department of Physiology and Pathophysiology

Rady Faculty of Health Sciences

University of Manitoba

Winnipeg

ABSTRACT

This study investigated whether heat shock protein-60 (Hsp60) modulates nuclear protein import (NPI) to promote vascular smooth muscle cell (VSMC) proliferation and atherosclerotic development. Rat VSMCs were treated with oxidized low density lipoprotein (oxLDL), which increased Hsp60 expression, NPI machinery expression, and cell proliferation versus controls. Overexpression of cytosolic Hsp60 induced VSMC proliferation and enhanced NPI. Conversely, Hsp60 knockdown followed by oxLDL treatment did not increase NPI, NPI machinery or proliferating cell nuclear antigen (PCNA), a marker of cell proliferation. Co-immunoprecipitation showed that at high intracellular levels, Hsp60 interacts with Ran, a protein involved in NPI. Plaques obtained from hypercholesterolemic rabbit aortas showed that Hsp60, PCNA and Nup62 expression were elevated during plaque growth and returned to baseline during plaque stabilization. Thus, intracellular Hsp60 enhances NPI and VSMC proliferation through a chaperone and signaling mechanism, processes that may contribute to atherosclerotic development.

ACKNOWLEDGEMENTS

My time in the Pierce laboratory spanned 7 years, over which I worked with many amazing lab members. I owe many thanks to my cell culture teacher and friend, Justin Deniset, for his eternal patience and for making the lab a fun and stimulating environment to work in. I am also thankful to Marketa Hlavackova for teaching me the art and science of the microinjection technique. Alex Austria and Thane Maddaford provided outstanding technical support and guidance with animal care. Graham Maddaford and David Nelson were the best summer students I could ever ask for and provided valuable assistance with western blotting. My fellow graduate student, Stephanie Caligiuri, was never too busy to help me with statistics questions or writing concerns and inspired me with her passion for research. Andrea Edel always brightened my day with her cheerful and optimistic attitude. Kim O'Hara was a tremendous help with cell culture work and provided important experimental advice. Lastly, I am deeply thankful to Elena Dibrov, whose laboratory expertise, scientific wisdom, and motherly guidance had an incredible impact on my research and life.

I am grateful for the funding I received from Canadian Institutes of Health Research (Frederick Banting and Charles Best Canada Graduate Scholarship) for my project.

I am especially thankful to my supervisor and research mentor, Dr. Grant Pierce. My co-enrollment in medicine made my project a significant challenge. I sincerely thank you for accepting and embracing that challenge, and for supporting me throughout this process. The lab truly became my second family and I strongly

believe this is a by-product of the supportive, fun, and hard-working culture that you promote and inspire. It was an honour and a privilege for me to be a part of your lab for 7 years.

Thank you to my parents, Don and Cheryl, and my sister, Raegan, for your love and support. You taught me to live and research with integrity and to finish what you start. To my amazing girlfriend, Shannon Cuciz, thank you for inspiring me to be a better researcher, physician, and man. I love you so much!

For my parents,

Don and Cheryl

It started with a science fair project in elementary school.

Thanks for supporting and fostering my inner science nerd!

TABLE OF CONTENTS

LIST OF TABLES

LIST OF FIGURES

LIST OF COPYRIGHTED MATERIAL

LIST OF ABBREVIATIONS

Human heat shock protein-60 expressed via adenovirus	adHsp60
Cytosolic heat shock protein-60 expressed via adenovirus	adHsp60^{mito-}
Green fluorescent protein expressed via adenovirus	AdGFP
Bone morphogenetic protein	BMP
Ca2+/calmodulin	CaM
CaM Kinase II	CaMKII
Cardiovascular disease	CVD
Cellular apoptosis susceptibility protein	CAS
Chaperonin in E.coli analogous to Hsp60	GroEL
Chaperonin in E.coli analogous to Hsp10	GroES
Chlamydia pneumoniae	*Cpn*
Classical nuclear localization signal	cNLS
Cluster of differentiation-68	CD68
Chemokine ligand 1	CXCL1
Cyclic adenosine monophosphate	cAMP
cAMP response element binding protein	CREB
Dulbecco's Modified Eagle's Medium	DMEM
Deoxyribonucleic acid	DNA
Endothelial cell	EC
Enhanced green fluorescent protein	EGFP
Empty adenovirus	AdQBI
ETS domain-containing protein 1	ELK1

Extracellular matrix	ECM
Extracellular signal-regulated kinase 1/2	ERK1/2
Fetal bovine serum	FBS
Glucocorticoid receptor	GR
Glycogen synthase kinase 3	GSK3
Guanosine diphosphate	GDP
Guanosine triphosphate	GTP
Hemagglutinin	HA
Heat shock element	HSE
Heat shock factor	Hsf
Heat shock protein	Hsp
Helper T lymphocytes	Th
Histone deacetylase	HDAC
Hsp70/Hsp90 organizing protein	Hop
Immunoglobulin G	IgG
Immunoglobulin M	IgM
Importin	Imp
Infectious forming units	IFU
Inhibitor of κB	IκB
Interferon gamma	IFN-γ
Interleukin	IL
Intercellular adhesion molecule	ICAM
Ischemic heart disease	IHD

Kruppel-like factor 4	KLF4
Low density lipoprotein	LDL
Least significant difference	LSD
Lectin-like oxidized low density lipoprotein receptor 1	LOX1
Lipoprotein	LP
Lysophosphatidylcholine	LPC
Matrix metalloproteinase	MMP
Mitogen-activated protein kinase	MAPK
Micro ribonucleic acid	miR or miRNA
Monocyte chemotactic protein-1	MCP1
Myocardial infarction	MI
Myocardin-related transcription factor	MRTF
Multiplicity of infection	MOI
Native low density lipoprotein	NaLDL
Non-targeting siRNA pool	Scrambled siRNA
Nuclear export signal	NES
Nuclear factor of interleukin-6	NF-IL6
Nuclear factor kappa-B	NF-κB
Nuclear factor Y	NF-Y
Nuclear localization signal	NLS
Nuclear pore complex	NPC
Nuclear protein import	NPI
Nuclear transport factor 2	NTF2

Nucleoporin	Nup
Optical density at 500nm	OD500
Oxidized low density lipoprotein	OxLDL
Pattern recognition receptor	PRR
Phosphate buffered saline	PBS
Platelet derived growth factor	PDGF
Proliferating cell nuclear antigen	PCNA
Ras-related nuclear protein	Ran
Ran binding protein	RanBP
Ran guanine nucleotide exchange factor	RanGEF
Ran GTPase-activating protein	RanGAP
Reactive oxygen species	ROS
Regulator of chromosome condensation-1	RCC-1
Regulatory T lymphocytes	Treg
Serum response factor	SRF
Short interfering ribonucleic acid	siRNA
Signal transducer and activator of transcription	STAT
Small heat shock protein	sHsp
Smooth muscle cell	SMC
Smooth muscle-myosin heavy chain	SM-MHC
Smooth muscle alpha actin	α-SMA
Standard error of the mean	SEM
Stem cell antigen 1	Sca1

Calponin-related alpha-smooth muscle 22	SM22α
Toll-like receptor	TLR
Transforming growth factor beta	TGF-β
T-complex polypeptide 1 ring complex	TRiC
Tumour necrosis factor alpha	TNF-α
Vascular cell adhesion molecule	VCAM
Vascular smooth muscle cell	VSMC
Very low density lipoprotein	VLDL

CONTRIBUTIONS

The purpose of this section is to outline my contributions to each experiment. This thesis is a collation of the experiments from 5 years of laboratory work and as such involved the combined efforts of myself, summer students, lab technicians, research associates, and other graduate students.

The oxLDL experiments examined the effect of oxLDL treatment on Hsp60, PCNA, nucleoporin, and nuclear transport receptor expression in VSMCs (Figures 7, 8, and 19-22). For all of these experiments, I did the cell culture and sample preparation. The western blots were completed by myself and summer students (under my supervision).

The Hsp60 knockdown experiments examined the effect of Hsp60 knockdown with or without subsequent oxLDL treatment on Hsp60 expression, PCNA expression, NPI machinery expression, and the rate of NPI in VSMCs (Figures 14-18, and Table 1). I performed the cell culture, sample preparation, and western blotting for these experiments. Summer students assisted with some of the western blotting for these experiments under my supervision. I performed the NPI assays for control samples as well as samples with Hsp60 knockdown plus or minus subsequent oxLDL treatment (Figures 16-18). Markéta Hlaváčková performed the NPI assays for the Hsp60 overexpression samples in Figures 16 and 17.

Another experiment examined Hsp60 immunostaining in VSMCs with Hsp60 knockdown (Figures 12 and 13). I performed the cell culture, sample treatment, and slide preparation and summer students acquired images from these slides.

Graham Maddaford performed quantification of Hsp60 staining in each treatment group under my supervision (Figure 13).

A co-immunoprecipitation experiment examined the protein-protein interactions between Hsp60 and nuclear transport receptors in VSMCs under stress stimuli (Figure 23). Kim O'Hara and I performed the cell culture and treatment, while summer students ran the co-immunoprecipitation experiment and western blotting under my supervision.

Hsp60 expression levels and intracellular localization were investigated in VSMCs with Hsp60 overexpression (Figures 9 and 10). I performed the cell culture and Justin Deniset did the sample treatment, slide preparation, image acquisition, and western blots for these experiments.

Cell titer assays were used to assess VSMC proliferation in response to oxLDL treatment and Hsp60 overexpression (Figures 6 and 11). I performed the cell culture and sample preparation and Elena Dibrov ran each of the cell titer assays.

The atherosclerotic rabbit model experiments examined the expression of Hsps, NPI machinery and PCNA in plaque tissue from rabbit aorta (Figures 25-27). For these experiments, I did the protein extraction, sample preparation, and helped Justin Deniset run the western blots. Justin Deniset ran the correlation statistics in Figure 28. Andrew Francis performed the en-face analysis and quantification of the percentage of the vessel lumen covered by atherosclerotic plaque tissue in Figure 24.

CHAPTER I: REVIEW OF LITERATURE

1. CARDIOVASCULAR DISEASE

Cardiovascular disease (CVD) remains the leading cause of mortality in the world[1]. CVD encompasses both acute and chronic injuries or pathologic processes that affect the cardiovascular system, which includes blood vessels and the heart. Major categories of CVD include ischemic heart disease, cerebrovascular disease, peripheral vascular disease, cardiomyopathies, as well as cardiac arrhythmias and infections.

Ischemic heart disease (IHD) is the leading cardiovascular cause of morbidity and accounts for almost half of CVD related deaths worldwide[1,2]. IHD involves alterations in the function of blood vessels that supply the metabolic needs of the heart. Specifically, these vessels become narrowed due to the accumulation of fatty plaques in the vessel wall. This process is known as atherosclerosis, which is the pathophysiologic mechanism that leads to IHD.

As plaques grow, they reduce blood flow to the heart and can lead to ischemia. Cardiac ischemia occurs when blood supply to the heart becomes inadequate to meet its metabolic demands[3]. In advanced stages of atherosclerosis, vulnerable plaques may rupture, leading to formation of a blood clot and the total blockage of blood flow to the heart[4]. When blood flow to the heart is stopped for a prolonged period, it results in death to the portion of the heart muscle supplied by that blood vessel, which is known as a myocardial infarction (MI)[3]. This event initiates structural remodeling of the heart muscle and blood vessels, which

eventually leads to heart failure. Heart failure is a clinical syndrome that results from the inability of the heart to pump sufficient blood to tissues to meet their metabolic demands or the inability of the heart to accommodate blood returning from the body[5].

Cardiovascular diseases have a multitude of etiologies and are the result of complex interactions between modifiable and non-modifiable risk factors. Non-modifiable risk factors include age, sex, and genetic factors[6–8]. Modifiable risk factors include smoking, high body mass index, sedentary lifestyle, hypercholesterolemia, diabetes, and hypertension[2,9]. Interventions that target these modifiable risk factors have the potential to lower the incidence of cardiovascular disease.

2. PATHOGENESIS OF ATHEROSCLEROSIS

2.1. Overview

Atherosclerosis is a chronic inflammatory disease[4] that leads to progressive narrowing and stiffening of arteries due to the build-up of lipids, inflammatory cells, and extracellular matrix in the intimal layer[10]. The intima, also known as the sub-endothelial space, is the area between the endothelium and the underlying medial layer of smooth muscle cells[10].

The development of atherosclerotic plaque is initiated through an injury to the endothelial layer of an arterial vessel caused by stimuli such as hypercholesteremia, smoking, hypertension[11–13]. This injury leads to endothelial

activation, which allows infiltration of low density lipoprotein (LDL) particles from the circulation into the sub-endothelial space[12,14]. Activation of the endothelium also stimulates expression of cell surface adhesion molecules and secretion of chemotactic molecules to attract monocytes and lymphocytes to the injury site[4,10,12,13].

LDL trapped in the sub-endothelial space is modified through oxidation to become oxidized LDL (oxLDL), which can further activate the endothelium[4,10,14,15]. Monocytes recruited to the site of endothelial injury migrate into the sub-endothelial space where they differentiate into macrophages[10,12]. These macrophages express scavenger receptors for oxLDL and are normally involved in its elimination from the vessel[10,16]. However, uptake of excessive oxLDL causes transformation of macrophages into a foam cell phenotype[10,17,18]. Foam cells form the lipid core of the plaque and, along with other pro-inflammatory macrophages, secrete cytokines (e.g. tumour necrosis factor alpha (TNF-α) and interleukin-1β (IL-1β)), proteolytic enzymes (e.g. matrix metalloproteinases (MMPs)), and growth factors (e.g. platelet derived growth factor (PDGF))[4,12,17].

Cytokines recruit more immune cells and growth factors promote growth and proliferation of immune cells within the lesion[4,19]. If the immune system is unable to resolve the inflammatory stimuli, the inflammatory response will proceed unchecked[4]. The pro-inflammatory environment stimulates migration of vascular smooth muscle cells (VSMCs) from the medial layer to the intimal layer where local growth factors stimulate VSMC proliferation (see Figure 1)[4,12,17,19]. VSMCs in the intimal layer secrete extracellular matrix (ECM) proteins (e.g. collagen and elastin)

to form a fibrous cap that helps stabilize the plaque[4,12,17]. At this point, the lesion begins to bulge into the vessel lumen, narrowing the area for blood flow[4,17].

As immune cell recruitment continues in the core of the plaque, there is defective removal of apoptotic macrophages/foam cells leading to necrosis and release of intracellular lipids to form a necrotic core[20]. Both macrophages and the necrotic core promote breakdown of the fibrous cap through release of proteolytic enzymes and the stimulation of VSMC apoptosis[10]. Advanced atherosclerotic lesions with a thin fibrous cap, large necrotic core, and high level of inflammation are more vulnerable to rupture[21]. When a vulnerable plaque ruptures, the pro-coagulant and pro-thrombotic factors in the inflamed tissue are released into the blood, leading to platelet aggregation, thrombosis of the vessel, and tissue ischemia[20,21].

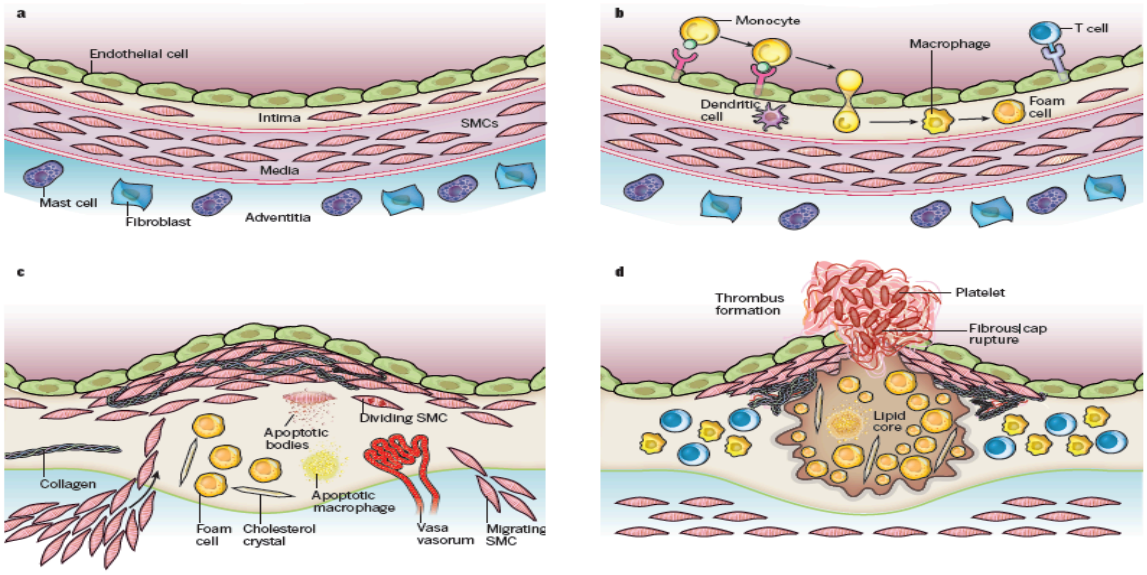

Figure 1. Stages in the development of atherosclerotic lesions.

The normal muscular artery and the cell changes that occur during disease progression to thrombosis are shown. **a,** The normal artery contains three layers. The inner layer, the tunica intima, is lined by a monolayer of endothelial cells that is in contact with blood overlying a basement membrane. In contrast to many animal species used for atherosclerosis experiments, the human intima contains resident smooth muscle cells (SMCs). The middle layer, or tunica media, contains SMCs embedded in a complex extracellular matrix. Arteries affected by obstructive atherosclerosis generally have the structure of muscular arteries. The arteries often studied in experimental atherosclerosis are elastic arteries, which have clearly demarcated laminae in the tunica media, where layers of elastin lie between the strata of SMCs. The adventitia, the outer layer of arteries, contains mast cells, nerve endings and microvessels. **b,** The initial steps of atherosclerosis include adhesion of blood leukocytes to the activated endothelial monolayer, directed migration of the leukocytes into the intima, maturation of monocytes (the most numerous of the leukocytes recruited) into macrophages, and their uptake of lipid, yielding foam cells. **c,** Lesion progression involves the migration of SMCs from the media to the intima, the proliferation of resident intimal SMCs and media-derived SMCs, and the heightened synthesis of extracellular matrix macromolecules, such as collagen, elastin, and proteoglycans. Plaque macrophages and SMCs can die in advancing lesions, some by aptopiosis. Extracellular lipid derived from dead and dying cells can accumulate in the central region of a plaque, often denoted the lipid or necrotic core. Advancing plaques also contain cholesterol crystals and microvessels. **d**, Thrombosis, the ultimate complication of atherosclerosis, often complicates a physical disruption of the atherosclerotic plaque. Shown is a fracture of the plaque's fibrous cap, which has enabled blood coagulation components to come into contact with tissue factors in the plaque's interior, triggering the thrombus that extends into the vessel lumen, where it can impede blood flow. Reprinted by permission from Macmillan Publishers Ltd: Nature, P Libby, PM Ridker, and GK Hansson. Progress and challenges in translating the biology of atherosclerosis, 473(7347): 317-325, © 2011.

2.2. OxLDL and atherosclerosis

Lipoproteins (LPs) are carrier proteins composed of varying amounts of lipids (cholesterol esters, phospholipids, triglycerides) and apolipoproteins. LPs regulate lipid metabolism and facilitate lipid transport between tissues. LPs are made by the liver and secreted as very low density lipoproteins (VLDL), which are converted to LDL in the blood stream[10]. LDL is responsible for cholesterol deposition in the tissues, which is mediated through extracellular receptor mediated endocytosis[22]. LDL particles can be subject to modifications such as oxidation, glycation, aggregation, association with proteoglycans, or incorporation into immune complexes[4,15]. Oxidation of LDL, in particular, has been found to be important in the pathogenesis of atherosclerosis[4,15,18,23].

Data from cell lines and animal models demonstrate a pro-atherogenic role of oxLDL through its effects on macrophages, endothelial cells (ECs), and VSMCs[23]. In atherosclerotic animal models, the data suggests antioxidant treatment, which has been shown to inhibit oxidation of LDL, impedes the development of atherosclerotic plaques[23]. In cohort studies, higher levels of oxLDL have been associated with more cardiovascular events[23]. Randomized clinical trials show that although anti-oxidants do not reduce cardiovascular events in healthy populations, they can benefit high-risk patients[23]. Instead, statin therapy is the single most effective intervention against atherothrombosis, underscoring the importance of cholesterol in the pathogenesis of atherosclerosis[14].

A proposed mechanism of the role of oxLDL in atherosclerosis is as follows: hypercholesterolemia is a risk factor for atherosclerosis and is associated with

chronically elevated LDL levels in the plasma component of blood[18]. High plasma LDL levels increase lipid delivery to endothelial cells and eventually overwhelm their capacity to metabolize endocytosed lipoproteins[24]. This leads to retention of large amounts of LDL within the ECM in the sub-endothelial space of the vessel wall[24]. The ECM acts a scaffold, facilitating progressive oxidation of LDL through interactions with lipoxygenases, reactive oxygen species (ROS), peroxynitrite, and myeloperixodase, resulting in the generation of a variety of oxLDL species[24,25]. OxLDL particles cannot enter cells through normal LDL receptors[18]. Under inflammatory conditions in the vascular wall, ECs, VSMCs, and macrophages express scavenger receptors, which allow them to internalize oxLDL molecules and mediate changes in cellular signalling[18]. Oxidized LDL retained in the vessel wall can cause endothelial activation through pro-inflammatory signaling molecules, like nuclear factor kappa B (NF-κB)[10,14,19].

As macrophages are responsible for removing injurious stimuli, they function to remove oxLDL from the vessel wall[18]. OxLDL internalization and processing by macrophages promotes a pro-inflammatory phenotype[18]. Dysregulated oxLDL uptake by macrophages results in formation of lipid-laden foam cells and development of fatty streaks[18]. OxLDL also acts as a chemotactic stimuli for monocytes and induces proliferation of macrophages[14,23].

In later stages of atherosclerotic development, oxLDL stimulates VSMC migration from the medial layer and their subsequent proliferation at the intimal layer[18,23]. *In vitro* treatment of rabbit VSMCs with a high dose of oxLDL induces cell proliferation[26–29]. In addition, oxLDL augments the effects of other pro-atherogenic

stimuli, including *Chlamydia pneumonia (Cpn)* infection and mechanical stretch on rabbit VSMC proliferation[26,27]. Treatment of cultured human coronary artery SMCs with oxLDL stimulated cell proliferation and migration in a dose dependent fashion[30]. Other studies showed that higher concentrations of oxLDL can cause VSMC apoptosis *in vitro*[31,32].

There was also early evidence that more extensively oxidized LDL results in apoptosis and mildly oxidized LDL leads to cell proliferation[33]. A subsequent study showed that mildly oxidized LDL triggers apoptosis indicating that the degree of LDL oxidation does not have differential effects on VSMCs[34]. Therefore, the amount of oxLDL in the vessel wall and the disease stage could influence whether oxLDL induces VSMC apoptosis or proliferation.

OxLDL can also stimulate macrophage and EC apoptosis as part of the formation of a vulnerable plaque[21,23]. Thus, oxLDL is involved in various stages of atherosclerotic plaque development including activation of ECs, macrophage transformation into foam cells, and VSMC migration and proliferation[18].

2.3. VSMCs and atherosclerosis

VSMCs reside in the medial layer of the vessel wall, where they regulate blood pressure by altering the lumenal diameter in response to changes in shear stress and chemical mediators[35,36]. However, unlike adult skeletal or cardiac muscle cells, mature VSMCs have phenotypic plasticity, which allows them to respond to vascular injury[37,38]. The phenotypic conversion of VSMC has important implications in atherogenesis.

2.3.1. VSMC phenotypes in the vessel wall

Mature VSMCs in the vasculature can dynamically adapt their structure and function in response to the changes in their extracellular environment[36]. They can differentiate into a contractile phenotype or de-differentiate into a synthetic phenotype[38]. In the medial layer of a mature vessel, there is a mixed population of smooth muscle cells, which exist in a phenotypic continuum between contractile and synthetic states[39].

Contractile VSMCs in the arterial media have a negligible rate of proliferation, very little synthetic activity, and express a subset of contractile proteins, ion channels and signalling molecules that regulate contractile function[35,36,38,40]. Contractile proteins (i.e. smooth muscle myosin heavy chain (SM-MHC) and smooth muscle alpha-actin (α-SMA)) can be used as markers of VSMCs and their relative levels reflect the extent of differentiation[35].

In cell culture most VSMCs are in the contractile phenotype[41], but can undergo phenotypic switching in response to chemical stimuli, such as growth factors[42–45]. *In vivo* models of atherosclerosis demonstrate heterogeneous patterns of smooth muscle cell (SMC) marker expression within lesions, which change throughout disease progression[46]. Specifically, intimal VSMCs have decreased SMC marker expression relative to medial VSMCs[47,48]. Taken together, the *in vivo* and *in vitro* results suggest that intimal cells are derived from medial VSMCs that have undergone phenotypic switching and have migrated to the intima[36].

Recent *in vivo* lineage studies show a proportion of medial SMCs undergoing phenotypic conversion during atherogenesis exhibit macrophage markers (e.g.

CD68)[49,50] and enhanced pro-inflammatory markers[51]. In addition, the majority of these macrophage-like cells do not express VSMC markers such as α-SMA, but express markers of mesenchymal stem cells (e.g. stem cell antigen 1 (Sca1)) and myofibroblasts (e.g. PDGF receptor)[49]. This raises the concept of a progenitor population of SMCs that proliferate and accumulate in the core of plaques[38]. However, there are also studies suggesting that not all cells expressing SMC markers are indeed SMCs in origin[40]. One hypothesis is that these could be hematopoietic stem cells (myeloid cells)[52], as myeloid-derived SMCs exist both in mice[53] and human plaques[54]. Other studies show evidence that myeloid cells do not differentiate into SMCs in ApoE null mice[55,56]. A recent lineage study in ApoE null mice lesions showed that myeloid cells do indeed make up a small proportion of the SMC-marker expressing population[51]. Therefore, within atherosclerotic plaques medial SMCs can transdifferentiate into macrophage-like cells and myeloid cells may also become smooth muscle-like cells[40,50,51].

Macrophage-like or synthetic VSMCs exhibit both beneficial and detrimental characteristics for atherosclerotic progression[36]. These cells produce ECM proteins and have enhanced responsiveness to mitogenic stimuli[40]. VSMC proliferation and ECM production lead to the formation of a fibrous cap, which helps stabilize the plaque from rupture and prevents thrombotic complications[40].

In response to atherogenic stimuli (e.g. oxLDL), synthetic VSMCs also produce pro-inflammatory mediators such as IL-1β and TNF-α[38]. These cytokines act through auto- and paracrine mechanisms to potentiate the inflammatory cascade. They mediate changes in local ECM structure, specifically the replacement

of collagen IV with collagen I and fibronectin[38]. These changes in ECM composition help drive phenotypic conversion of contractile VSMCs to a synthetic state[36]. IL-1β participates in a positive feedback loop which leads to an increase in scavenger receptors (e.g. LOX1) for oxLDL[38]. This leads to increased lipid accumulation and eventually VSMC-derived foam cells[57]. TNF-α upregulates NF-κβ, a pro-inflammatory transcriptional regulator, which increases expression of adhesion molecules (e.g. VCAM and ICAM), MMPs, and chemokines (e.g. CXCL1, MCP1)[38]. Collectively these mediators enhance the recruitment of monocytes and medial SMC to the plaque core. MMPs secreted by synthetic VSMCs also promote degradation of the fibrous cap, which eventually leads to plaque rupture[58–60]. Hence, synthetic VSMCs are crucial for early vessel wall repair but drive plaque destabilization in advanced lesions with high levels of inflammation and oxLDL.

2.3.2. Regulation of VSMC phenotype and proliferation

SMC phenotype is regulated by the complex interaction of environmental signals from growth factors, ECM interactions, mechanical forces, atherogenic stimuli (i.e. modified lipids, ROS, cytokines), and cell-cell interactions[36,61]. These extracellular signals modulate transcription factor[62] and micro RNA (miR)[61,63] expression to alter SMC marker gene expression.

The best characterized model for intracellular regulation of SMC-selective genes involves the transcriptional co-activators serum response factor (SRF), myocardin, and myocardin related transcription factors (MRTF)[61,64]. These factors bind CArG sequences in the promoter sequences of SMC marker genes (e.g. SM-MHC, α-SMA) to drive transcription of these genes[65,66]. Myocardin deficiency in ApoE null

mice results in increases in inflammatory pathway signalling and VSMC conversion to a macrophage-like phenotype[62,64].

In cultured VSMCs treated with atherogenic growth factors and oxidized phospholipids, Kruppel-like factor 4 (KLF4), ETS Domain-containing protein 1 (ELK-1) and histone deacetylases (HDACs) cooperatively silence SMC marker genes through binding of G/C-rich repressor elements in the promoters of these genes, thereby preventing SRF-myocardin transcriptional activation[67–71]. SMC-specific conditional knockout of KLF4 led to reduced numbers of SMC-derived macrophage-like cells, significant reductions in lesion size, and increased plaque stability[49]. Hence, KLF-4 is a key transcriptional regulator of phenotypic conversion of VSMC towards a macrophage-like state as part of atherosclerotic plaque development[49].

Expression of miRs are controlled by extracellular signals (i.e. transforming growth factor beta (TGF-β) and PDGF) that modulate SMC phenotype switching[61,63]. In response to these signals, different groups of miRs are expressed: one that promotes the contractile phenotype and another that promotes the synthetic phenotype as well as migration and proliferation of SMCs[72]. miR143/145 promotes VSMC differentiation to the contractile phenotype through inhibition of transcriptional repressors (i.e. KLF4 and ELK-1) of SMC-marker genes[73–75]. In addition, induction of miR-21 can promote VSMC differentiation[76]. Myocardin-induced inhibition of VSMC proliferation is thought to be mediated through induction of miR-1[77]. In contrast, miR 221 and miR-146a both promote de-differentiation to a synthetic phenotype and VSMC proliferation[78,79].

The most highly characterized environmental signalling molecules that regulate VSMC phenotype are PDGF and TGF-β[36]. PDGF, a mediator released by activated vascular cells, promotes a synthetic phenotypic through downregulation of SMC markers[44,45] as well as stimulation of VSMC migration and proliferation[80,81]. TGF-β and homolog bone morphogenetic protein (BMP) promote SMC marker gene expression and differentiation to the contractile phenotype[82,83].

VSMC in the medial layer of the vessel wall synthesize and are surrounded by an ECM composed of collagen, elastin, proteoglycans, and glycoproteins[84]. ECM proteins are connected to VSMCs through extracellular receptors called integrins that interact differently with certain ECM proteins to modulate VSMC responsiveness to specific growth factors. ECM protein composition within the vessel wall differs between healthy versus atherogenic conditions.

In a healthy vessel wall, the ECM is rich in laminin and collagen IV, which suppress phenotypic switching[38], maintaining VSMCs in a contractile phenotype with reduced sensitivity to mitogenic stimuli[40]. A pro-inflammatory environment within the vessel wall leads to re-constitution of the ECM with collagen I, osteopontin, syndecan-4, and fibronectin[38]. Through differential interaction with integrins these ECM components collectively mediate phenotypic conversion and induce VSMC growth[38].

ECM component production by VSMC is regulated by specific growth factors and cytokines (e.g. IL-1β and TNF-α)[38]. Moreover, de-differentiated VSMCs increase production of MMPs[36], which have an important role in ECM remodelling. In a chronically damaged vessel wall, MMPs are abundant in the sub-intimal space[85] and

degrade ECM proteins (mainly collagen)[86–88] and liberate growth factors to facilitate phenotypic conversion as well as migration and proliferation[89–91].

The vessel wall is subjected to a variety of physical and chemical stressors that influence VSMC proliferation. Physical stresses are hemodynamic factors within the vessel wall, including shear stress and hydrostatic pressure[41]. Wall shear stress varies depending on the nature of blood flow. In an endothelial cell/VSMC co-culture system, low shear stress (associated with slow flow *in vivo*) stimulates VSMC phenotypic switching and proliferation via endothelial release of PDGF[41,69,92]. Conversely, high shear stress (associated with laminar flow *in vivo*) inhibits proliferation but induces apoptosis through endothelial-derived nitric oxide[41,93,94] and miRs (e.g. miR143/145)[95,96]. Interestingly, proliferation is inhibited when cultured VSMCs are directly subjected to shear stress[97]. Thus, under normal hemodynamic conditions there is a homeostatic balance between VSMC proliferation and apoptosis in the vasculature[41].

This balance is disrupted in vascular pathologies such as hypertension and atherosclerosis where there are aberrant mechanical forces on the vessel wall[98,99]. High blood pressure produces sufficient wall force to mechanically stretch VSMCs and prolonged cyclic mechanical stretch can stimulate VSMC proliferation *in vitro*[100,101]. In addition, experimental models of hypertension show an increased VSMC mass in the vessel wall indicative of VSMC proliferation[102,103]. In atherosclerosis, the neointimal layer protrudes into the vessel lumen, which disturbs blood flow patterns[41]. This produces areas of reduced flow and low shear

stress downstream of the lesion, leading to increased VSMC proliferation in these areas[41,104].

Several chemical stressors present in atherosclerotic lesions, including oxLDL[28,29], hypoxia[105], ROS[106,107], and heat shock proteins (Hsps)[108], can directly stimulate VSMC proliferation.

In conclusion, VSMCs assume varying roles throughout the different stages of atherosclerotic development[61]. VSMC phenotypic conversion, migration, and cell proliferation represent key processes in the transformation of fatty streaks into fibrous-capped plaques. In advanced lesions, the balance of VSMC migration and proliferation with VSMC senescence and apoptosis influences plaque stability[40].

3. CELLULAR STRESS RESPONSES

The cellular stress response is a reaction to any form of damage that pushes the cell out of its homeostatic set point[109]. When exposed to environmental stressors, cells can mount an adaptive response to promote survival or in the face of more severe damage initiate controlled cell death[110]. Some of the protective mechanisms include the heat shock response, unfolded protein response, DNA damage response and oxidative stress response[110]. Proteins in these stress-response pathways are conserved across human, yeast, bacterial, and archaeal genomes, underscoring their importance in protecting cells from environmental stressors[109]. Impairment in the function of these pathways may contribute to pathology, such as atherosclerosis.

3.1. Heat shock response

The heat shock response is defined as the activation of a subset of genes which were previously inactive or expressed at low levels, in response to mild hyperthermia or other stresses[111]. This phenomenon was first described in 1962, when Ritossa discovered a unique puffing pattern on the chromosomes of salivary gland cells in *Drosophila* subjected to an elevated temperature[112]. Puffs are chromosomal sites of rapid RNA synthesis and thus represent regions of gene activation[113,114]. It was subsequently found that the puffs induced by heat shock treatment were associated with the expression of a new family of proteins, now called heat shock proteins (Hsps)[113]. In addition to elevated temperature, other stressors including oxidative stress, heavy metals, bacterial and viral infections have been shown to turn on the heat shock response and induce the expression of Hsps[115,116].

3.1.1. Heat shock proteins

Hsps are a family of evolutionarily conserved chaperone proteins that are induced in response to a variety of stress stimuli to attenuate cellular damage and promote survival[117]. These chaperones protect cells in the face of proteotoxic stress by facilitating proper folding or refolding of proteins to prevent protein aggregation[118]. Beyond their role in the stress response, Hsps have several roles in maintaining cellular homeostasis including, regulation of protein breakdown[119,120], cell signaling pathways[121,122], and intracellular protein trafficking[123,124], as well as regulation of apoptotic pathways[115,117,125]. Hsps are named according to their molecular weight and are divided into the following sub-families based on their

amino acid constitution and function: Hsp110, Hsp90, Hsp70, and Hsp40; small Hsps; and human chaperonins (Hsp60/Hsp10, TRiC)[126].

The Hsp70 and Hsp90 families have critical roles in cellular proteostasis and exhibit similar structural properties[118,127]. In humans some Hsp70 and Hsp90 family members are constitutively expressed, while other members have low basal expression and are induced under stress conditions[118,126,128]. These chaperones primarily function in the cytosol and the nucleus, but both families also have isoforms that localize to the mitochondria and endoplasmic reticulum[118,127,129,130].

Hsp70 functions include facilitating the folding of newly synthesized polypeptide chains, re-folding of misfolded proteins to prevent their aggregation, movement of proteins across intracellular membranes, and control of proteins involved in cell signaling and apoptosis[118,123,131–133]. Hsp90 mediates the folding, activation, transport, and degradation of proteins involved in cell cycle regulation, cellular signaling, and apoptosis[127,133–135].

Hsp70 and 90 share similar structural motifs, both possessing an ATP-binding domain as well as binding domains for client proteins and regulatory co-chaperones[136–138]. The chaperone activity of these proteins is ATP dependent such that ATP and ADP-bound forms assume different conformations to enable the binding of different substrates[139–141]. Thus, the configuration and corresponding function of both protein families is dependent on their ATPase activity, which can be modulated by co-chaperones (e.g. Hsp70-Hsp40; Hsp70/Hsp90 organizing protein, Hop; Hsp110-Hsp70)[127,141,142] and post-translational modifications (i.e. phosphorylation and acetylation)[143]. For example, Hsp110 in complex with Hsp-70

acts as a nucleotide exchanger for ADP-bound Hsp70 to cooperatively facilitate disassembly of protein aggregates[144].

Under physiological conditions, Hsp70 assists in the folding of nascent polypeptides[118] and Hsp90 facilitates their final maturation[139]. Together, Hsp70 and Hsp90 facilitate the sequential folding and regulation of several groups of client proteins including steroid hormone receptors[139]. Tumorigenic cells are dependent on the Hsp70 and Hsp90 buffering systems to promote survival, making these chaperones attractive anti-cancer targets[118].

The small Hsps (sHsps) are lower molecular weight (12-42kDa) chaperones with a conserved α-crystallin domain[145]. At baseline, most proteins in this sub-family have low levels of expression[110,146]. sHsps interact with a range of client proteins, particularly those involved in gene expression, signal transduction, apoptosis, and cytoskeletal organization[147,148]. Hsp27 is a seminal family member which is induced as part of the heat shock response in most tissues[149,150]. Hsp27, like Hsp70 and Hsp90, is a pro-survival chaperone[146,151]. Induction of Hsp27 has been shown to protect cells against stress-induced apoptosis[151–153]. In addition, Hsp27 interacts with actin to maintain cytoskeletal integrity and promote survival in the face of stress stimuli[110,147].

sHsps are ATP-independent chaperones which form dynamic oligomeric structures around unfolded proteins to hold these client proteins in a partially competent state[154] until transfer to ATP dependent chaperone complexes like Hsp70/40 to refold the protein[155–157]. Alternatively, sHsps can transfer unfolded

proteins to proteasomes for degradation[119,120]. The chaperone activity of sHsps is regulated by phosphorylation[157], temperature[158], and pH[159].

The chaperonin family includes Hsp60, the eukaryotic homolog of GroEL, and its co-chaperone Hsp10 (eukaryotic homolog of GroES) as well as the TRiC protein family[126]. Hsp60 has an intracellular role as a housekeeping and stress-induced protein chaperone that aids in the folding and maintenance of a diverse set of client proteins[160–162]. Hsp60 exhibits its chaperone activity through the assembly of 2 groups of Hsp60 monomers into a barrel-like structure containing a central core which binds unfolded proteins[163–166]. Protein unfolding and re-folding within this multimeric Hsp60 structure is ATP dependent and assisted by its co-chaperone, Hsp10[166,167].

Within the cell, the majority (80-85%) of Hsp60 is localized to the mitochondria, with a smaller fraction (15-20%) localized to the cytosol and plasma membrane[168–170]. In response to stress, mitochondrial Hsp60 redistributes into the cytosol[171] and can be released from cells in vesicles[160,172–175]. Extracellular Hsp60 functions as a signaling molecule, promoting an inflammatory response through toll-like receptor (TLR) activation of various cell types[108,175–178]. For example, direct exposure of cultured VSMCs to recombinant Hsp60 promotes pro-inflammatory cytokine release, migration, and proliferation[108,176,178]. Alternatively, intracellular increases in Hsp60 expression in response to stress can promote apoptosis or proliferation depending on the cell type[26,27,162,171,179]. For example, artificial increases in intracellular Hsp60 protein levels through adenoviral transfection can directly stimulate VSMC proliferation[26,27].

3.1.2. Regulation of heat shock protein expression

Heat shock protein gene expression is controlled by transcription factors known as heat shock factors (Hsf)[180]. Upon stress-induced activation, these factors bind heat shock elements (HSEs) in the promoter regions of Hsp genes to facilitate transcription[181–184]. In vertebrates there are four members in the Hsf family (Hsf1-4)[184,185]. Hsf1 is expressed in most mammalian tissues and is considered the master regulator of Hsp gene expression[184]. In $Hsf1^{-/-}$ mice, fibroblasts do not increase transcription of hsp genes in response to heat shock treatment[186]. Alternatively, cells lacking the Hsf2 gene can produce a heat shock response, but with a different complement of Hsps than cells with an intact Hsf2 gene[187]. Thus, Hsf2 interacts cooperatively with DNA-bound Hsf1 to promote transcription of a unique repertoire of Hsp genes[187]. Hsf3 and Hsf4 are expressed only in specific tissues and their roles are poorly characterized in mammals[184].

In the absence of stress, Hsf1 is constitutively expressed as a monomer that lacks DNA binding activity and trans-activating capacity on HSEs[116,181]. However, under basal conditions, Hsf1 can modulate the expression of non-heat shock genes[188,189]. In response to proteotoxic stress stimuli, Hsf1 is rapidly activated through a multi-step process involving homotrimerization, accumulation in the nucleus, post-translational modification and interaction with chaperone complexes to enable HSE binding competence and trans-activation capacity[181]. DNA-bound Hsf1 complexes initiate transcription of Hsp genes through the liberation of paused RNA polymerase II on the the Hsp promoter regions[190].

There are a number of models proposed for stress-induced Hsf1 activation[116]. Chaperone displacement is the most widely accepted model and is based on negative feedback regulation of Hsf1 by stress-induced Hsps, namely Hsp90[116,191]. In this model, Hsp90 directly associates with Hsf1 monomers to constitutively repress homotrimerization[192,193]. In response to stress stimuli, there is an increase in aberrantly folded proteins causing Hsp90 to dissociate from Hsf1 to chaperone these denatured proteins[194]. This process liberates Hsf1 and enables transition of the inactive monomer into a homotrimer complex[194]. An alternative model of Hsf1 activation theorizes that Hsf1 has an intrinsic stress-sensing capacity, which explains the rapid activation of Hsf1 at the onset of stress[116]. *In vitro* experiments show monomeric Hsf1 can trimerize in response to heat shock and other chemical stressors[195,196].

Post-translational modifications (i.e. phosphorylation, sumoylation, and acetylation) and interactions with chaperone complexes are the primary mechanisms that modulate Hsf1 transactivation[116]. Phosphorylation is an important control mechanism of the transactivation potential of Hsf1. Although there are 19 phosphorylation sites identified on Hsf1[116,197], only 2 sites induce Hsf1 transactivation[198,199]. Interestingly, many phosphorylation events repress Hsf1 transcriptional potential[197]. Protein kinases involved in various cell signalling pathways, including mitogen activated protein kinases (MAPKs)[200,201], glycogen synthase kinase 3 (GSK3)[200,201], and calcium/calmodulin-dependent kinase II (CaMKII)[199] have been shown to phosphorylate different sites on Hsf1. Hsps and their co-chaperones have also been shown to regulate the activity of Hsf1[191]. Hsp90-

containing multi-chaperone complexes associate with trimeric Hsf1 to inhibit their transactivation potential[202]. Hsp70 and its co-chaperone Hsp40 can bind the transactivation domain of Hsf1 to repress its transcriptional activation function[203].

Hsp expression can also be regulated by other transcription factors (e.g. NF-κB, STAT proteins, NF-IL6, NF-Y, CREB), which are activated in response to pro-inflammatory cytokines (e.g. TNF-α, IFN-γ, IL-6). For example, TNF-α can increase Hsp60 expression through NF-κB[204]. In addition, interferon-gamma (IFN-γ) stimulates Hsp70 and Hsp90 through signal transducer and activator of transcription-1 (STAT1) and Hsf1 co-activation[205]. Interleukin-6 (IL-6) can induce Hsp90 expression through interactions of nuclear factor IL-6 (NF-IL6) and STAT3[206]. Lastly, NF-κB, nuclear transcription factor Y (NF-Y), and cAMP response element binding protein (CREB) induce Hsp70 expression through a variety of cooperative mechanisms that vary with cell type[207].

3.2. Heat shock protein-60 and atherosclerosis

The pro-inflammatory environment within atherosclerotic plaques effectively induces Hsps in vascular cells[208]. It is not surprising, then, that Hsps have been implicated in atherosclerotic development, with certain Hsps (Hsp27 and Hsp70) playing protective roles, while others (Hsp90 and Hsp60) are pro-atherogenic[208]. However, experimental atherosclerotic models and clinical studies have proven that Hsp60 is the only Hsp with the potential to directly contribute to atherosclerotic development[209]. Hsp60 plays an important role in atherosclerosis in

its role as an intracellular chaperone, intercellular signalling molecule, and cell surface autoantigen.

3.2.1. Intracellular mechanisms

Within surgically excised human atherosclerotic plaques, ECs, VSMCs, and macrophages all display positive Hsp60 staining[210]. In that same study, advanced lesions showed increased Hsp60 expression in VSMCs and lymphocytes[210]. ECs subjected to shear stress *in vitro* and *in vivo* demonstrate increased Hsp60 expression[211]. Furthermore, ECs from the aortic sinus in apoE deficient mice had high intracellular levels of Hsp60 early in the development of atherosclerosis[212]. As atherogenesis proceeded, Hsp60 was strongly expressed in the SMC-rich necrotic core[212]. In advanced, calcified plaques Hsp60 expression was not detectable[212]. These studies suggest that intracellular Hsp60 has an important role within different vascular cells throughout atherosclerosis. In particular, intracellular Hsp60 has been suggested to promote VSMC proliferation under atherosclerotic conditions[208]. VSMCs infected with *Cpn*, an atherogenic stimulus, demonstrate increased cell proliferation, which coincides with increased Hsp60 expression[162]. Furthermore, mechanical stretch and *Cpn* infection each have a synergistic effect on Hsp60 expression and VSMC proliferation in oxLDL-treated cells[26,27]. In addition, intracellular overexpression of Hsp60 independently stimulates VSMC proliferation[26].

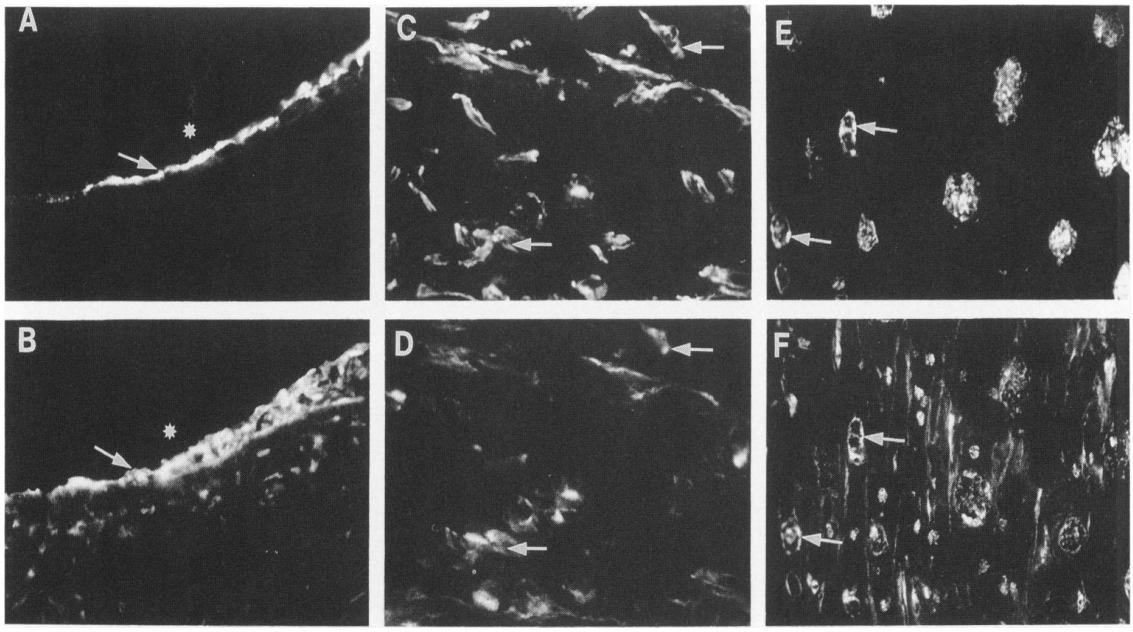

Figure 2. Expression of Hsp60 in vascular cells within human atherosclerotic plaques

The upper panel shows endothelial cells (A), vascular smooth muscle cells (VSMCs) (C), and macrophages (E) stained for cell-specific markers. The lower panel shows the corresponding photos of these cells stained for Hsp60 (B, D, F). Asterisks (*) indicate the lumen of the vessel. Arrows indicate selected double positive cells on corresponding pictures, which demonstrate expression of Hsp60 in endothelial cells, VSMCs and macrophages. This image was published in American Journal of Pathology, 142, R Kleindienst, Q Xu, J Willeit, FR Waldenberger, S Weimann, G Wick, Immunology of Atherosclerosis. Demonstration of Heat Shock Protein 60 Expression and T Lymphocytes Bearing alpha/beta or gamma/delta Receptor in Human Atherosclerotic Lesions, 1927-1937, Copyright © 1993, AMERICAN SOCIETY FOR INVESTIGATIVE PATHOLOGY. Published by ELSEVIER INC. All rights reserved.

3.2.2. Extracellular mechanisms

Under pro-atherosclerotic conditions, damaged vascular cells can secrete Hsp60 through exosomal pathways[176,213,214], which acts as an autocrine and paracrine hormone[215,216] capable of activating vascular cells through pattern recognition receptors (PRRs) such as Toll-like receptors (TLRs)[217]. For example, chlamydial and human-derived Hsp60 can directly activate EC, VSMC, and macrophage cellular functions that are important in atherogenesis[218]. Moreover, exposure of cultured VSMC to chlamydial and human Hsp60 stimulates cell proliferation through a TLR-dependent mechanism[108,178]. Thus, vascular cells recognize extracellular Hsp60 as a danger signal that promotes inflammation[215].

Clinical studies demonstrate a strong association between Hsp60 levels in the circulation and atherosclerotic vascular disease[219–222]. Initial clinical studies determined that elevated levels of soluble Hsp60 were associated with early atherosclerosis[219,220]. Subsequently, a large case control study showed that increased circulating levels of Hsp60 were associated with an increased risk of atherosclerosis[221].

3.2.3. Autoimmune mechanisms

Endothelial cells activated by atherosclerotic risk factors can express biochemically modified Hsp60 and cell adhesion molecules on their cell surface[209,223–225]. This altered membrane protein expression triggers an autoimmune response whereby T-cells migrate to the activated endothelium and orchestrate production of antibodies and effector T cells against autologous Hsp60. These antibodies and T cells can have cytotoxic effects on Hsp60 expressing

vascular cells within lesions[226–228]. Soluble Hsp60 can be released from these damaged cells[209], whereupon it can activate vascular and immune cells to propagate inflammation.

Human and bacterial Hsp60 have considerable sequence homology[229,230]. Consequently humans exposed to microbial Hsp60 (e.g. chlamydial Hsp60) through infection or vaccinations develop similar cellular and humoral immunity responses as they do when exposed to human Hsp60[209,230,231]. Thus, protective immunity against microbial Hsp60 may promote cross-reactivity with autologous Hsp60 when endothelial cells are stressed by atherogenic stimuli[209,231].

The concepts and implications of Hsp60 autoimmunity and Hsp60 cross-reactivity by the humoral immune response are exhibited in a number of clinical and experimental studies. In human atherosclerotic plaques, the expression of chlamydial and human Hsp60 is associated with Hsp65 antibodies[232]. Circulating antibodies against mycobacterial Hsp65 can also react with endogenous Hsp60 expressed on the surface of endothelial cells in human plaques[233]. Higher titers of Hsp65-reactive antibodies were found in individuals with atherosclerosis as compared to individuals without the disease[234]. Furthermore, higher titers of anti-human Hsp60 autoantibodies are correlated with advanced stages of atherosclerosis[235]. Consequently, anti-Hsp65 antibody titers may be a valuable prognostic marker for atherosclerosis[234].

In hypercholesterolemic rabbits, addition of recombinant mycobacterial Hsp65 induces endogenous Hsp65 expression in the plaque and stimulates production of T-cell populations against Hsp65, which drives atherosclerotic

development[236]. Indeed, effector T-cells reactive to Hsp60 are prominent in the early development of human atherosclerotic lesions[235]. Therefore, cellular immunity to Hsp60 plays a role in the initiation of atherosclerosis, while the humoral response to Hsp60 is responsible for disease propagation[209].

In addition to its pro-inflammatory effects on T cells, Hsp60 can also have anti-inflammatory effects through the induction and maintenance of regulatory T cells[231,237,238]. Soluble Hsp60 can activate regulatory T cells through TLR mediated signalling pathways[239]. Regulatory T cells are able to modulate Hsp60-reactive cytotoxic T-cell activity via anti-inflammatory cytokines and cell-cell contact[239]. This concept has been examined in various atherosclerotic animal models. Oral and nasal immunization of atherogenic mice with Hsp60 and small Hsp60-peptides produced a significant reduction in atherosclerotic plaque size through increases in regulatory T cells[240,241]. In addition, oral and nasal immunization with mycobacterial Hsp65 protects against atherosclerosis in LDL receptor deficient mice[242,243]. Lastly, subcutaneous immunization of ApoE null mice with Hsp65 attenuates the development of atherosclerotic lesions[244]. Hence, developing immune tolerance against Hsp60 through vaccination with Hsp60 and Hsp60-derived peptides could be a treatment strategy for atherosclerosis[209,231].

4. NUCLEOCYTOPLASMIC TRAFFICKING

Within the eukaryotic cell, the nucleus is separated from the cytosol by a double-layered nuclear membrane, known as the nuclear envelope[245]. The nuclear envelope houses the genetic material of the cell[245]. Nucleocytoplasmic trafficking

describes the movement of molecules between the cytosolic and nuclear compartments[246]. Transport into and out of the nucleus is through proteinaceous channels in the nuclear envelope, called nuclear pore complexes (NPCs)[247]. In order to mediate changes in gene expression, transcription factors enter and mRNAs exit the nucleus through NPCs[246,247]. Thus, nucleocytoplasmic transport is integral to both gene transcription and translation, and, therefore, survival of the cell[246,248].

4.1. Structure of the NPC

The NPC is a large, dynamic channel that spans both layers of the nuclear envelope and thereby acts as a door to the nucleus[249–251]. It is composed of multiple copies of approximately 30 different nuclear pore proteins (also known as nucleoporins)[252]. Nucleoporins (Nups) are arranged into 8 multimeric subunits that collectively form a barrel-like structure (Figure 3)[251,253]. This configuration produces an aqueous central pore through which nuclear transport complexes translocate[253–255]. The central portion of the NPC also has channels that are believed to allow the movement of small molecules and ions[256,257].

At the cytosolic and nuclear poles of the pore, nucleoporin-derived filaments extend into the cytosol or nucleoplasm[255,257] and can interact with proteins involved in transport in the respective compartments[251]. The cytosolic filaments contain sequence motifs that allow them to associate with proteins involved in nuclear import[258,259]. The nuclear filaments are significantly longer than cytoplasmic filaments and are connected at their distal ends to form a ring structure [257,260,261]. The distal ends of these filaments associate with the nuclear lamina, which holds

NPCs in place within the nuclear membrane[260,262]. The distal ends of nuclear filaments can also interact with nuclear export machinery[263].

The different structural and functional properties of each substructure of the NPC can be attributed to the presence of different nucleoporins in these regions. For example, nucleoporin 62 (Nup62) is found in the central core of the NPC, while Nup153 functions on the nucleoplasmic face of the NPC, and Nup358 functions on the cytoplasmic face[264]. Interestingly, certain nucleoporins can regulate gene expression through mobilization into the nucleoplasm[265–267].

Under normal conditions, individual NPCs are anchored to the nuclear membrane resulting in a characteristic spatial distribution[262]. However, defects in the nuclear lamina[268] or mutations in nucleoporins[269,270] can alter the distribution of NPCs within the nuclear envelope.

4.2. Receptor mediated nuclear transport

The NPC acts as a gatekeeper for the nucleus, allowing only select macromolecules to enter or exit. Small molecules can passively diffuse through the NPC, whereas proteins larger than 40 kilodaltons (kDa) are actively transported through NPCs by specialized nuclear transport receptors and their adaptor proteins[251]. To be recognized by these nuclear transport receptors, proteins require specific import or export sequences, known respectively as nuclear localization signals (NLSs) and nuclear export signals (NESs)[251]. There are numerous nuclear import pathways, which differ by their transport receptors and adaptor proteins as well as the cargo proteins and nuclear localization sequences they recognize[271].

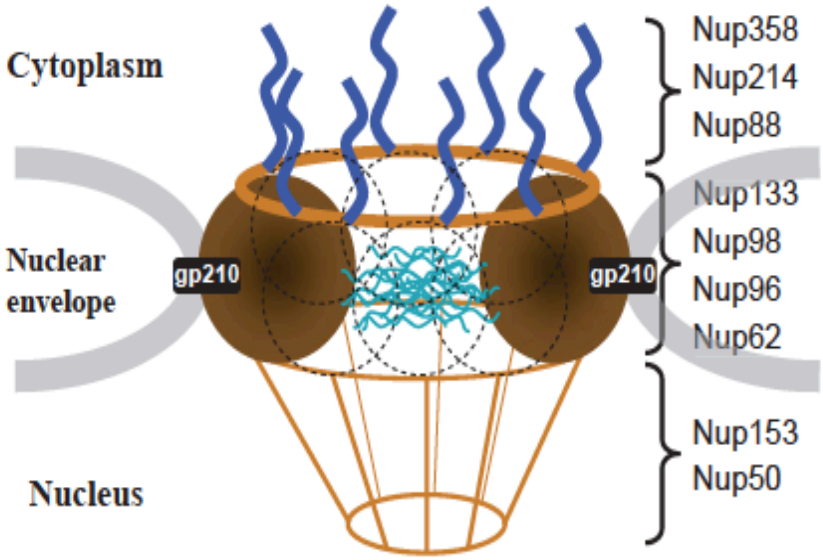

Figure 3. Structure of the NPC.

The NPC is composed of cytoplasmic fibrils, aqueous central channel, rings, spokes, nuclear fibrils, and nuclear basket. The relative distribution of Nups is also shown. Nup358, Nup62, and Nup153, play a role in the classical nuclear protein import pathway. Reproduced by permission from John Wiley & Sons Inc.: Genes to Cells, T Sekimoto, Y Yoneda, Intrinsic and extrinsic negative regulators of nuclear protein transport processes, 17(7): 525-535, © 2012 The Authors Journal compilation, © 2012 by the Molecular Biology Society of Japan/Blackwell Publishing Ltd.

4.2.1. Classical NPI pathway

The transport of cytosolic proteins through the NPC into the nucleus is known as nuclear protein import (NPI)[272]. The classical nuclear import pathway involves a transport receptor, importin-β (Imp-β) and its adaptor protein, importin-α (Imp-α) that recognizes cargo proteins containing a classical NLS (cNLS)[272,273]. A GTPase protein, Ras-related nuclear protein (Ran) and its accessory proteins give the pathway directionality[274,275]. Transporter proteins, cellular apoptosis susceptibility protein (CAS) and nuclear transport factor-2 (NTF2) are responsible for resetting the pathway, as they move proteins involved in import back to their initial compartment[276,277].

The import process begins with a cytosolic protein containing a cNLS. The cNLS consists of a small segment of positively charged amino acids[271] that can exist in either a mono-partite (PKKKRRV)[278] or a bi-partite (KRPAATKKAGQAKKKK)[279] form. cNLS motifs are recognized by the NLS-binding domain of Imp-α[280,281]. This results in a conformation change in Imp-α, which exposes its importin-β binding (IBB) domain to enable its association with Imp-β and form a heterotrimeric import complex[282,283]. Imp-β then interacts with Phenylalanine-Glycine (FG) repeats on nucleoporins (i.e. Nup62 and Nup153) from the NPC to translocate the import complex across the nuclear membrane (Figure 4)[275,284,285]. This mechanism of FG-Nup selective gating is known as the karyopherin (also known as importin)-centric, binding affinity model of nuclear import[246].

The nucleus contains a high concentration of Ran bound to GTP (RanGTP) relative to the cytoplasm[274,286]. This sets-up a RanGTP concentration gradient across

the nuclear membrane that provides energy for nuclear import[274]. Once the import complex enters the nucleus, RanGTP binds Imp-β to facilitate its dissociation from Imp-α and the cargo protein (Figure 4)[287,288]. Imp-α interacts with Nup50 to facilitate the dissociation of the cargo protein into the nucleoplasm[289,290]. Cargo-free Imp-α assumes an autoinhibitory structure, such that the free Imp-β and NLS-binding domains interact to prevent the re-association of the import complex[291]. Imp-β is displaced from Nup50 through binding of RanGTP and CAS[271,276]. Thus, export complexes of Imp-β:RanGTP and Imp-α:CAS:RanGTP move down the RanGTP concentration gradient through the NPC back to the cytoplasm (Figure 4)[271,276,292].

On the cytoplasmic side of the nuclear membrane, there is a high concentration of Ran bound to GDP (RanGDP) relative to the nucleus[288]. This establishes a RanGDP concentration gradient in the opposite direction of RanGTP[274]. Accessory proteins for Ran, including Ran GTPase-activating protein (RanGAP) and Ran binding proteins (RanBPs), are localized to the cytoplasmic side of the nuclear membrane (Figure 4)[247,293]. Ran has low intrinsic GTPase activity[294] and GTP hydrolysis is inhibited when Ran is associated with Imp-β or α[288,295]. When RanGAP and RanBP1 interact with RanGTP they catalyze GTP hydrolysis and destabilize the interaction between Ran and Imp-β or α[247,295–297]. This liberates Imp-β or α for another cycle of nuclear import and the generation of RanGDP (Figure 4)[247]. In its GDP-bound form, Ran has a low affinity for the importins, RanBPs, and RanGAP[271]. RanGDP is recognized by NTF2[277,298], which is localized to the cytosolic side of the nuclear envelope through interactions with Nups[299]. NTF2 transports RanGDP down its concentration gradient back into the nucleus (Figure 4)[277,300]. Upon nuclear

import, RanGDP associates with Ran Guanine Nucleotide Exchange Factor (RanGEF) an accessory protein that is localized to the nucleus (Figure 4)[247,274]. RanGEF (also known as regulator of chromosome condensation 1, RCC1) converts Ran-GDP to Ran-GTP[301] to prepare Ran for another round of nuclear protein import (Figure 4). Hence, cytoplasmic RanGAP and nuclear RanGEF are responsible for maintaining the Ran-GTP and Ran-GDP concentration gradients that provide directionality of importins and their cargo proteins[247,271].

4.2.2. Regulation of NPI

An important feature of selective transport of proteins into the nucleus is that the process is dynamically regulated[271]. Regulation enables adjustment of NPI according to cellular need[271]. NPI is primarily controlled by phosphorylation[248] which connects this process with a number of signalling pathways including the cell cycle, gene expression, and the immune response[271]. Other post-translational modifications including methylation, acetylation, and sumoylation have roles in regulating NPI[271]. Modulation of intracellular localization of cargo proteins, nuclear sequestration of transport receptors, and alterations in nuclear transport machinery gene expression are additional mechanisms by which NPI is regulated[271,302].

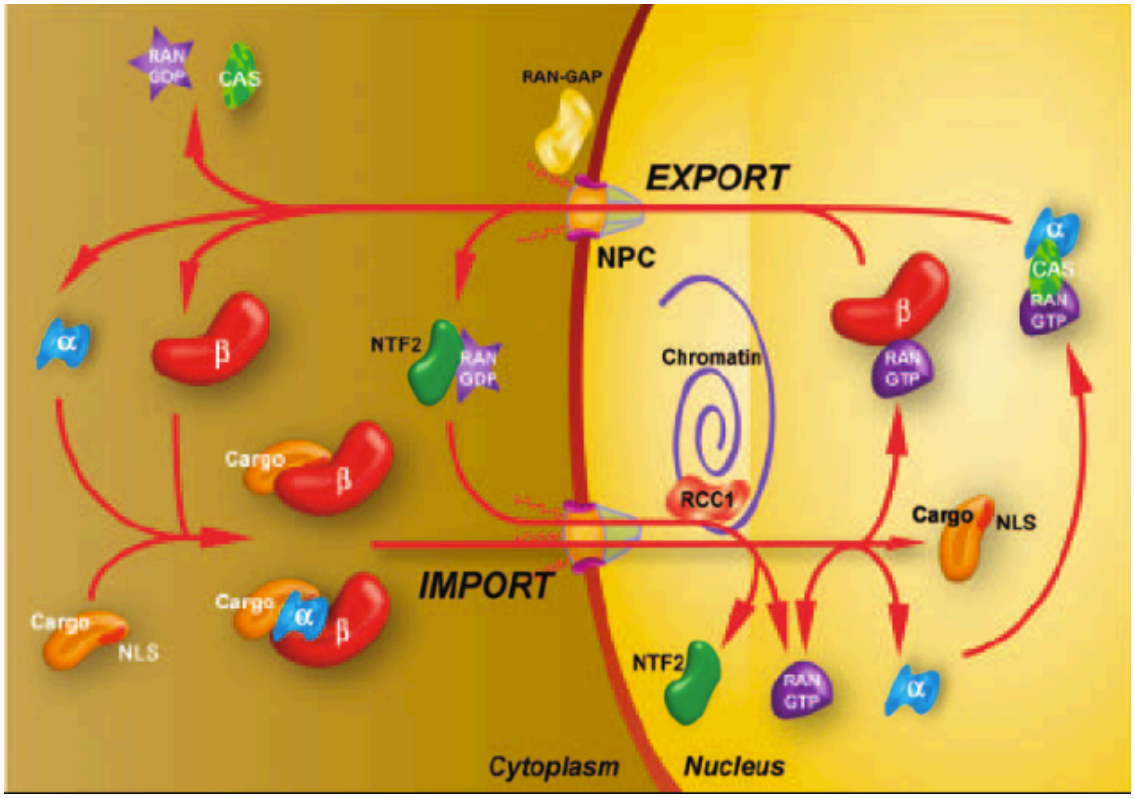

Figure 4. Mechanisms of NPI.

Cargo targeted for nuclear import have NLSs on their surface which interact with a number of distinct importin-alpha/beta heterodimers or importin-beta isoforms directly. These complexes are targeted to and translocated across the nuclear envelope through the NPC. Upon reaching the nucleus, RanGTP binds to importin-beta causing a conformational change that releases the bound cargo. The importins are then recycled to the cytoplasm as a RanGTP-importin-beta complex or, in the case of importin-alpha, by its export carrier CAS. The complex then dissociates in the cytoplasm after the hydrolysis of RanGTP, which is facilitated by RanGAP at the cytoplasmic face of the NPC. RanGDP is then imported to the nucleus by NTF2 and the guanine exchange factor RCC1 converts it to RanGTP. Reprinted by permission from MacMillan Publishers Ltd: Gene Therapy, AP Lam, DA Dean. Progress and prospects: nuclear import of non-viral vectors, 17(4):439-447, © 2010.

Intra- and inter-molecular NLS masking are two of the mechanisms through which phosphorylation can control nuclear transport[303]. NLS masking involves modulating NLS accessibility on cargo proteins to alter Imp-α binding and dictate whether heterotrimeric import complexes can be formed[303]. Intramolecular masking of the NLS involves phosphorylation- or dephosphorylation-induced conformational changes to the cargo protein, which either hides or exposes the NLS to inhibit or promote nuclear import[304–307]. Intermolecular masking of the NLS occurs through direct binding of inhibitory factors to the NLS of a protein[308,309]. For example, under baseline conditions the transcription factor NF-κB is associated with its repressor protein, IκBα, which masks the NLS[310,311]. Stress-stimuli induce phosphorylation and proteolysis of IκBα, which unmasks the NLS of NF-κB[308,312]. Intermolecular masking also influences nuclear transport in multi-subunit proteins in which each subunit contains one NLS[313]. Oligomerization of these subunits can increase or decrease the number of NLS copies available for Imp-α binding and thereby affects nuclear import efficiency[313].

Importin-cargo binding affinity and the activity of NPI machinery can also be controlled by phosphorylation. The phosphorylation of amino acids adjacent to the NLS changes the affinity of Imp-α for a NLS-containing protein[314–317]. Phosphorylation and dephosphorylation of importins can modulate their ability to interact with cargo proteins to form import complexes[318,319]. Phosphorylation of specific nucleoporins alters their binding affinity for Imp-β[320]. Mitogen-activated protein kinases (MAPKs) are involved in cell growth and viability pathways and can directly mediate phosphorylation of particular Nups[321].

Another method of regulating NPI is by modulating subcellular localization of cargo proteins and transport receptors. Cytoplasmic retention of NLS-containing proteins can be a consequence of intermolecular NLS masking[322,323]. For example, under baseline conditions Hsp90 chaperones are associated with glucocorticoid receptors (GRs)[324]. This interaction inhibits binding of nuclear transport receptors and thereby promotes cytosolic retention of GRs[324]. When a steroid hormone binds the receptor, Hsp90 dissociates, enabling NLS-dependent nuclear import of the steroid receptor and its hormone[324]. In contrast another molecular chaperone, Hsp70, has been postulated to promote NPI by facilitating the association of transport receptors with transport substrates[248,325]. Microtubules can facilitate translocation of NLS-containing proteins closer to the nucleus where transport receptors are readily available[326,327]. In response to stress-stimuli, Imp-α is sequestered in the nucleus to prevent its recycling back to the cytosol and inhibit NPI[328].

Modulating the expression profile of nuclear transport machinery is another mechanism for regulating NPI[302]. As different importins recognize unique sets of cargo proteins, the presence or absence of a specific importin can determine whether a particular cargo protein can enter the nucleus[329]. This plays a role in the regulation of development, as different importins are expressed during different stages of development[330]. Moreover, in adults the expression of certain importins and nucleoporins can be tissue specific[331–333]. Different Nups also interact more efficiently with certain importins[334], meaning modulation of the expression profile of Nups can also influence NPI[335]. For example, during cell proliferation there is an

upregulation of FG-Nups (i.e. Nup62)[26,27,101], which increases docking sites that are specific for Imp-β. Consequently, the expression level of Nup62 protein is correlated with the rate of classical NPI[27,29,101].

Alterations in the levels of transport receptors and accessory proteins can directly influence the rate of NPI. Elevated levels of Imp-β increase the rate of NPI[336]. Another study demonstrated that Imp-α, Ran, and NTF2 were the rate limiting factors of NPI[337]. Furthermore, changes in expression levels of specific import receptors and Nups has the potential to cause disease[338,339].

4.3. NPI and atherosclerosis

Regulation of nuclear protein import is essential for controlling intracellular localization of signalling proteins and fine-tuning cellular responses. In response to particular stress stimuli, NPI becomes dysregulated, which can lead to aberrant localization of signalling mediators and pathologic cell responses[339]. Pathological changes in NPI occur through altered expression and availability of importins and nucleoporins as well as alterations in the Ran cycle[340]. Atherosclerosis involves stress stimuli induced pathologic cell responses in VSMCs, ECs, and macrophages. There is evidence that alterations in NPI mediate pathological VSMC responses associated with atherosclerosis[339].

A number of studies have examined nuclear protein import in VSMCs under atherosclerotic conditions. OxLDL is a proposed stimulator of VSMC proliferation and apoptosis, two key processes in atherosclerotic development[23]. At low concentrations or short exposure time, oxLDL stimulates VSMC proliferation

through extracellular signal-regulated kinase 1/2 (ERK1/2) MAPK-dependent increases in NPI via increased Nup62 expression[29]. Alternatively, at higher concentrations or longer exposure times, oxLDL inhibits VSMC proliferation and promotes apoptosis through p38 MAPK-dependent decreases in NPI via decreased Nup62 expression[29]. In addition, at both low and high concentrations, oxLDL stimulates nuclear localization of cell cycle regulatory proteins (i.e. cyclin and proliferating cell nuclear antigen (PCNA)) in VSMCs[28]. Thus, oxLDL induces VSMC proliferation or apoptosis through MAPK-dependent alterations in nucleoporin expression, which modulates the rate of nuclear import and the localization of cell cycle regulatory proteins. Intermittent mechanical stretch, which is analogous to high blood pressure *in vivo*, also stimulates VSMC proliferation through ERK1/2 MAPK increases in Nup62 and NPI[101]. Furthermore, subjecting VSMCs to mechanical stretch synergistically enhanced cell proliferation, NPI, and Nup62 expression in oxLDL treated cells[27].

Lysophosphatidylcholine (LPC) is a phospholipid component of oxLDL that functions as an intracellular signalling molecule with mitogenic properties[341,342]. LPC mediates VSMC proliferation through increased RanGAP activity and the resultant increases in NPI[343]. Given that LPC mediates its mitogenic effect through ERK1/2 MAPK activation[342,343] and that RanGAP has docking sites for ERK1/2[339,344], it is postulated that increases in RanGAP activity are mediated by ERK1/2 MAPK[343]. Hydrogen peroxide, a ROS generated in atherosclerotic vascular cells, inhibits NPI and cell proliferation at least partially through cytosolic accumulation of RanGTP[345] and degradation of Nup153[346]. Cytosolic re-localization of RanGTP in hydrogen

peroxide treated cells is an ERK1/2 MAPK-dependent process[345]. Ceramide is a bioactive sphingolipid present in atherosclerotic SMCs that has anti-proliferative signalling properties[347,348]. Ceramide inhibits VSMC proliferation through inhibition of NPI via cytosolic re-localization of CAS and nuclear sequestration of Imp-α[347].

In a rat arterial balloon injury model, where VSMC are known to de-differentiate, migrate, and proliferate, RanGAP expression is elevated in neointimal cells post injury[349]. When RanGAP protein expression is experimentally reduced, VSMCs exposed to mitogens assume a more contractile phenotype and have reduced migration and proliferation as compared to control cells[349]. Thus, RanGAP expression can be modulated to effect changes in VSMC phenotype, proliferation, and migration.

Alterations in the components of NPI and the resulting alterations in nucleocytoplasmic trafficking are involved in pathological VSMC cell responses in atherosclerosis. Consequently, therapeutic targeting of proteins associated with nuclear import could be used to modulate aberrant NPI in atherosclerosis[339]. However, it is unknown whether changes in NPI occur within vascular cells in atherosclerotic plaques. In addition, a more complete understanding of the intracellular mechanism by which pro-atherogenic stimuli induce changes in NPI could provide more optimal therapeutic targets.

CHAPTER II: RATIONALE AND HYPOTHESES

Rationale

Proliferation of VSMCs is a key a step in atherosclerotic plaque development[40]. NPI is an important cellular pathway that is modulated as part of VSMC proliferation[29]. Hsp60 is a molecular chaperone that facilitates protein folding and trafficking under stress conditions[160,229]. The proliferation of VSMCs is stimulated by various stress stimuli, including oxLDL[26,27,29], which accumulates in the subendothelial layer in atherosclerosis[18]. A proposed mechanism of oxLDL-induced VSMC proliferation involves induction of Hsp60 and an increased rate of NPI[26,27,29]. OxLDL also augments the effects of other atherogenic stimuli (*Cpn* infection and mechanical stretch) on VSMC proliferation, NPI, and Hsp60 expression[26,27,29]. Therefore, further work is needed to understand the mechanistic link between Hsp60 and NPI in VSMC proliferation in response to oxLDL.

Experimental atherosclerosis models and clinical samples have supported the hypothesis that Hsp60 directly participates in the development of atherosclerotic lesions[209]. For example, Hsp60 is expressed in vascular cells in varying quantities throughout atherosclerotic development[210]. However, it is not fully understood how intracellular Hsp60 plays a role in atherosclerotic development *in vivo*. Given the work in cell culture, which demonstrates a relationship between Hsp60 and NPI in VSMC proliferation[26], this merits investigation into the relationship between Hsp60 and NPI during atherosclerotic progression. NPI can be modulated through altered expression of nuclear transport receptors and nucleoporins[101,336,337]. This raises the

question of whether Hsp60 expression is related to the expression of NPI-associated proteins (i.e. nuclear transport receptors and nucleoporins) in vascular cells in an atherosclerotic animal model.

Thus, we plan to investigate whether Hsp60 modulates NPI via alterations in nucleoporins and transport receptors to lead to VSMC proliferation *in vitro* and promote atherosclerotic development *in vivo*.

Hypotheses

1. It is hypothesized that when VSMCs are exposed to oxLDL, Hsp60 will alter cellular proliferation by regulating NPI.

2. It is hypothesized that nucleoporins and nuclear transport receptors for NPI will be altered during atherosclerotic development through a Hsp60-dependent mechanism.

CHAPTER III: OBJECTIVES

The following objectives address the first hypothesis:

1. To determine whether oxidized LDL can induce Hsp60, augment proteins associated with NPI, and stimulate cell proliferation in rat VSMCs.
2. To evaluate whether Hsp60 overexpression can independently stimulate VSMC proliferation in rat VSMCs.
3. To determine the effect of Hsp60 siRNA knockdown on NPI, expression of NPI-associated proteins, and cell proliferation in oxLDL-treated rat VSMCs.
4. To assess whether Hsp60 interacts with nuclear transport proteins under stress conditions to regulate NPI.

The following objectives address the second hypothesis:

1. To evaluate how the expression of a proliferative cell marker, heat shock proteins, and NPI-associated proteins vary in rabbit aortic vessels during atherosclerotic development.
2. To determine the relationships between Hsp60 expression, NPI-associated protein expression, and proliferative marker expression in rabbit aortic vessels during atherosclerotic development.

CHAPTER IV: MATERIALS AND METHODS

Reagents

Product	Source
4-(*N*-Maleimidomethyl)cyclohexane-1-carboxylic acid 3-sulfo-*N*-hydroxysuccinimide ester sodium salt	Sigma-Aldrich, Co. (St. Louis, MO)
5X siRNA Buffer	ThermoScientific (Rockford, IL)
20X Coupling Buffer, 25 ml	ThermoScientific (Rockford, IL)
Adenosine 5'-Disphosphate Sodium Salt From Bacterial Source	Sigma-Aldrich, Co. (St. Louis, MO)
$ALEXA_{488}$-Bovine Serum Albumin (BSA)	ThermoScientific (Rockford, IL)
Antibiotic-Antimycotic	Life Technologies Corporation (Grand Island, NY)
Ascorbate (200uM)	Sigma-Aldrich, Co. (St. Louis, MO)
Benzamidine	Sigma-Aldrich, Co. (St. Louis, MO)
BLUeye Pre-Stained Protein Ladder	FroggaBio Inc. (North York, ON)
Bovine Serum Albumin (BSA)	Sigma-Aldrich, Co. (St. Louis, MO)
Calcium Chloride	Sigma-Aldrich, Co. (St. Louis, MO)
CellTiter 96® Aqueous Non-Radioactive Cell Proliferation Assay	Promega (Madison, WI)
CellTiter-Glo-Luminescent Cell Viability Assay	Promega (Madison, WI)
Clarity™ Western ECL Substrate	Bio-Rad Laboratories (Mississauga, ON)
DAPI	Sigma-Aldrich, Co. (St. Louis, MO)
Dextrose U.S.P. (Anhydrous Granular)	Mallinckrodt Specialty Chemicals Company (Paris, KY)
DharmaFECT® 2 Transfection Reagent	ThermoScientific (Rockford, IL)
Dimethyl sulfoxide	Sigma-Aldrich, Co. (St. Louis, MO)
Dithiothreitol (DTT)	Sigma-Aldrich, Co. (St. Louis, MO)
DSS, No-Weigh™ Format	ThermoScientific (Rockford, IL)
Dulbecco's Modified Eagle Medium (DMEM)	Life Technologies Corporation (Grand Island, NY)
EDTA	Sigma-Aldrich, Co. (St. Louis, MO)
EGTA	Sigma-Aldrich, Co. (St. Louis, MO)
Elution Buffer, pH 2.0	ThermoScientific (Rockford, IL)
Ethanol, 99%	Fisher Scientific (Nepean, ON)
FastCast™ Resolver A, 10%	Bio-Rad Laboratories (Mississauga, ON)
FastCast™ Stacker A	Bio-Rad Laboratories (Mississauga, ON)
Ferric chloride $FeCl_3$	Sigma-Aldrich, Co. (St. Louis, MO)

FluorSave™ Reagent 0.05% NaN_3	Merck Millipore (Billerica, MA)
Fungizone	ThermoScientific (Rockford, IL)
Glycine	Sigma-Aldrich, Co. (St. Louis, MO)
HEPES (1M)	Life Technologies Corporation (Grand Island, NY)
HEPES (powder form)	Sigma-Aldrich, Co. (St. Louis, MO)
HyClone™ Fetal Bovine Serum (Canada), Standard	GE Healthcare Life Sciences HyClone Laboratories (Logan, UT)
Insulin from bovine pancreas (10nM)	Sigma-Aldrich, Co. (St. Louis, MO)
IP Lysis/Wash Buffer	ThermoScientific (Rockford, IL)
Laemmli Sample Buffer	Bio-Rad Laboratories (Mississauga, ON)
Leupeptin	Sigma-Aldrich, Co. (St. Louis, MO)
Luminata™ Forte Western HRP Substrate	Merck Millipore (Billerica, MA)
Magnesium Chloride	Fisher Scientific (Fair Lawn, NJ)
β-Mercaptoethanol	Sigma-Aldrich, Co. (St. Louis, MO)
MES hydrate	Sigma-Aldrich, Co. (St. Louis, MO)
Neutralization Buffer	ThermoScientific (Rockford, IL)
Non-targeting siRNA pool	GE Healthcare Life Sciences (Mississauga, ON)
Paraformaldehyde, 16% w/v aq. Soln., methanol free	Alfa Aesar (Ward Hill, MA)
PBS pH 7.2 (1X)	Life Technologies Corporation (Grand Island, NY)
Penicillin-Streptomycin	Life Technologies Corporation (Grand Island, NY)
Phosphate Buffered Saline	Sigma-Aldrich, Co. (St. Louis, MO)
Pierce® BCA Protein Assay Kit	ThermoScientific (Rockford, IL)
Pierce® Crosslink Magnetic IP/Co-IP Kit	ThermoScientific (Rockford, IL)
Pierce® Protein A/G Magnetic Beads	ThermoScientific (Rockford, IL)
Ponceau S Solution	Sigma-Aldrich Chemie GmbH Eschenstr. (Taufkirchen, Germany)
Potassium Acetate	Sigma-Aldrich, Co. (St. Louis, MO)
Potassium Chloride	Fisher Scientific (Fair Lawn, NJ)
PMSF	Sigma-Aldrich, Co. (St. Louis, MO)
Protease Inhibitor Cocktail	Sigma-Aldrich, Co. (St. Louis, MO)
Rat Hspd1 siRNA	GE Healthcare Life Sciences (Mississauga, ON)
Re-Blot Plus Strong Antibody Stripping Solution (10X)	Merck Millipore (Billerica, MA)
SimplyBlue™ SafeStain	ThermoScientific (Rockford, IL)
Skim Milk Powder	Wal-Mart (Winnipeg, MB)
Sodium chloride, crystalline powder PDV, 99+%	Alfa Aesar (Heysham, England)
Sodium dodecyl sulfate (SDS)	Sigma-Aldrich, Co. (St. Louis, MO)
Sodium deoxycholate	Sigma-Aldrich, Co. (St. Louis, MO)
Sodium Hydroxide Certified A.C.S.	Fisher Scientific (Fair Lawn, NJ)
Sodium pyruvate (2.5 uM)	Sigma-Aldrich, Co. (St. Louis, MO)

Sodium selenite (1nM)	Sigma-Aldrich, Co. (St. Louis, MO)
Supersignal® West Femto Chemiluminescent Substrate	ThermoScientific (Rockford, IL)
SuperSignal® West Pico Chemiluminescent Substrate	ThermoScientific (Rockford, IL)
SV40 large T antigen nuclear localization signal	ThermoScientific (Rockford, IL)
TBS BUFFER, 20X LIQUID	AMRESCO® (Solon, Ohio)
TEMED	Bio-Rad Laboratories (Mississauga, ON)
TGX Stain-Free™ FastCast™ Resolver B	Bio-Rad Laboratories (Mississauga, ON)
TGX Stain-Free™ FastCast™ Stacker B	Bio-Rad Laboratories (Mississauga, ON)
Trans-Blot® Turbo™ 5x Transfer Buffer	Bio-Rad Laboratories (Mississauga, ON)
TransBlot® Turbo™ Mini-size Nitrocellulose	Bio-Rad Laboratories (Mississauga, ON)
TransBlot® Turbo™ Mini-size Transfer Stacks	Bio-Rad Laboratories (Mississauga, ON)
Transferrin (5ug/mL)	Life Technologies Corporation (Grand Island, NY)
Tris(2-carboxyethyl)phosphine hydrochloride	Sigma-Aldrich, Co. (St. Louis, MO)
Tris-HCl	Sigma-Aldrich, Co. (St. Louis, MO)
Triton®-X-100	Fisher Scientific (Fair Lawn, NJ)
Trizma® base	Sigma-Aldrich, Co. (St. Louis, MO)
TrypLE™ Express	Life Technologies Corporation (Grand Island, NY)
Tween® 20	Fisher Scientific (Fair Lawn, NJ)
*ultra*PURE™ Ammonium Persulfate	Life Technologies, Inc. (Gathersburg, MD)

Antibodies

Primary Antibody	Type	Host	Source
Hsp60 [LK-1]	Monoclonal	Mouse	Abcam Inc. (Cambridge, MA)
Hsp60 (Mab11-13)	Monoclonal	Mouse	Enzo Life Sciences, Inc. (Farmingdale, NY)
Hsp70/Hsc70	Polyclonal	Rabbit	Enzo Life Sciences, Inc. (Farmingdale, NY)

Hsp90	Monoclonal	Rat	Enzo Life Sciences, Inc. (Farmingdale, NY)
Importin-α/KPNA2 [EPR11716(B)]	Monoclonal	Rabbit	Abcam Inc. (Cambridge, MA)
Importin-β/NTF97[3E9]	Monoclonal	Mouse	Abcam Inc. (Cambridge, MA)
MAb414/Nup62	Monoclonal	Mouse	Covance Inc. (Princeton, NJ)
Nup153	Monoclonal	Mouse	Covance Inc. (Princeton, NJ)
Proliferating Cell Nuclear Antigen (PCNA)	Monoclonal	Mouse	Invitrogen Corporation (Camarillo, CA)
Ran [EPR10791(B)]	Monoclonal	Rabbit	Abcam Inc. (Cambridge, MA)
Ran	Monoclonal	Mouse	BD Biosciences (Mississauga, ON)

Secondary Antibody	**Type**	**Host**	**Conjugate**	**Source**
Anti-mouse IgG	Polyclonal	Goat	HRP	Merck Millipore (Billerica, Massachusetts)
Anti-mouse IgG	Polyclonal	Goat	HRP	Abcam Inc. (Cambridge, MA)
Anti-mouse IgG	Polyclonal	Goat	Alexa488	ThermoFisher Scientific Inc. (Waltham, MA)
Anti-Rabbit IgG	Polyclonal	Goat	HRP	Abcam Inc. (Cambridge, MA)
Anti-Rat IgG	Polyclonal	Rabbit	HRP	Sigma-Aldrich, Co. (St. Louis, MO)

Methods

Procedures used in all studies

Vascular smooth muscle cell isolation and culture

Primary VSMCs were isolated from the thoracic aorta of male Sprague-Dawley rats or male New Zealand white rabbits using an explant technique as previously described[350]. Animal care was conducted as per the Guide for the Care and Use of Laboratory Animals published by the US National Institute of Health (NIH Publication No. 85-23, revised 1996). The Animal Care Protocol and Review Committee of the University of Manitoba approved this study.

Aortic rings were incubated in growth media (20% FBS, 10% fungizone, and 1% 1M Hepes in Dulbecco's Modified Eagle's Medium, DMEM) for 7-10 days with media changes every 48 hours. After this time, rings were transferred to another 10cm plate and VSMCs then migrated from the aortic tissue and adhered to the bottom of the plate. After another 5-7 days the tissue was removed to allow cells to grow to confluency. Cells were trypsinized and seeded onto coverslips in 6 well plates at a density of $4x10^4$ cells/well for NPI measurement or immunocytochemistry. Cells were seeded directly into 6 well plates at $1.5x10^5$ cells/well for western blotting. Alternatively, cells were seeded onto 96 well plates at a density of $5x10^3$ cells/well for measurement of cell proliferation or onto 10cm plates at a density of $8.4x10^5$ cells/plate for co-immunoprecipitation. VSMCs were then left to adhere to plates or coverslips for 24 hours, whereupon they were incubated in starvation media (DMEM, 5μg/ml transferrin, 1nM selenium, 200μM

ascorbate, 10nM insulin, 2.5μM sodium pyruvate, 1% fungizone) for 72 hours to synchronize cells prior to treatment. Notably, adenovirally-transfected cells underwent a different sequence of events prior to treatment. Cells were synchronized in starvation media on 10cm plates for 72 hours and then passaged onto 96 well plates, 6 well plates, or 10cm plates where they were given 3 hours to adhere to plates prior to infection.

Experimental treatments were adenovirally transfected human Hsp60, short interfering RNA against Hsp60 (Hsp60 siRNA), non-targeting siRNA (also known as scrambled siRNA), native LDL (naLDL), oxLDL, Hsp60 siRNA followed by oxLDL, or heat shock. For the duration of all treatments, cells were placed in a Sanyo MCO-18AIC(UV) incubator at 37^0C and 5% CO_2 unless otherwise stated.

Adenoviral transfection

Recombinant adenovirus-expressing human Hsp60 (adHsp60) or human Hsp60 without a mitochondrial localization sequence (adHsp60^{mito-}) were formulated using the AdEasy Vector System (Qbiogen), as previously described[162]. A hemagglutinin (HA) tag was added to the Hsp60 sequence to allow differentiation between endogenous and exogenous Hsp60. The recombinant adenoviral constructs were then transfected into QBI-293A cells, which give rise to viral particles. The concentration of the viral stock was determined through the tissue culture infectious dose 50 ($TCID_{50}$) method. VSMCs were treated with the adenovirus using a multiplicity of infection (MOI) of 20, 125, 150, or 200 viral particles/cell for 48 hours in 0.5% FBS supplemented DMEM without antibiotics. Different MOIs were used based on the subsequent assay performed on the cells.

Importantly, each of the different MOIs ensured transfer of the reporter gene into 100% of VSMCs in their respective experiments. An adenovirus with a green fluorescent protein reporter gene (adGFP) was used as an infection control. An empty adenovirus (adQBI) was used as an infection control in other experiments.

siRNA transfection

siRNA against rat Hsp60 was used to reduce Hsp60 protein expression in rat VSMCs. Hsp60 siRNA and non-targeting siRNA was obtained commercially through Thermo Scientific. siRNA transfection of VSMCs was performed using Thermo Scientific DharmaFECT transfection reagents and protocol. In brief, siRNA was combined with liposomes in FBS-free DMEM, resulting in the formation of siRNA-containing liposome carriers. This mixture was added to 0.5% FBS in DMEM without antibiotics to become the transfection media. The transfection media was then added to Rat VSMCs in 6 well plates, such that the final concentration of siRNA in each well was 25nM. A siRNA concentration of 25nM was chosen as it yielded the highest transfection efficiency in Rat VSMCs. Rat VSMCs were treated with Hsp60 siRNA, non-targeting siRNA (negative control), or no siRNA (control) for 48 hours.

Plasma lipoprotein isolation, oxidation, and treatment

Plasma was collected from male New Zealand white rabbits fed a 0.5% cholesterol-supplemented diet for at least 8 weeks. Low density lipoprotein (LDL) was then isolated through sequential ultra-centrifugation, as previously described[28,29,351,352]. EDTA was added to prevent oxidation of LDL throughout the isolation. In brief, the LDL fraction was subjected to dialysis against 0.15M NaCl and

0.1mM EDTA (pH 7.4). Subsequently, the dialyzed LDL was sterile filtered (0.2μm pore size) and stored at 4^0C. A cholesterol assay was then performed to determine the concentration of cholesterol.

An iron-ADP free radical producing system was used to oxidize LDL[28,29,351,352]. Specifically, 1mg/ml LDL stock was incubated with 0.05mM $FeCl_3$ and 0.5mM ADP in sterile filtered 150mM NaCl (pH 7.4) at 37^OC for 3 hours. For naLDL, neither $FeCl_3$ nor ADP was added to the sterile filtered 150mM NaCl (pH 7.4).

Rat VSMCs were treated with 0.5% FBS in DMEM supplemented with 25 or 50μg/ml of naLDL or oxLDL for 6 or 24 hours. The control group of VSMCs were incubated with 0.5% FBS in DMEM without added LDL for the same time periods. Alternatively, rat VSMCs transfected with Hsp60 or scrambled siRNA for 48 hours were subsequently treated with oxLDL at 50μg/ml for 6 hours.

Statistical analysis

Data are represented as mean +/- standard error of the mean (SEM) unless otherwise stated. Differences between treatment groups were evaluated by one-way ANOVA with a Fisher least significant difference (LSD) post-hoc test with the exception of treatment group data from the atherosclerotic rabbit study, which used a Student-Neuman-Keuls (SNK) post-hoc test. A probability of $p<0.05$ was considered statistically significant. In the atherosclerotic rabbit study, Pearson correlation and linear regression were used to evaluate the relationship between Hsp60 expression and PCNA or Nup62 expression.

1. Involvement of Hsp60 in the modulation of stress-induced VSMC proliferation

Measurement of cell proliferation

After treatment with adHsp60, adHsp60^{mito-} or oxLDL, VSMC number was assessed using a colorimetric enzyme assay (CellTiter96 AQueous Non-Radioactive Cell Proliferation Assay). This assay was based on the activity of a cytosolic enzyme expressed in viable cells. An increase in cell number following experimental treatment was indicative of cell proliferation. Cell proliferation was also assessed by evaluating changes in the protein expression of proliferating cell nuclear antigen (PCNA) through western blotting analysis.

Western blot analysis

Rat VSMCs treated with naLDL, oxLDL, Hsp60 siRNA +/- oxLDL, or scrambled siRNA +/- oxLDL and rabbit VSMCs treated with adHsp60 or adHsp60 mito- were subjected to western blot analysis. After treatment, cells were collected by trypsinization, then washed and lysed in sample buffer.

For rat VSMCs, electrophoresis and western blotting were performed with stain-free gel technology as previously described[353–355]. VSMC lysate samples were loaded into wells of 10% or 12% TGX-stain free denaturing polyacrylamide gels at $5x10^4$ cells/well. Proteins were separated by SDS-PAGE using a Bio-Rad gel apparatus. Following electrophoresis, gels were irradiated with UV light to activate binding of trihalocompound to tryptophan residues on proteins in the gel[354]. This caused proteins on the gel to fluoresce and thereby allowed visualization of the

quality of SDS-PAGE separation[354]. Proteins were then transferred using the Trans-Blot Turbo Transfer System onto nitrocellulose membranes. Post-transfer images of the membranes were taken using the stain-free imaging application on the ChemiDoc MP. This was done to assess transfer efficiency and to show the total protein content in each lane[356].

Subsequently, membranes were blocked with milk and incubated with anti-Hsp60 (Abcam) or anti-PCNA primary antibodies. HRP-conjugated anti-mouse or anti-rabbit IgGs were used as secondary antibodies. Protein bands were visualized on a ChemiDoc MP apparatus after application of Supersignal West Pico Chemiluminescent Substrate, Luminata Forte Western HRP Substrate, Clarity Western ECL Substrate, or Supersignal West Femto Maximum Sensitivity Substrate. The density of each band was quantified using Image Lab software (Bio-Rad). Protein expression was determined by normalizing the density of a protein band by the total protein loaded into a given lane. The total protein content in each lane was calculated from the post-transfer image of the membrane using Image Lab software. This quantification method of western blot data uses the total lane density of transferred protein on membranes, in place of housekeeping proteins, for loading controls[353,356].

For rabbit VSMCs, electrophoresis and western blotting were not performed with stain-free technology. VSMC lysate samples were loaded into wells of 10% denaturing polyacrylamide gels at $5x10^4$ cells/well. Proteins were separated using SDS-PAGE and then electrophoretically transferred onto nitrocellulose membranes. Subsequently, membranes were blocked with milk and incubated with anti-Hsp60

(Enzo Life Sciences) primary antibody. HRP-conjugated anti-mouse IgGs were used as secondary antibodies. Protein bands were visualized on a Fluor-S MAX apparatus after application of Supersignal West Pico Chemiluminescent Substrate or Luminata Forte Western HRP Substrate. The density of each band was quantified using Quantity One software (Bio-Rad). Protein expression in each sample was normalized by a β-tubulin loading control.

Immunocytochemistry

After transfection with adHsp60, adHsp60^{mito-}, Hsp60 siRNA, or scrambled siRNA, VSMCs on coverslips were washed twice with 1XPBS and fixed with 4% paraformaldehyde for 15 minutes. Cells were then permeabilized with 0.1% Triton-X100 in PBS and blocked with 5% milk in PBS with 0.1% Triton-X100 for 2 hours at room temperature. Coverslips were incubated overnight at 4^0C with anti-Hsp60 (Abcam) primary antibody in 1% skim milk in PBS with 0.1% Triton-X100. After washing the cells, Alexa488-conjugated goat anti mouse IgG in 1% skim milk in PBS with 0.1% Triton-X100 was added for 1 hour in the dark. Subsequently, the cells were washed and incubated with DAPI for 2 minutes in the dark. Coverslips were mounted on microscope slides using 10µl FluorSave to preserve fluorophore signal. Stained VSMCs were visualized with a 40X objective on a Nikon TE 2000s microscope using filters specific for DAPI or Alexa488 fluorescence. Images were acquired using NIS Elements software (Nikon) and cell fluorescence was quantified using this same software.

2. Involvement of Hsp60 in the modulation of nuclear protein import during stress-induced VSMC proliferation

Measurement of nuclear protein import

The rate of nuclear protein import was assessed using a microinjection technique as previously described[101]. VSMCs treated with adHsp60, adHsp60^{mito-}, Hsp60 siRNA +/- oxLDL, or scrambled siRNA +/- oxLDL were assessed for nuclear protein import. Following treatment, coverslips with VSMCs were removed from wells and placed in a Leyden dish containing 2ml of pre-warmed perfusate buffer (6mM KCl, 1mM MgCl2, 1mM CaCl2, 10mM dextrose, 6mM HEPES, pH 7.4). The Leyden dish was mounted in a microperfusion chamber to maintain the cells at 37^0C. An Alexa488-BSA-nuclear localization signal (NLS) fluorescent substrate was prepared through the conjugation of Alexa488-BSA to the SV40 large T antigen NLS (CGGGPKKKRKVED)[345]. Using a Flaming/Brown micropipette puller (Sutter Instruments, Model p-97), thin-walled glass capillary tubes (1.0 mm, 3 inch) were separated into micropipettes for cell injection. A micropipette was loaded with the fluorescent NLS-containing substrate and inserted into the cell cytoplasm using a MS314 micromanipulator (Fine Science Tools) (Figure 5). The substrate was then injected into the cell cytoplasm using a PV830 Pneumatic PicoPump (World Precision Instruments). The micropipette was slowly removed from the cell after injection. Images of the cell after microinjection were acquired on a confocal laser-scanning microscope (Zeiss LSM5 Pascal). To observe the nuclear import of the Alexa-BSA-NLS fluorescent protein in each microinjected cell, images were taken

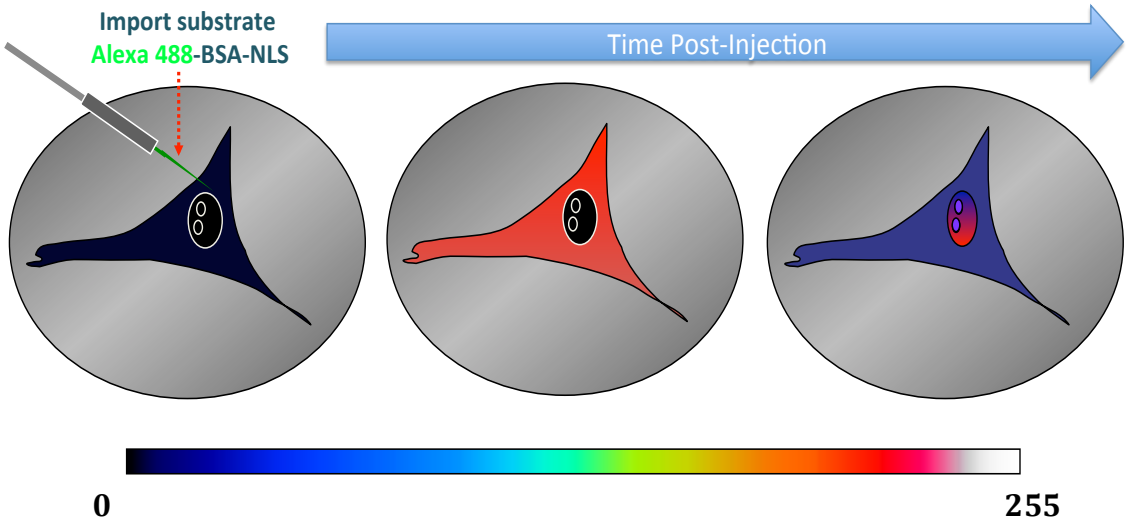

Figure 5. Schematic of microinjection technique used to measure NPI.

VSMCs were microinjected with a fluorescent-tagged NLS-protein marker. The fluorescent protein marker moves from the cytoplasm into the nucleus to increase the ratio of nuclear to cytoplasmic fluorescence over time. The pseudo-colour scale represents level of fluorescence from 0 (black) to 255 (white) arbitrary units. Re-used with permission from Deniset, JF. *Heat Shock Protein-60 Mediated Induction of Vascular Smooth Muscle Cell Proliferation through Nucleocytoplasmic Trafficking*, JF Deniset, M Hlavackova, TE Hedley, MN Chahine, E Dibov, and GN Pierce, © 2013.

pre-injection and post-injection up to 30 minutes (Figure 5). Importantly, the fluorescent BSA does not move into the nucleus over this time period without a NLS. In addition, as this marker protein contains a classical NLS, it models the nuclear import characteristics of all proteins using the classical nuclear import pathway. Image J software was used to quantify the ratio of nuclear to cytoplasmic fluorescence at each time point. To calculate nuclear to cytoplasmic fluorescence, a cytosolic area adjacent to the nucleus and equivalent nuclear area were used.

Heat shock treatment

Rat VSMCs were heat-shocked at 42^0C for 1 hour and then returned to a Sanyo MCO-18AIC (UV) incubator at 37^0C and 5% CO_2 for 48 hours. Control plates remained in the same incubator at 37^0C and 5% CO_2 for this entire duration. Both control and heat shocked VSMCs were maintained in 2.5% FBS-supplemented DMEM for this experiment.

Co-immunoprecipitation

Co-immunoprecipitation was performed with the Pierce Crosslink Magnetic IP/Co-IP kit. After heat shock treatment or adenoviral transfection, Rat VSMCs were collected and lysed with an IP Lysis/Wash buffer (Thermo Scientific Pierce). Cell lysates were then centrifuged at 13,000g to pellet cell debris. The supernatant containing VSMC protein was removed and subjected to a BCA protein assay to determine protein concentration. Anti-Hsp60 (Abcam) or anti-Ran (Abcam) antibodies (IgG isotypes) were covalently cross-linked to magnetic beads coated with recombinant proteins capable of binding IgG. The antibody-conjugated beads

were incubated with specific concentrations of VSMC protein samples. This was done to separate Ran and Hsp60 proteins from the rest of the proteins in the samples. Beads were washed to remove non-bound material and then incubated in an elution buffer, which caused bound protein to dissociate from the antibody-crosslinked beads. The eluted protein for each sample was collected, put into sample buffer and then loaded into TGX-stain free gels for SDS-PAGE. Finally, the eluted proteins were subjected to western blotting techniques to assess what proteins were co-immunoprecipitated with Ran or Hsp60.

Western blot analysis

Co-immunoprecipitated protein samples from rat VSMCs treated with heat shock, adHsp60, or adHsp60^{mito-} were subjected to western blot analysis. In addition, rat VSMCs treated with oxLDL, Hsp60 siRNA +/- oxLDL, or scrambled siRNA +/- oxLDL were subjected to western blot analysis. Electrophoresis and western blotting were performed with stain-free gel technology as previously described[353–355]. VSMC lysate samples were loaded into wells of 10% or 12% TGX-stain free denaturing polyacrylamide gels at $5x10^4$ cells/well. Proteins were separated by SDS-PAGE using a Bio-Rad gel apparatus. After gel activation using UV radiation, proteins were transferred onto nitrocellulose membranes. Post-transfer images of the membranes were taken using the stain-free imaging application on the ChemiDoc MP. Subsequently, membranes were blocked with milk and incubated with anti-Hsp60 (Abcam), anti-Ran (BD Biosciences), anti-Importin-α, anti-Importin-β, anti-Nup153, or anti-Mab414 (Nup62) primary antibodies. HRP-conjugated anti-mouse or anti-rabbit IgGs were used as secondary antibodies.

Protein bands were visualized on a ChemiDoc MP apparatus after application of Supersignal West Pico Chemiluminescent Substrate, Luminata Forte Western HRP Substrate, Clarity Western ECL Substrate, or Supersignal West Femto Maximum Sensitivity Substrate. The density of each band was quantified using Image Lab software (Bio-Rad).

3. Expression and relationship of Hsp60, NPI-associated proteins, and PCNA during atherosclerotic development

Atherosclerotic rabbit model

Male New Zealand White rabbits weighing between 2.7 and 3.0 kg (Spilak Farms) were used for this study. Upon arrival, rabbits were housed in individual cages in temperature- and humidity-controlled rooms and were subjected to a 12-hour light cycle. Animal care was conducted as per the Guide for the Care and Use of Laboratory Animals published by the US National Institute of Health (NIH Publication No. 85-23, revised 1996). The University of Manitoba Protocol Management Review committee approved the experimental protocols of this study. Rabbits were fed a diet containing 1% cholesterol (Ren's Pet Depot) for 4 weeks and then switched to a regular rabbit chow (Nutrena, Nature Wise Performance Rabbit Formula) for an additional 0, 2, 4, 8, 16, 22, or 28 weeks. This dietary course results in two distinct stages of atherosclerosis: a robust growth phase of atherosclerotic plaques followed by a stabilization phase, in which plaque growth plateaus[357]. Control rabbits were given regular rabbit chow for 12 weeks and subsequently

terminated. Cholesterol-fed rabbits were terminated at the end of their respective cholesterol withdrawal periods. Immediately after termination, aortas were excised from the proximal aortic arch to the end of the thoracic aorta at the base of the diaphragm. Aortas were then subjected to en-face analysis[358] to determine the proportion of luminal area covered by atherosclerotic plaques. This involved opening the aortas longitudinally and taking digital photographs of the vessel lumens[358]. Images were analyzed using Nikon imaging software (Elements). The percentage of lesional area was calculated by dividing the area covered with lesions by the total area of the aorta. Aortas were then stored at -80^{0}C for western blot analysis.

Western blot analysis

A segment of aortic tissue containing atherosclerotic lesions was excised from each aortic arch. Aortic tissue samples were ground using liquid nitrogen and re-suspended in RIPA buffer (50mM TrisHCl pH 7.5, 150mM NaCl, 1mM EDTA, 1mM EGTA, 1% Triton X-100, 0.1% SDS, 0.5% Na Deoxycholate, 1µg/ml Leupeptin, 1mM PMSF, 1mM protease inhibitor cocktail, 1mM DTT and 1mM Benzimidine). Samples were then subjected to several freeze-thaw cycles, which consisted of flash freezing in liquid nitrogen followed by sonication in a room temperature water bath. Subsequently, samples were centrifuged at 14,000 rpm and the supernatant was collected. Sample protein concentrations were determined using a BCA protein assay kit. For these samples electrophoresis and western blotting were not performed with stain-free technology. Proteins were separated on a 9%, 12%, or 15% polyacrylamide gel and then transferred onto nitrocellulose membranes via

electrophoresis. Subsequently, membranes were blocked with milk and incubated with anti-Hsp60 (Enzo Life Sciences), anti-Hsp70, anti-Hsp90, anti-PCNA, anti-Ran (BD Biosciences), anti-Importin-β, or anti-Mab414 (Nup62) primary antibodies. HRP-conjugated anti-mouse, anti-rabbit, and anti-rat IgGs were used as secondary antibodies. Protein bands were visualized on a Fluor-S MAX apparatus after application of Supersignal West Pico Chemiluminescent Substrate or Luminata Forte Western HRP Substrate. The density of each band was quantified using Quantity One software (Bio-Rad). Protein expression in each sample was normalized by a total actin loading control.

CHAPTER V: RESULTS

1. Involvement of Hsp60 in the modulation of stress-induced VSMC proliferation

Oxidized LDL stimulates VSMC proliferation and induces Hsp60 expression

Consistent with previous work on rabbit VSMCs[26–29], oxLDL induced cell proliferation in rat VSMCs after 24 hour treatment at a concentration of 25μg/ml (Figure 6). This effect was not dose-dependent, as 50μg/ml oxLDL treatment for the same duration did not stimulate VSMC proliferation (Figure 6).

Previous work also demonstrated that Hsp60 is involved in VSMC proliferation[26,162]. Thus, the effect of 25μg/ml oxLDL treatment on expression of Hsp60 and PCNA (protein marker of proliferation) was examined (Figures 7A and 7B). After six hours of oxLDL treatment, Hsp60 expression was significantly upregulated relative to untreated control cells (Figure 7B). In addition, PCNA expression displayed a trend towards statistically significant elevation compared to control samples (Figure 7A). After twenty-four hours of oxLDL treatment, Hsp60 expression returned to baseline (Figure 8B) and PCNA expression continued to show a trend towards statistically significant elevation versus control samples (Figure 8D). Consistent with the cell proliferation assay, elevated levels of oxLDL did not alter Hsp60 or PCNA expression, as 50μg/ml oxLDL treatment for 6 hours produced no significant changes in Hsp60 (Figure 8A) or PCNA (Figure 8C) levels.

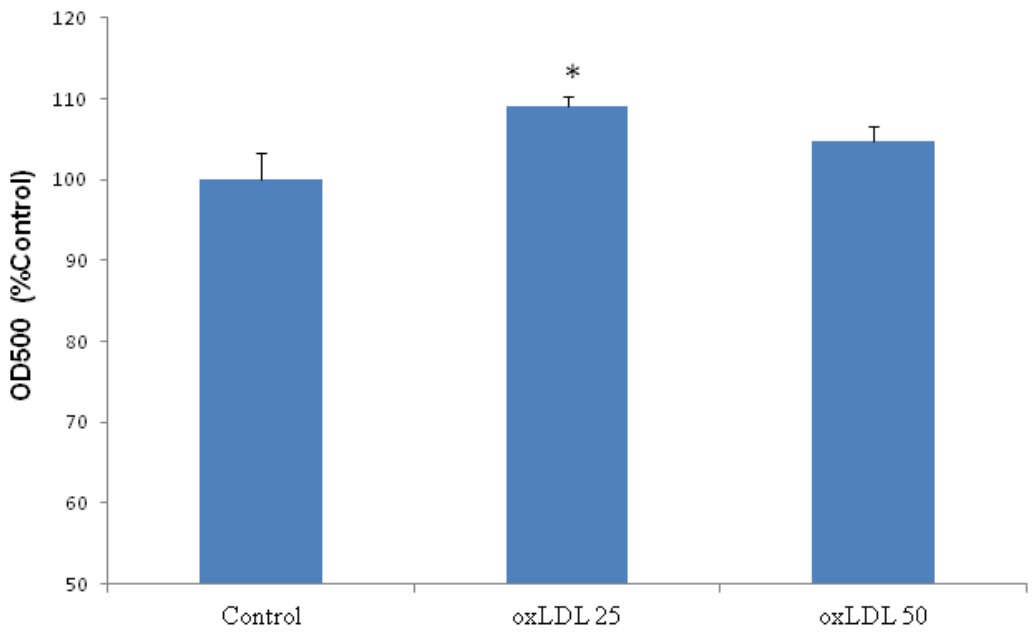

Figure 6. OxLDL stimulates VSMC proliferation.

Rat VSMC measurement in response to treatment with oxLDL at 25 or 50 μg/ml for 24 hours. Control cells were incubated in identical medium without oxLDL. Cell number determined by optical density (OD) at 500nm. Data represented as percentage optical density of control. *$P < 0.05$ versus control. Values are means ± SEM; n=8.

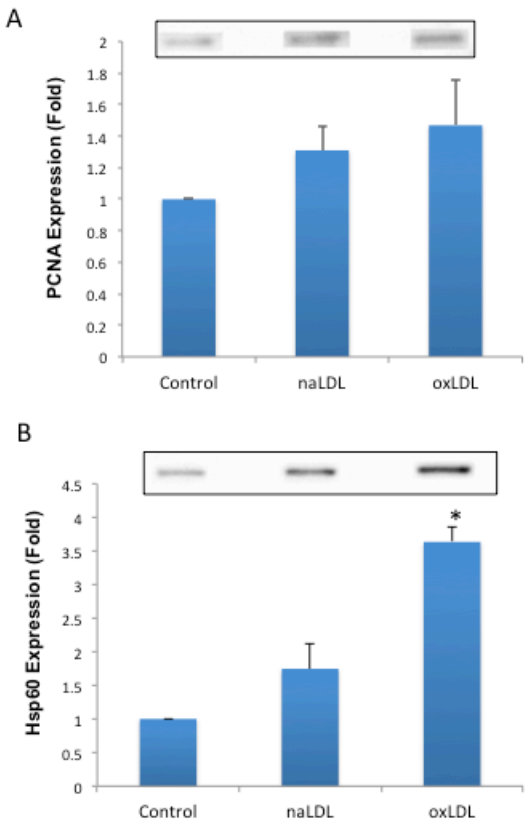

Figure 7. Effect of oxLDL treatment on PCNA and Hsp60 protein expression in VSMCs.

Western blot analysis and representative images of PCNA (A) and Hsp60 (B) expression in rat VSMCs treated with naLDL or oxLDL at 25µg/ml for 6 hours. Control cells were incubated in identical medium without LDL. On each Western blot, density of a specific protein band was normalized by total protein loaded into each lane. Normalized protein expression is represented as fold change to control samples. The values in each graph represent the means ± SEM of three independent experimental replicates (n=3) from the same primary rat aorta explant. *$P < 0.05$ versus control and naLDL.

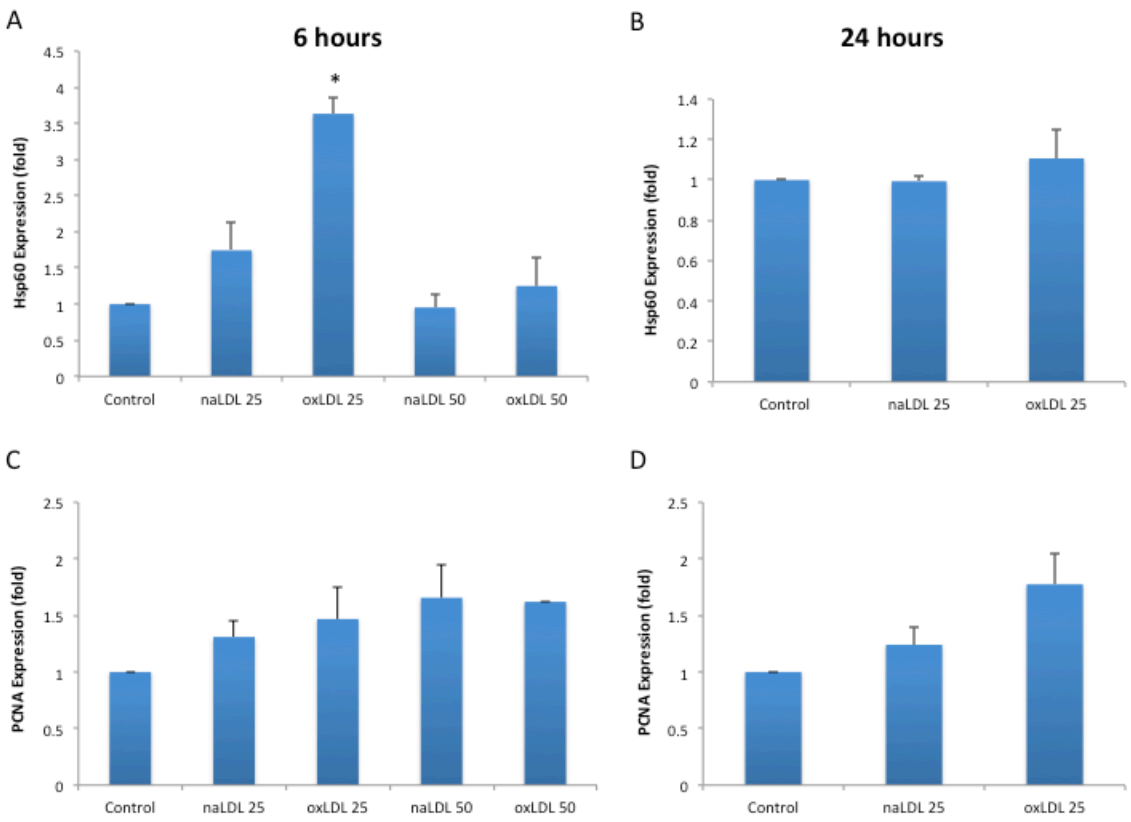

Figure 8. Effect of oxLDL treatment for 6 or 24 hours on Hsp60 and PCNA protein expression in VSMCs.

Western blot analysis of Hsp60 (A, B) and PCNA (C, D) expression in rat VSMCs treated with naLDL or oxLDL at 25 or 50 μg/ml for 6 hours (A, C) or 25μg/ml for 24 hours (B, D). Control cells were incubated in identical medium without LDL. On each Western blot, density of a specific protein band was normalized by total protein loaded into each lane. Normalized protein expression is represented as fold change to control samples. Values are means ± SEM; n=3. *$P < 0.05$ versus 6 hour control and naLDL at 25μg/ml for 6 hours.

Hsp60 overexpression independently stimulates VSMC proliferation

Previous work demonstrated that Hsp60 overexpression induced cell proliferation in rabbit VSMCs[26,162]. However, the subcellular localization of Hsp60 that induced the proliferative effect was not identified. To confirm the proliferative action of Hsp60 in rat VSMCs and to identify the subcellular localization of Hsp60 that mediates the proliferative action, adenoviral transfection was used to overexpress two forms of Hsp60: a cytosolic form (adHsp60^{mito-}) that lacked a mitochondrial targeting sequence and a form that possessed the same mitochondrial targeting sequence as endogenous Hsp60 (adHsp60). Both adHsp60 and adHsp60^{mito-} were over expressed at similar levels (Figure 9) but with different localization within the VSMC. Whereas the adHsp60^{mito-} was expressed throughout the cytosolic compartment, adHsp60 was primarily localized to the mitochondria (Figure 10). Both adHsp60 and adHsp60^{mito-} were capable of a significant stimulation of cell number as compared to enhanced green fluorescent protein (EGFP) transfected controls (Figure 11).

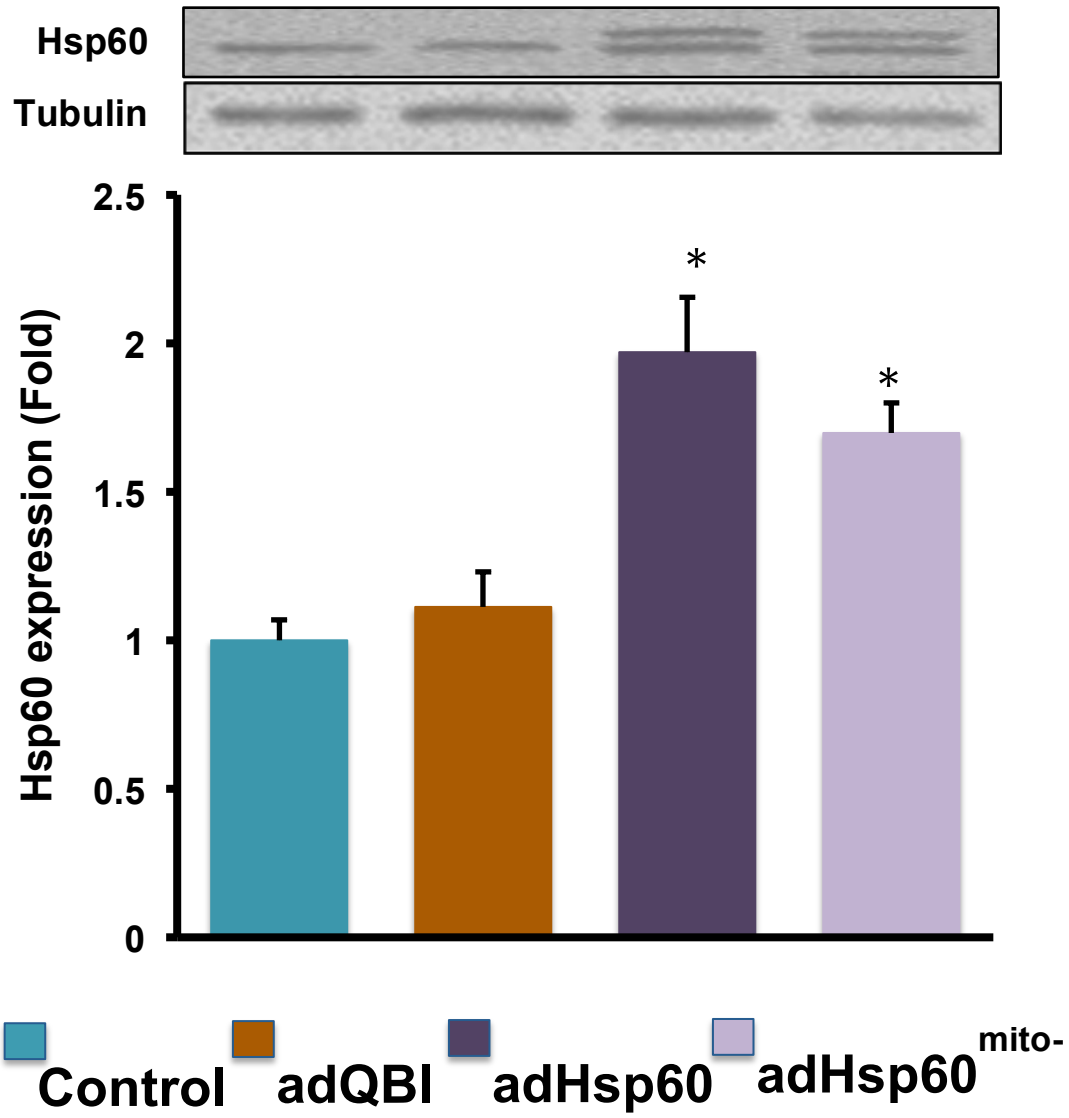

Figure 9. Hsp60 overexpression.

Western Blot analysis and representative images of Hsp60 expression in rabbit VSMCs transfected with Hsp60 with (adHsp60) or without (adHsp60^{mito-}) a mitochondrial targeting sequence. Rabbit VSMCs transfected with an empty adenovirus (adQBI) were used as an infection control. MOIs of 1:100-150 were used for the adenoviruses. Normalized protein expression levels were represented as fold change to control samples. Values are means ± SEM; n= 4-5. *$P < 0.05$ vs. control and adQBI (Student-Neuman-Keuls). Adapted with permission from Deniset, JF. *The Role of Chlamydia Pneumoniae Infection and Stress Responses in Vascular Remodelling.* 2013, University of Manitoba.

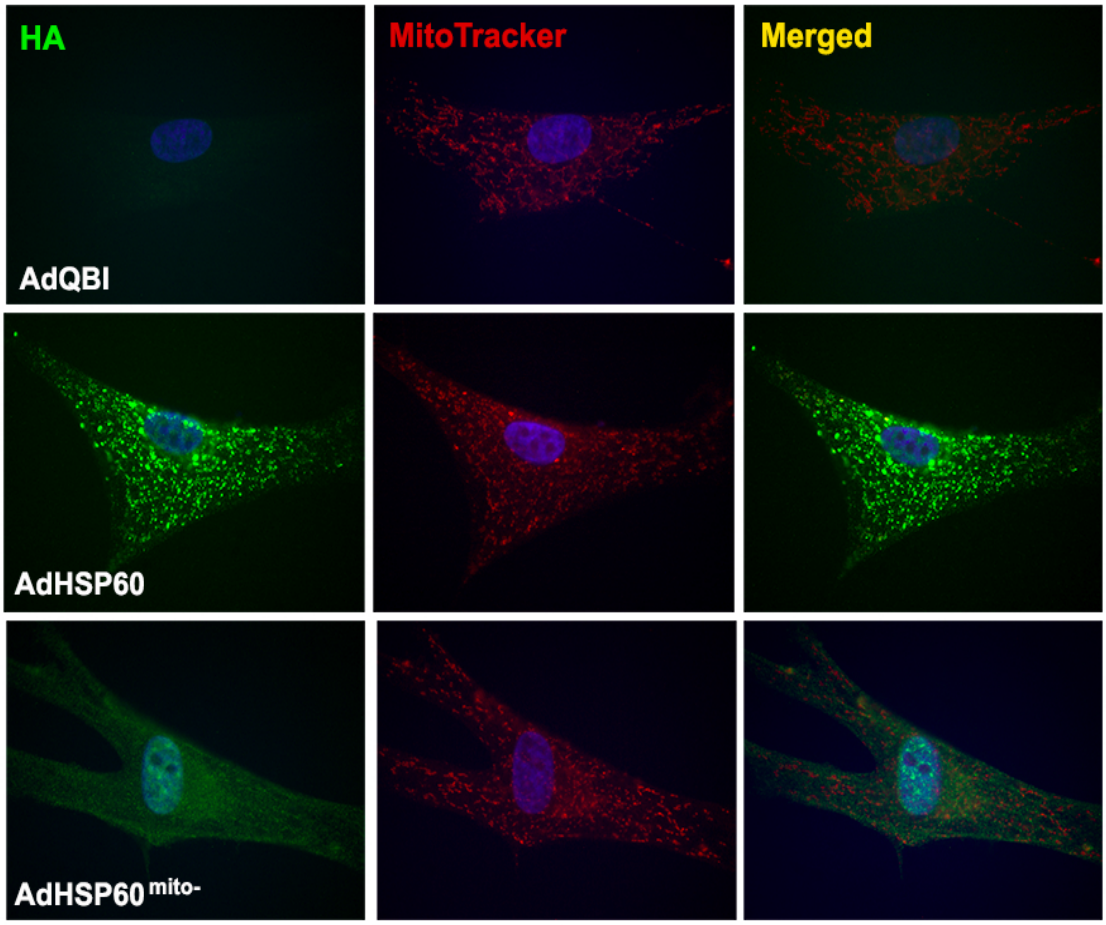

Figure 10. Intracellular localization of overexpressed Hsp60

Rabbit VSMCs were transfected with Hsp60 with (adHsp60) or without (adHsp60^{mito-}) a mitochondrial targeting sequence to induce Hsp60 overexpression. Both forms of Hsp60 were tagged with hemagglutinin (HA) to differentiate transfected Hsp60 from endogenous Hsp60. MOIs of 1:100-150 were used for the adenoviruses. The figure shows representative immunocytochemistry images of HA co-localization with mitochondrial and nuclear staining. **left column:** HA expression, green; **middle column:** MitoTracker, red; **right column:** Merged staining. **all images:** DAPI nuclear stain, blue. Adapted with permission from Deniset, JF. *The Role of Chlamydia Pneumoniae Infection and Stress Responses in Vascular Remodelling.* 2013, University of Manitoba.

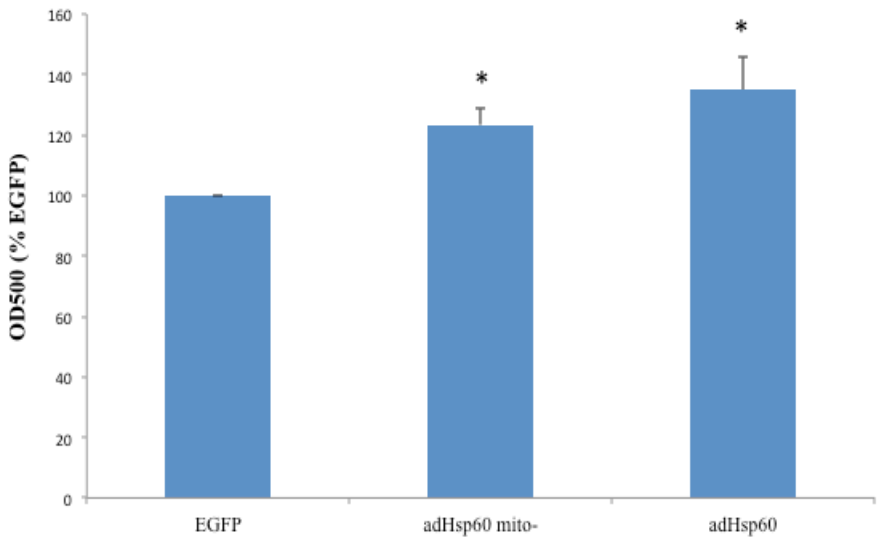

Figure 11. Hsp60 overexpression induces VSMC proliferation.

Rat VSMC number in response to transfection with enhanced green fluorescent protein (EGFP) or Hsp60 with (adHsp60) or without (adHsp60^{mito-}) a mitochondrial targeting sequence. Both adenoviruses were used at a MOI of 1:20. Cell number determined by optical density (OD) at 500nm. Data represented as % EGFP. *P < 0.05 versus EGFP. Values are means ± SEM; n=6.

Hsp60 knockdown does not affect cell proliferation in VSMCs treated with oxLDL

To further confirm whether Hsp60 plays a role in VSMC proliferation, Hsp60 expression was inhibited in rat VSMCs treated with oxLDL, and the expression of PCNA was evaluated. Intracellular Hsp60 levels were reduced using siRNA specific for Hsp60. Immunocytochemistry demonstrated that transfection of rat VSMCs with Hsp60 siRNA reduced Hsp60 staining as compared to control cells and cells transfected with a non-targeting siRNA pool (scrambled siRNA) (Figure 12). Quantification of images obtained through immunocytochemistry showed that Hsp60 siRNA significantly reduced Hsp60 protein expression compared to untreated control cells and scrambled siRNA transfected cells (Figure 13). Moreover, western blotting confirmed that transfection of rat VSMCs with Hsp60 siRNA significantly knocked down Hsp60 protein expression as compared to control and scrambled siRNA transfected cells (Figure 14). This reduction in Hsp60 levels was preserved in rat VSMCs transfected with Hsp60 siRNA that were subsequently treated with oxLDL for 6, 12, or 24 hours (Figures 14A, 14B, and 14C).
When Hsp60 expression was reduced through siRNA, oxLDL treatment for 6 hours had no effect on PCNA expression levels (Figure 15). In addition, this same 6 hour oxLDL treatment had no effect on PCNA levels in cells pre-treated with scrambled siRNA (Figure 15).

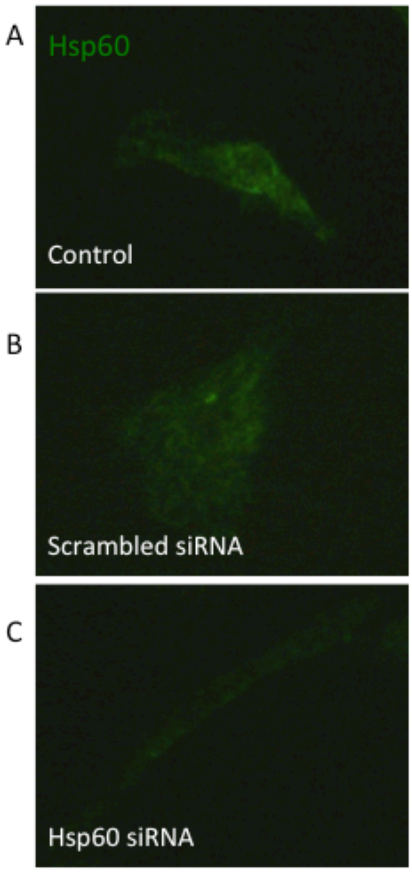

Figure 12. Cellular Hsp60 staining.

Representative immunocytochemistry images of Hsp60 expression (green). Rat VSMCs were treated with scrambled siRNA (B) or Hsp60 siRNA (C) for 48 hours. Control cells were incubated in identical medium without siRNA (A) for 48 hours.

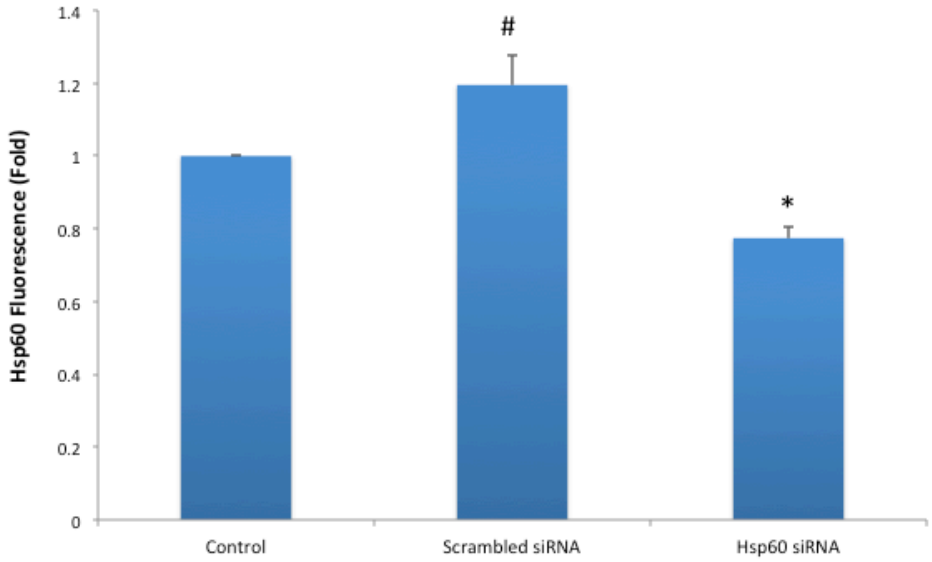

Figure 13. Intracellular Hsp60 expression is significantly reduced through transfection with Hsp60 siRNA.

Quantification of cellular Hsp60 staining. Rat VSMCs were treated with scrambled or Hsp60 siRNA for 48 hours. Control cells were incubated in identical medium without siRNA for 48 hours. Hsp60 expression is represented as fold change in fluorescence relative to control samples. The tissue from one rat aorta was used to generate enough VSMCs for 3 replicates of each treatment group. For each experimental replicate multiple fields were acquired. Each field contained 1-3 cells. The average fluorescence for a given treatment group was calculated from 14 total cells from the multiple fields acquired for each experimental replicate (n=14). Values are means ± SEM. *$P < 0.05$ versus control and scrambled siRNA; #$P < 0.05$ versus control.

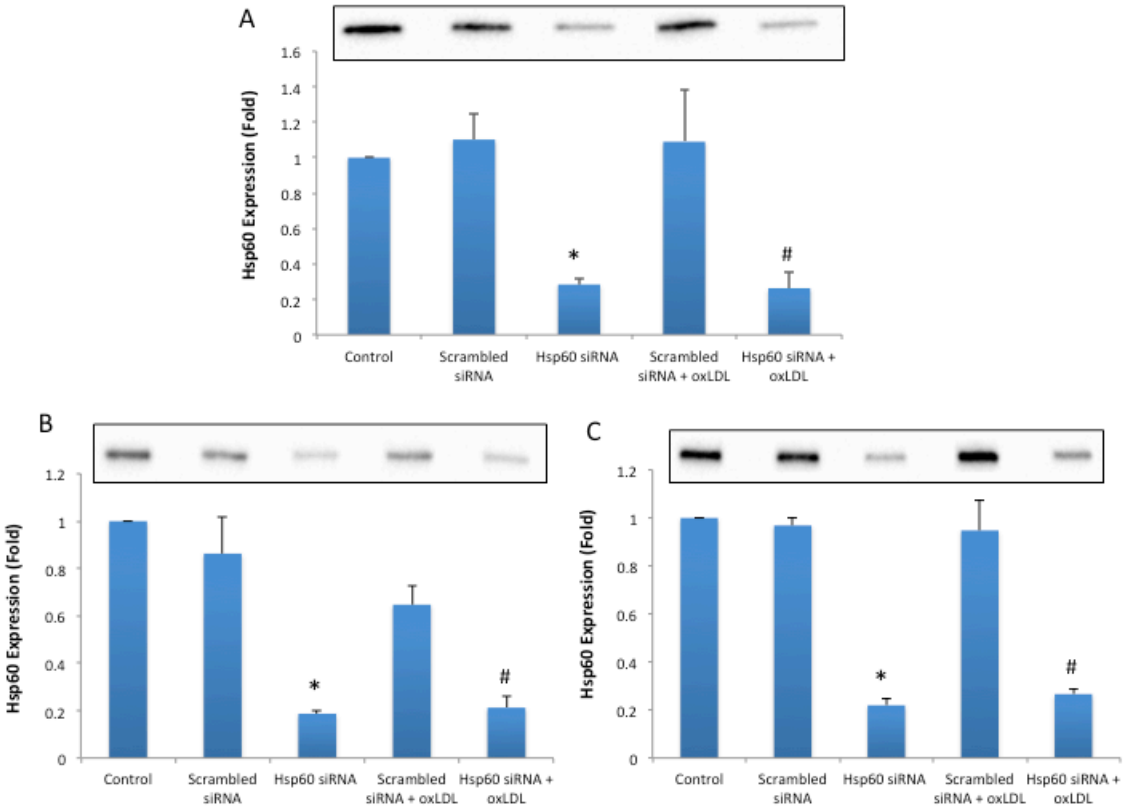

Figure 14. Hsp60 siRNA reduces Hsp60 expression with or without oxLDL treatment.

Western blot analysis and representative images of Hsp60 expression in rat VSMCs transfected with scrambled or Hsp60 siRNA with or without subsequent 50 μg/ml oxLDL treatment (scrambled siRNA + oxLDL, Hsp60 siRNA + oxLDL) for 6 hours (A), 12 hours (B), or 24 hours (C). Control cells were incubated in identical medium without siRNA and/or LDL. On each Western blot, Hsp60 protein band density was normalized by total protein loaded into each lane. Hsp60 expression is represented as fold change to control samples. Values are means ± SEM; n=3. *$P < 0.05$ versus control and scrambled siRNA. #$P < 0.05$ versus control and scrambled siRNA + oxLDL.

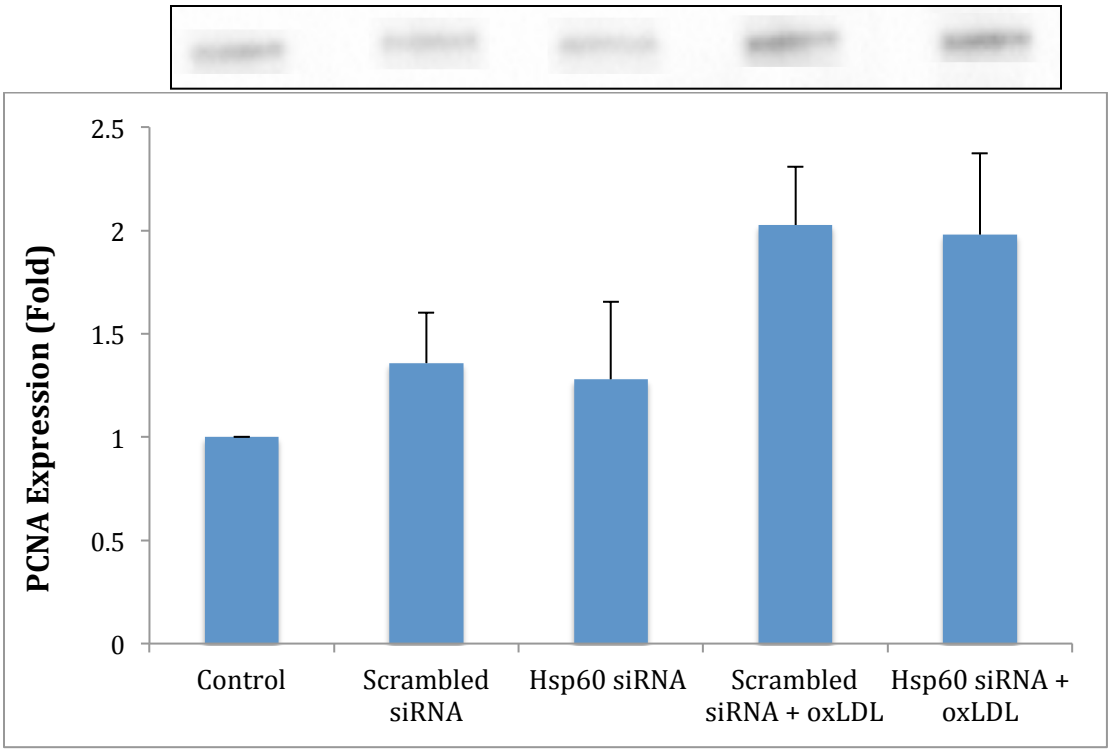

Figure 15. Hsp60 knockdown does not affect PCNA expression in oxLDL treated VSMCs.

Western blot analysis and representative image of PCNA expression in rat VSMCs transfected with scrambled or Hsp60 siRNA with or without subsequent 50µg/ml oxLDL treatment (scrambled siRNA + oxLDL, Hsp60 siRNA + oxLDL) for 6 hours. Control cells were incubated in identical medium without siRNA and/or LDL. On each Western blot, density of a specific protein band was normalized by total protein loaded into each lane. Protein expression is represented as fold change to control samples. Values are means ± SEM; n=3.

2. Involvement of Hsp60 in the modulation of nuclear protein import during stress-induced VSMC proliferation

If Hsp60 is involved in cell proliferation as demonstrated above, and if nuclear protein import is tightly associated with cell proliferation[101,339,343], then Hsp60 may modulate nuclear protein import. This was tested through assessment of nuclear protein import in VSMCs with altered levels of Hsp60.

Overexpression but not knockdown of Hsp60 alters NPI

To observe the effect of Hsp60 levels on nuclear protein import, NPI was measured in VSMCs where Hsp60 was overexpressed (adHsp60, adHsp60^{mito-}), knocked down (Hsp60 siRNA), or knocked down in the presence of oxLDL (Hsp60 siRNA + oxLDL). Both adHsp60 and adHsp60^{mito-} treated VSMCs showed significant increases in NPI compared to control cells and cells treated with scrambled siRNA, Hsp60 siRNA, or Hsp60 siRNA + oxLDL (Figures 16 and 17B). In VSMCs treated with Hsp60 siRNA, NPI was unchanged relative to control cells (Figures 16 and 17B). VSMCs exposed to oxLDL after pre-treatment with Hsp60 siRNA did not exhibit alterations in NPI compared to control cells (Figures 16 and 18B). In addition, VSMCs transfected with scrambled siRNA and then subjected to oxLDL did not demonstrate changes in NPI relative to control cells (Figures 16 and 18B).

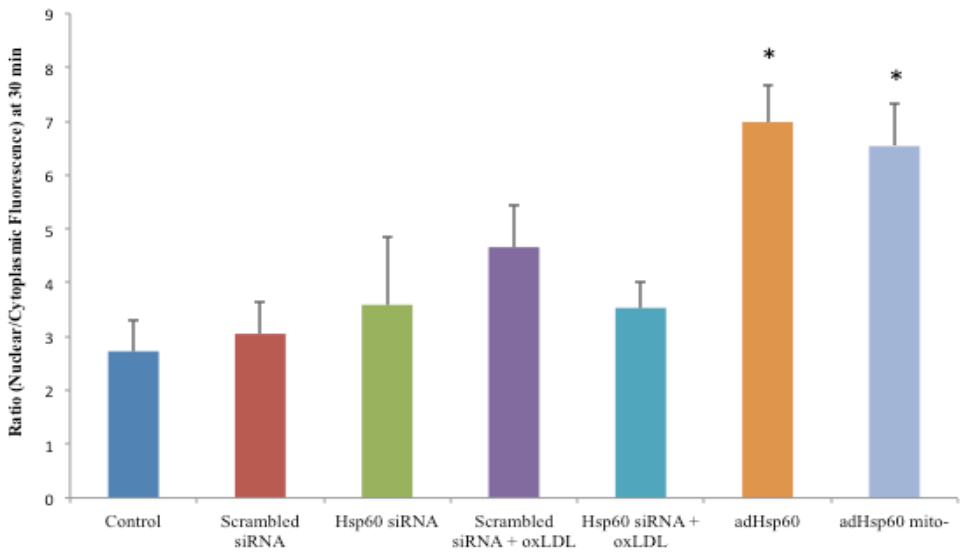

Figure 16. Knockdown of Hsp60 followed by oxLDL treatment has no effect on NPI whereas overexpression of Hsp60 stimulates NPI.

The graph represents the nuclear to cytoplasmic fluorescence 30 minutes after microinjection of ALEXA488-BSA-NLS substrate in: untreated (control) rat VSMCs (dark blue), rat VSMCs transfected with scrambled (red) or Hsp60 (green) siRNA, rat VSMCs treated with 50µg/ml oxLDL for 6 hours following transfection with scrambled (purple) or Hsp60 (teal) siRNA, and rabbit VSMCs transfected with human Hsp60 (adHsp60, orange) or human Hsp60 without a mitochondrial targeting sequence (adHsp60^{mito-}, light blue) at MOIs of 1:100-1:150. *$P < 0.05$ versus control, scrambled siRNA, Hsp60 siRNA, and Hsp60 siRNA + oxLDL. To calculate nuclear to cytoplasmic fluorescence for a given VSMC, the fluorescence of a nuclear area was divided by an equivalent cytosolic area adjacent to the nucleus. For each treatment group, the average nuclear/cytoplasmic fluorescence was determined from 3 to 10 VSMCs (n=3-10) depending on the treatment. These VSMCs were taken from multiple fields (1-2 cells/field) in 1 or more biological replicates of each experimental condition. Values are means ± SEM.

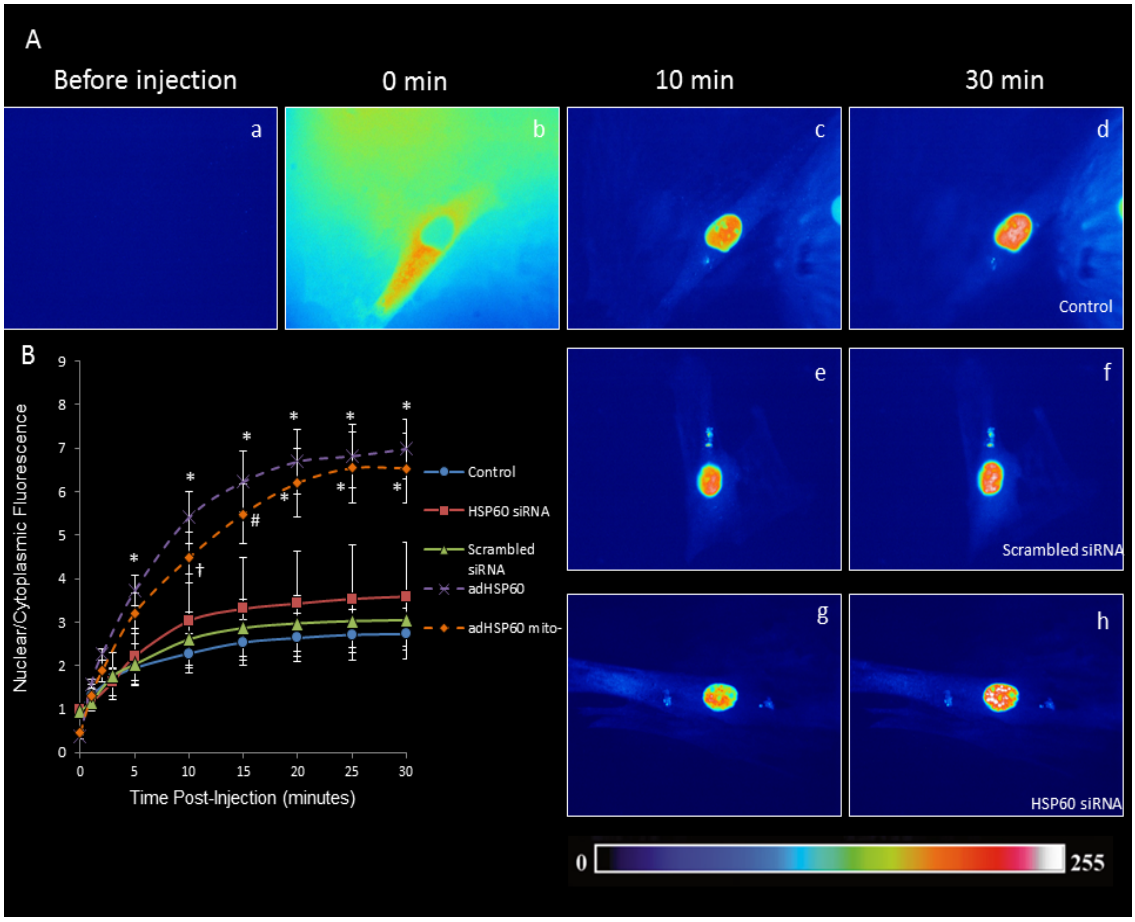

Figure 17. Effect of Hsp60 knockdown and Hsp60 over-expression on rate of NPI in VSMCs.

(A) Representative images of rat VSMCs microinjected with ALEXA488-BSA-NLS substrate following 48 hour siRNA transfection: scrambled siRNA (e-f), Hsp60 siRNA (g-h), or untreated (control) cells (a-d). Images were taken before injection (a), at injection (b), 10 min post-injection (c, e, g), and 30 min post-injection (d, f, h). The pseudo-colour scale represents level of fluorescence from 0 (black) to 255 arbitrary units (white). Laser scanning settings are the same for all cells and experiments. (B) The curve demonstrates NPI over time in control rat VSMCs (blue), rat VSMCs transfected with scrambled (green) or Hsp60 siRNA (red), and rabbit VSMCs transfected with human Hsp60 (adHsp60, purple) or human Hsp60 without a mitochondrial targeting sequence (adHsp60^{mito-}, orange). *P < 0.05 versus control, scrambled siRNA, and Hsp60 siRNA at that timepoint; #P < 0.05 versus control and scrambled siRNA at that timepoint; †P < 0.05 versus control at that timepoint. To calculate nuclear to cytoplasmic fluorescence for a given VSMC, the fluorescence of a nuclear area was divided by an equivalent cytosolic area adjacent to the nucleus. For each treatment group, the average nuclear/cytoplasmic fluorescence was determined from 4 to 10 VSMCs (n=4-10) depending on the treatment. These VSMCs were taken from multiple fields (1-2 cells/field) in 2 or more biological replicates of each experimental condition. Values are means ± SEM.

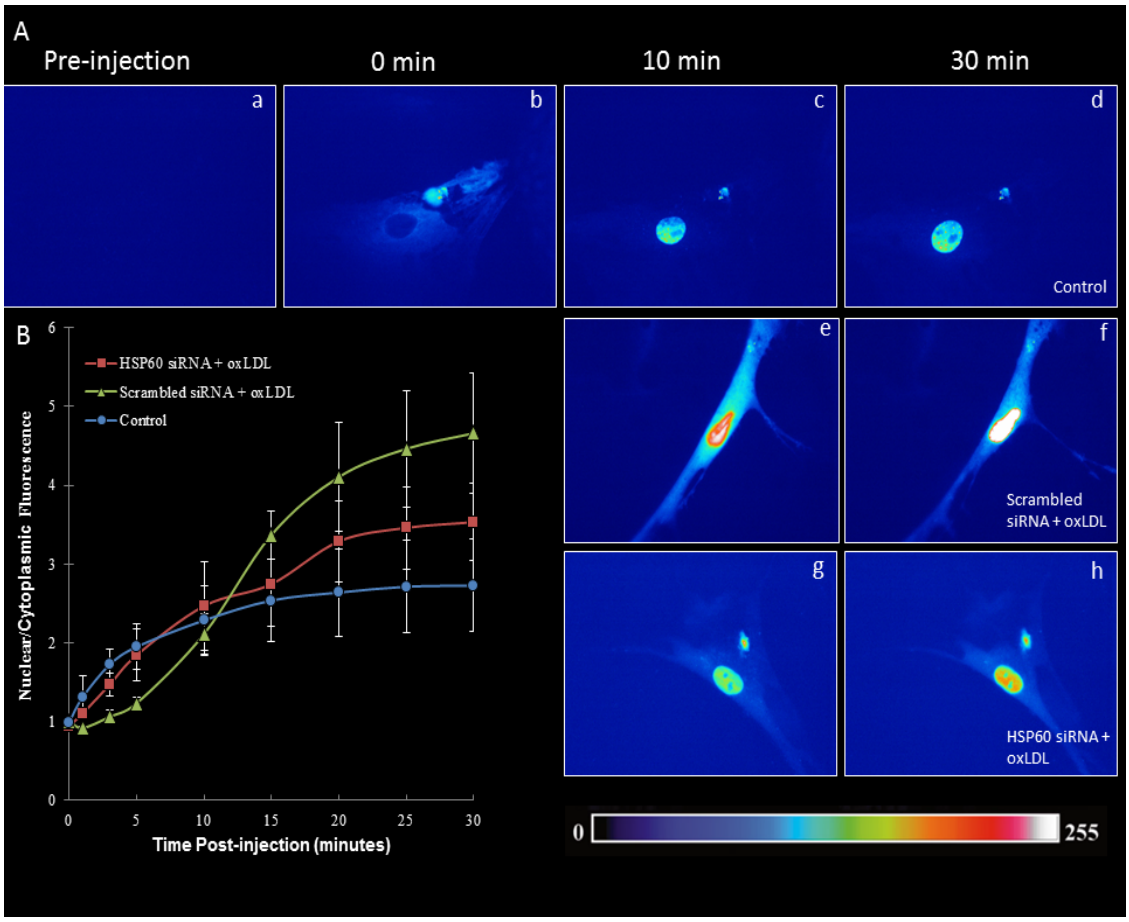

Figure 18. Effect of Hsp60 knockdown + oxLDL treatment on rate of NPI in VSMCs.

(A) Representative images of rat VSMCs microinjected with ALEXA488-BSA-NLS substrate after 48 hour siRNA transfection followed by 6 hour oxLDL treatment: untreated (control) cells (a-d), scrambled siRNA + oxLDL (e-f), Hsp60 siRNA + oxLDL (g-h). Images were taken before injection (a), at injection (b), 10 min post-injection (c, e, g), and 30 min post-injection (d, f, h). The pseudo-colour scale represents level of fluorescence from 0 (black) to 255 arbitrary units (white). Laser scanning settings are the same for all cells and experiments. (B) The curve demonstrates NPI over time in control rat VSMCs (red) and rat VSMCs treated with oxLDL following transfection with scrambled siRNA (scrambled siRNA + oxLDL, green) or Hsp60 siRNA (Hsp60 siRNA + oxLDL, blue). To calculate nuclear to cytoplasmic fluorescence for a given VSMC, the fluorescence of a nuclear area was divided by an equivalent cytosolic area adjacent to the nucleus. For each treatment group, the average nuclear/cytoplasmic fluorescence was determined from 3 to 5 VSMCs (n=3-5) depending on the treatment. These VSMCs were taken from multiple fields (1-2 cells/field) in 1 or more biological replicates of each experimental condition. Values are means ± SEM.

OxLDL stimulates expression of nucleoporins and nuclear transport receptors

To further understand how oxLDL affects NPI as part of VSMC proliferation, the expression of components of the nuclear import pathway was evaluated in rat VSMCs treated with oxLDL. OxLDL treatment at 25μg/ml for 6 hours significantly increased expression of NPC proteins, Nup62 (Figures 19A and 20A) and Nup153 (Figures 19B and 20C), relative to control and naLDL treated cells. This same oxLDL treatment significantly increased expression of nuclear transport receptors, Imp-α (Figures 19C and 21A) and Ran (Figures 19E and 22A), compared to control and naLDL treated cells. After 24 hours of oxLDL treatment at 25μg/ml, the expression of Nup62 (Figure 20B), Nup153 (Figure 20D), and Ran (Figure 22B) returned to baseline, while Imp-α (Figure 21B) remained significantly elevated relative to control. Interestingly, 50μg/ml oxLDL treatment for 6 hours resulted in a significant elevation of Imp-β relative to control and naLDL treated cells (Figure 21C). Both naLDL and oxLDL treatment at 50μg/ml for 6 hours stimulated significant increases in Nup62 expression versus control cells (Figure 20A). Thus, the effect of oxLDL treatment on nucleoporin and nuclear transport receptor expression was primarily observed after 6 hours at a concentration of 25μg/ml.

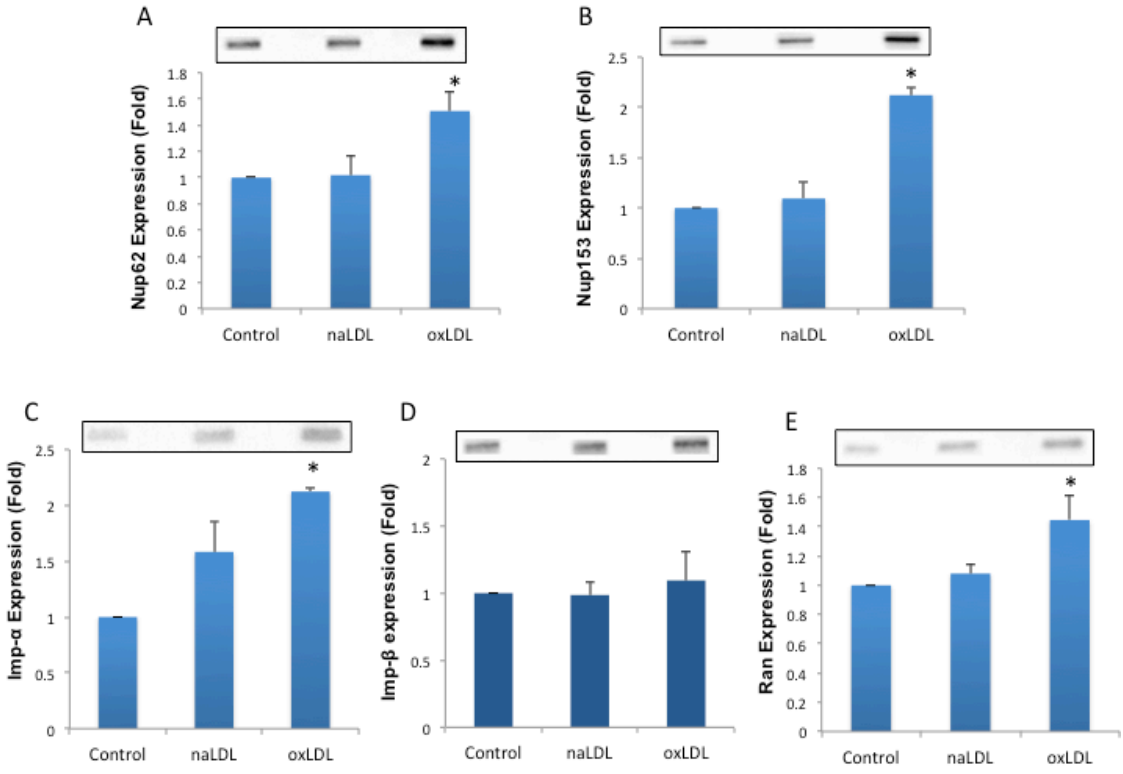

Figure 19. OxLDL treatment stimulates expression of nucleoporins and nuclear transport receptors.

Western blot analysis and representative images of nucleoporin (Nup62, A; Nup153, B) and nuclear transport receptor (Imp-α, C; Imp-β, D; Ran, E) expression in rat VSMCs treated with naLDL or oxLDL at 25μg/ml for 6 hours. On each western blot, density of a specific protein band was normalized by total protein loaded into each lane. Normalized protein expression is represented as fold change to control samples. The values in each graph represent the means ± SEM of three independent experimental repeats (n=3) from the same primary rat aorta explant. *$P < 0.05$ versus control and naLDL.

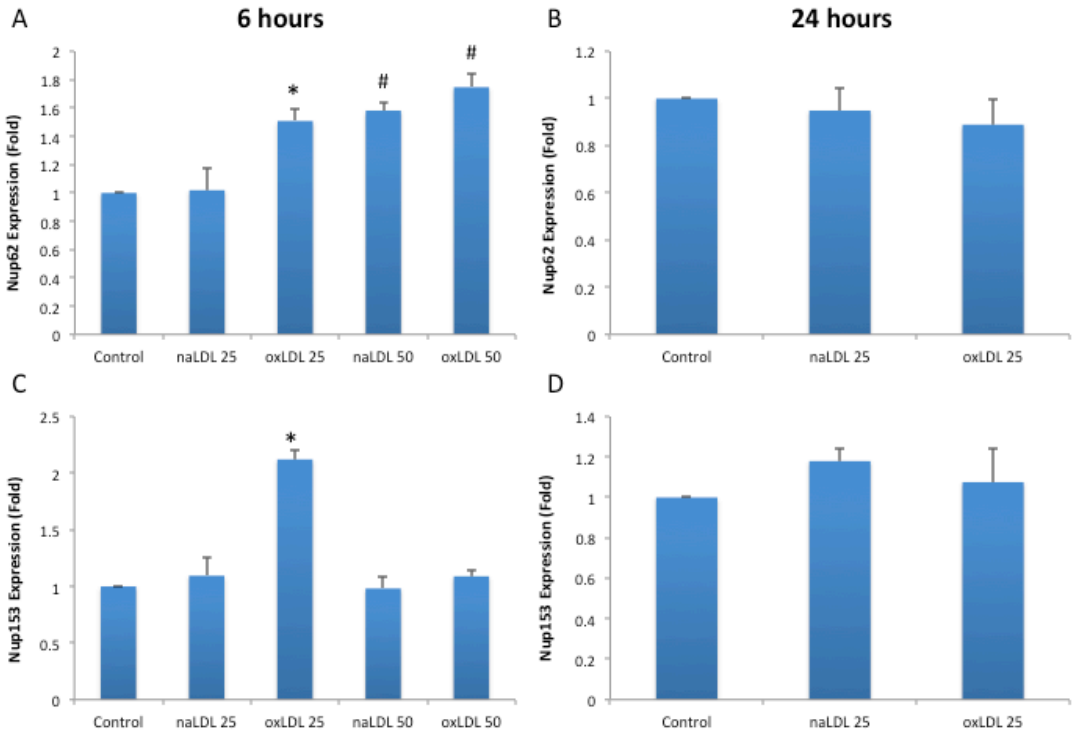

Figure 20. Effect of oxLDL treatment for 6 or 24 hours on nucleoporin expression.

Western blot analysis of nucleoporin expression (Nup62, A & B; Nup153, C & D) in rat VSMCs treated with naLDL or oxLDL at 25 or 50 µg/ml for 6 hours (A, C) or 25µg/ml for 24 hours (B, D). On each Western blot, density of a specific protein band was normalized by total protein loaded into each lane. Normalized protein expression is represented as fold change to control samples. Values are means ± SEM; n=3. *$P < 0.05$ versus 6 hour control and naLDL at 25µg/ml for 6 hours. #$P < 0.05$ versus 6 hour control.

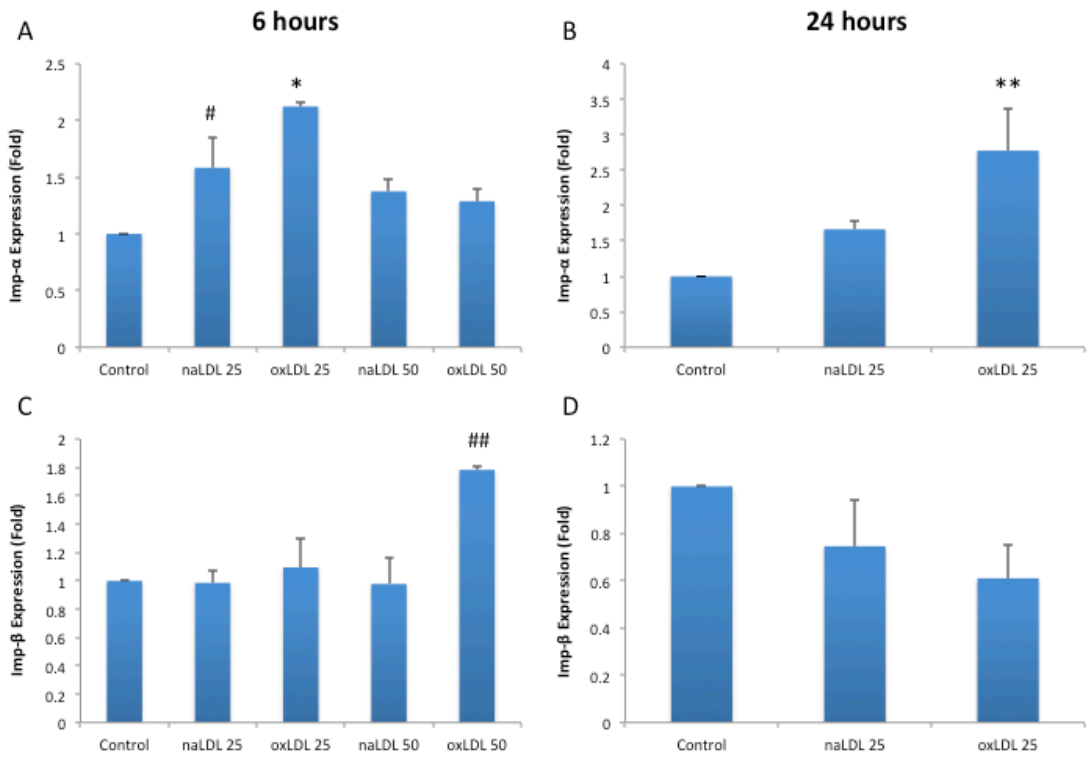

Figure 21. Effect of oxLDL treatment for 6 or 24 hours on importin expression.

Western blot analysis of importin expression (Imp-α, A & B; Imp-β, C & D) expression in rat VSMCs treated with naLDL or oxLDL at 25 or 50 μg/ml for 6 hours (A, C) or 25μg/ml for 24 hours (B, D). On each Western blot, density of a specific protein band was normalized by total protein loaded into each lane. Normalized protein expression is represented as fold change to control samples. Values are means ± SEM; n=3. *$P < 0.05$ versus 6 hour control and naLDL at 25μg/ml for 6 hours. #$P < 0.05$ versus 6 hour control. **$P < 0.05$ versus 24 hour control. ##$P < 0.05$ versus 6 hour control and naLDL at 50μg/ml for 6 hours.

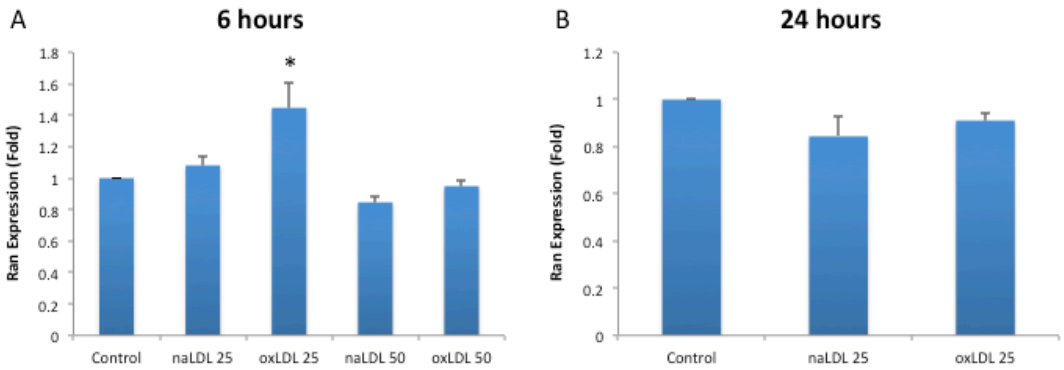

Figure 22. Effect of oxLDL treatment for 6 or 24 hours on Ran expression.

Western blot analysis of Ran expression (A, B) in rat VSMCs treated with naLDL or oxLDL at 25 or 50 μg/ml for 6 hours (A) or 25μg/ml for 24 hours (B). On each Western blot, density of a specific protein band was normalized by total protein loaded into each lane. Normalized protein expression is represented as fold change to control samples. Values are means ± SEM; n=3. *$P < 0.05$ versus 6 hour control and naLDL at 25μg/ml for 6 hours.

Hsp60 knockdown does not change nucleoporin and nuclear transport receptor expression in VSMCs treated with oxLDL

Previous work showed that oxLDL treatment of VSMCs significantly increased NPI[29]. We demonstrated that oxLDL treatment increased expression of nucleoporins and nuclear transport receptors (Figure 19). Thus, an inhibition of Hsp60 expression in the presence of oxLDL treatment would be hypothesized to block these effects. Figure 18 demonstrated that Hsp60 knockdown followed by oxLDL treatment did not change the rate of NPI relative to controls. Table 1 shows that Hsp60 knockdown followed by oxLDL treatment for 6 hours produced no significant changes in the expression of nuclear pore proteins (Nup62, Nup153) and nuclear transport receptors (Imp-α, Imp-β, Ran).

Table 1. OxLDL treatment in the presence of Hsp60 knockdown does not change expression of nuclear transport receptors or nucleoporins.
Western blot analysis of nuclear transport receptor (Ran, Imp-α, and Imp-β), and nucleoporin (Nup62 and Nup153) expression in rat VSMCs transfected with scrambled or Hsp60 siRNA with or without subsequent 50μg/ml oxLDL treatment (scrambled siRNA + oxLDL, Hsp60 siRNA + oxLDL) for 6 hours. Control cells were incubated in identical medium without siRNA and/or LDL. On each Western blot, density of a specific protein band was normalized by total protein loaded into each lane. Protein expression is represented as fold change to control samples. Values are means ± SEM); n=3.

		Treatment Group (Fold vs. Control)		
Protein	**Scrambled siRNA**	**Hsp60 siRNA**	**Scrambled siRNA + oxLDL**	**Hsp60 siRNA + oxLDL**
Ran	1.47 ± 0.44	1.26 ± 0.22	1.07 ± 0.13	0.80 ± 0.22
Imp-α	1.06 ± 0.16	1.33 ± 0.17	1.73 ± 0.68	1.73 ± 0.88
Imp-β	1.23 ± 0.24	1.65 ± 0.53	2.74 ± 0.51	2.37 ± 0.69
Nup62	1.03 ± 0.20	1.03 ± 0.42	1.14 ± 0.08	1.05 ± 0.12
Nup153	1.22 ± 0.16	1.84 ± 0.24	1.16 ± 0.36	0.98 ± 0.22

Induction of Hsp60 promotes interaction with Ran

Co-immunoprecipitation was used to determine whether Hsp60 interacted with cytosolic nuclear transport proteins to regulate NPI under stress conditions. Rat VSMCs were subjected to heat shock to induce Hsp60 expression. Hsp60 was co-immunoprecipitated with Ran under either untreated control conditions or after heat shock (Figure 23A). The relative amount of Hsp60 and Ran complexes was greater in heat shocked cells than control cells (Figure 23A). Importantly, Hsp60 was not co-immunoprecipitated with other nuclear transport proteins, Imp-α or Imp-β (Figure 23A). To confirm if increases in Hsp60 levels directly promotes its interaction with Ran, rat VSMCs were transfected with human Hsp60 with or without a mitochondrial targeting sequence (adHsp60 and adHsp60^{mito-}). In this experiment Hsp60 was not co-immunoprecipitated with Ran in control or EGFP treated cells (Figure 23B). Both adHsp60 and adHsp60^{mito-} treatment stimulated Hsp60 co-immunoprecipitation with Ran (Figure 23B). In addition, overexpression of cytosolic Hsp60 (adHsp60^{mito-}) resulted in an increased amount of Hsp60 and Ran complexes relative to adHsp60 treated cells (Figure 23B).

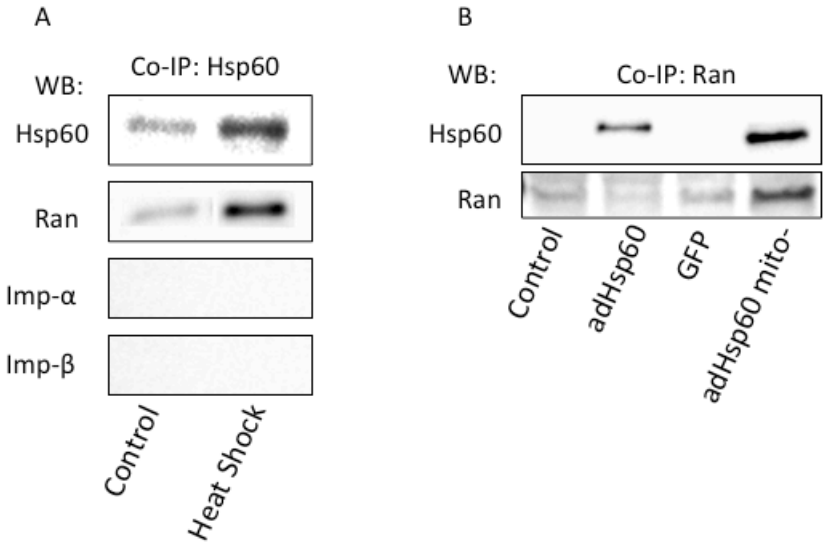

Figure 23. Heat shock treatment and Hsp60 overexpression promote interaction of Ran with Hsp60

(A) Co-immunoprecipitation was performed with Hsp60 antibody conjugated to Pierce Protein A/G coated beads. Rat VSMCs were heat shocked at 42 degrees Celsius for 1 hour and then were collected for co-immunoprecipitation after 48 hours. Western blot analysis was done for nuclear transport receptors (Ran, Imp-α, and Imp-β) and Hsp60. Ran was the only nuclear transport receptor co-immunoprecipitated with Hsp60. (B) Co-immunoprecipitation was performed with Ran antibody conjugated to Pierce Protein A/G coated beads. Rat VSMCs were transfected with green fluorescent protein (GFP) or Hsp60 with (adHsp60) or without a mitochondrial targeting sequence (adHsp60^{mito-}) for 48 hours. A MOI of 1:125 was used for GFP and adHsp60, whereas a MOI of 1:200 was used for adHsp60^{mito-}. Western blot analysis was done for Hsp60 and Ran. Hsp60 was co-immunoprecipitated with Ran.

3. Expression and relationship of Hsp60, NPI-associated proteins, and PCNA during atherosclerotic development

Dietary cholesterol withdrawal induces atherosclerotic plaque development

We have previously shown that prolonged cholesterol withdrawal produces an atherosclerotic model in rabbits[357]. Male New Zealand white rabbits were fed a high cholesterol diet for 4 weeks and then switched to regular rabbit chow for 0, 2, 4, 8, 16, 22, or 28 weeks prior to termination. This dietary course induces rapid growth of atherosclerotic plaques 0-8 weeks after cholesterol withdrawal followed by stabilization of plaque growth from 8-28 weeks after cholesterol withdrawal (Figure 24).

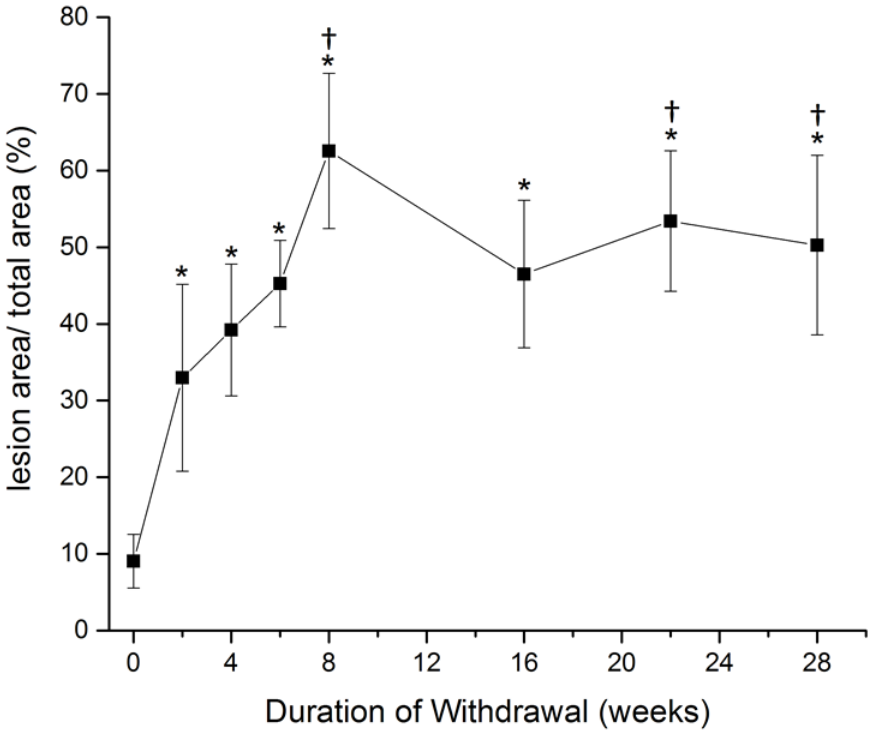

Figure 24. Progression and plateau of aortic atherosclerotic lesions after prolonged withdrawal from cholesterol feeding

Rabbits were fed a high-cholesterol diet for 4 weeks and then switched onto a regular diet for 0, 2, 4, 8, 16, 22, or 28 weeks. The graph represents the percentage of aortic lumenal area covered by atherosclerotic lesions as a function of withdrawal time from a 4 week high-cholesterol diet. Values are means ± SEM; n=7-10. *$P < 0.05$ versus animals fed regular diet for 4 week duration (no plaques present); †$P < 0.05$ versus 0 weeks of diet withdrawal. Reproduced from *Am J Physiol Heart Circ Physiol,* AA Francis, JF Deniset, JA Austria, RK LaVallee, GG Maddaford, TE Hedley, E Dibrov, GN Pierce. Effects of dietary flaxseed on atherosclerotic plaque regression, 304(12):H1743-51, 2013.

Atherosclerotic plaque development alters the proliferative status of cells in aortic tissue

The proliferative status of aortic cells during atherosclerotic development was evaluated using a marker of cell proliferation, PCNA. PCNA levels were significantly elevated during atherosclerotic plaque growth from 0-8 weeks followed by a return to baseline at 22 weeks of cholesterol withdrawal during plaque stabilization (Figure 25).

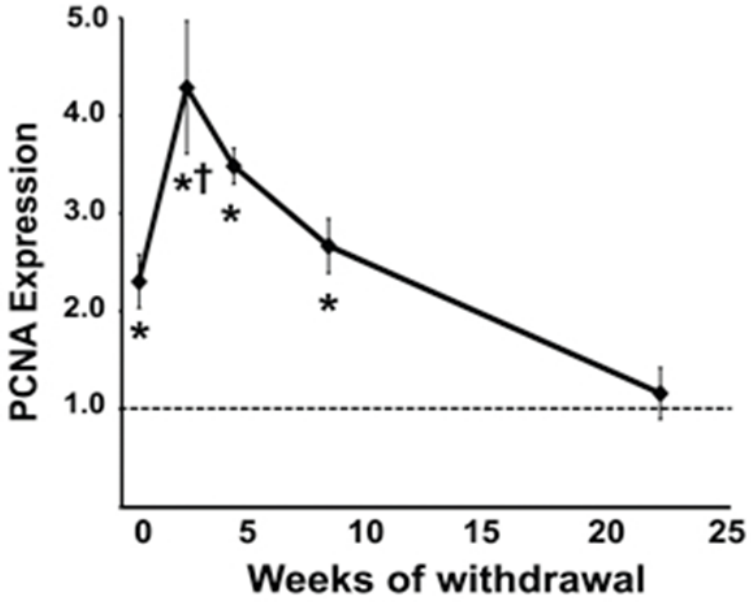

Figure 25. Expression of PCNA in rabbit aortic tissue during atherosclerotic development.

Western blot analysis of PCNA expression after 0, 2, 4, 8, and 22 weeks of withdrawal from cholesterol feeding. Protein expression levels are normalized to total actin and are represented as fold change to control samples. Values are means ± SEM, n=3-4. *$P < 0.05$ versus 22 weeks of cholesterol withdrawal; †$P < 0.05$ versus 8 weeks of cholesterol withdrawal. Re-used with permission from Deniset, JF. *The Role of Chlamydia Pneumoniae Infection and Stress Responses in Vascular Remodelling.* 2013, University of Manitoba.

Atherosclerotic plaque development induces alterations in expression of Hsps and NPI machinery

Hsps 60, 70, and 90 had differential expression patterns during atherosclerotic progression in this model (Figure 26). Hsp60 expression was induced during the growth phase, with significantly elevated levels at 2 and 4 weeks of cholesterol withdrawal relative to 8 and 22 weeks (Figure 26A). Conversely, Hsp70 and Hsp90 both demonstrated decreased expression during the growth phase (Figures 26B and 26C). Hsp70 expression was significantly decreased at 4-weeks of cholesterol withdrawal compared to 22 weeks (Figure 26B). Hsp90 expression was significantly depressed at 2 and 4 weeks of cholesterol withdrawal versus 22 weeks (Figure 26C). However, Hsp90 expression spiked at 8 weeks, with significant elevation relative to 0, 2, and 4 weeks (Figure 26C). During the stabilization phase (8-22 weeks after cholesterol withdrawal), Hsps 60, 70, and 90 expression normalized to control levels (Figure 26).

The expression of NPI-associated proteins (Nup62, Imp-β, and Ran) also followed distinct patterns during the growth phase in this model of atherosclerosis (Figure 27). Nup62 expression was significantly elevated at 2 weeks of cholesterol withdrawal relative to 22 weeks (Figure 27A). Nup62 then reached maximal levels at 4 weeks of cholesterol withdrawal, with significant elevation compared to 8 and 22 weeks (Figure 27A). In contrast, Imp-β and Ran expression remained at control levels at 0-4 weeks of cholesterol withdrawal and then spiked to maximal levels at 8 weeks (Figures 27B and 27C). At 8 weeks of cholesterol withdrawal, Ran, but not Imp-β levels were significantly increased compared to 0, 2, and 4 weeks of

cholesterol withdrawal (Figures 27B and 27C). Similar to Hsps, expression of proteins associated with NPI normalized to control levels during the stabilization phase of atherosclerosis (8-22 weeks of cholesterol withdrawal) (Figure 27).

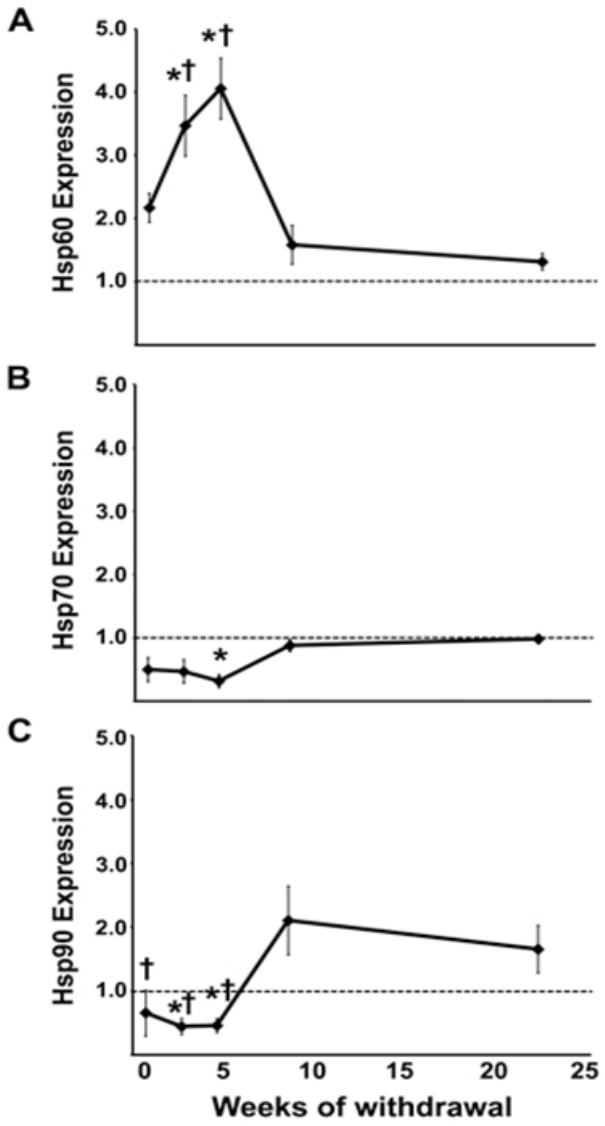

Figure 26. Expression of Hsps in rabbit aortic tissue during atherosclerotic development.

Western blot analysis of Hsp60 (A), Hsp70 (B), and Hsp90 (C) expression after 0, 2, 4, 8, and 22 weeks of withdrawal from cholesterol feeding. Protein expression levels are normalized to total actin and are represented as fold change to control samples. Values are means ± SEM), n=3-4. **P* < 0.05 versus 22 wks of cholesterol withdrawal; †*P* < 0.05 vs. 8 wks of cholesterol withdrawal. Re-used with permission from Deniset, JF. *The Role of Chlamydia Pneumoniae Infection and Stress Responses in Vascular Remodelling.* 2013, University of Manitoba.

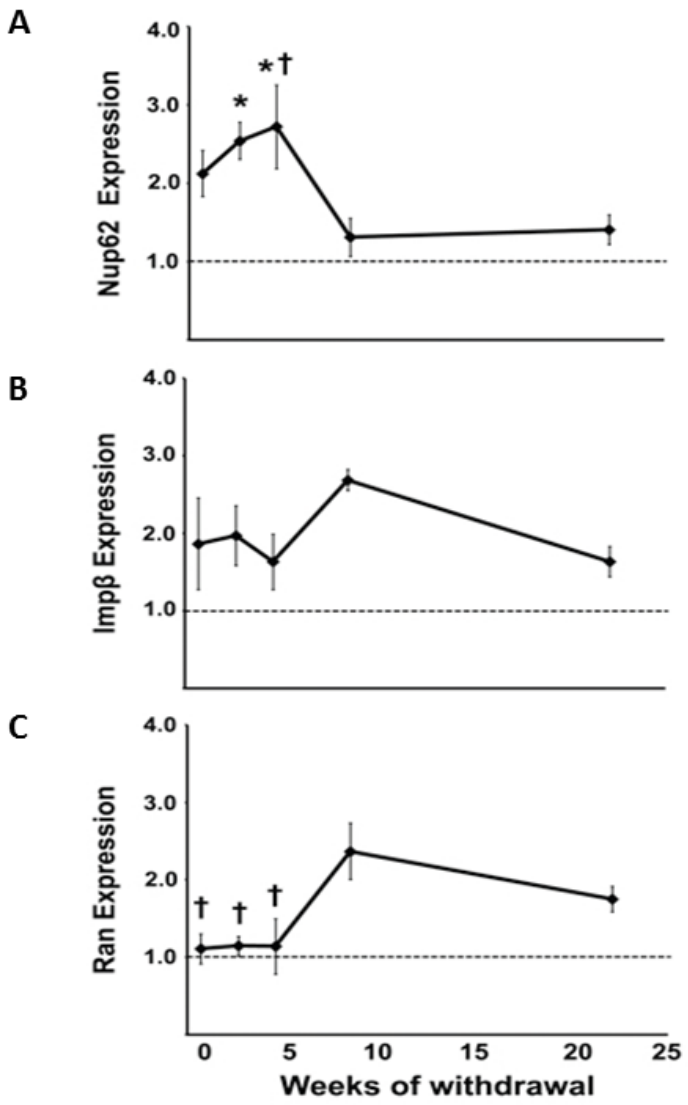

Figure 27. Expression of NPI machinery in rabbit aortic tissue during atherosclerotic development

Western blot analysis of Nup62 (A), Imp-β (B), and Ran (C) expression after 0, 2, 4, 8, and 22 weeks of withdrawal from cholesterol feeding. Protein expression levels are normalized to total actin and are represented as fold change versus control samples. Values are means ± SEM, n=3-4. **P* < 0.05 versus 22 weeks of cholesterol withdrawal; †*P* < 0.05 versus 8 weeks of cholesterol withdrawal. Re-used with permission from Deniset, JF. *The Role of Chlamydia Pneumoniae Infection and Stress Responses in Vascular Remodelling.* 2013, University of Manitoba.

Aortic levels of Hsp60 correlate with PCNA and Nup62 expression

To assess the relationship between Hsp60, nuclear transport proteins, and the proliferative status during atherosclerotic development, correlation analysis was performed. Since Nup62 and PCNA exhibited a similar expression pattern to Hsp60 over the entire cholesterol withdrawal period, correlation analysis was done using Hsp60 and these parameters (Figure 28). Hsp60 expression displayed a strong positive correlation with both PCNA and Nup62 expression ($r^2 = 0.3027$ and $r^2 = 0.3164$, $p < 0.01$) (Figures 28A and 28B).

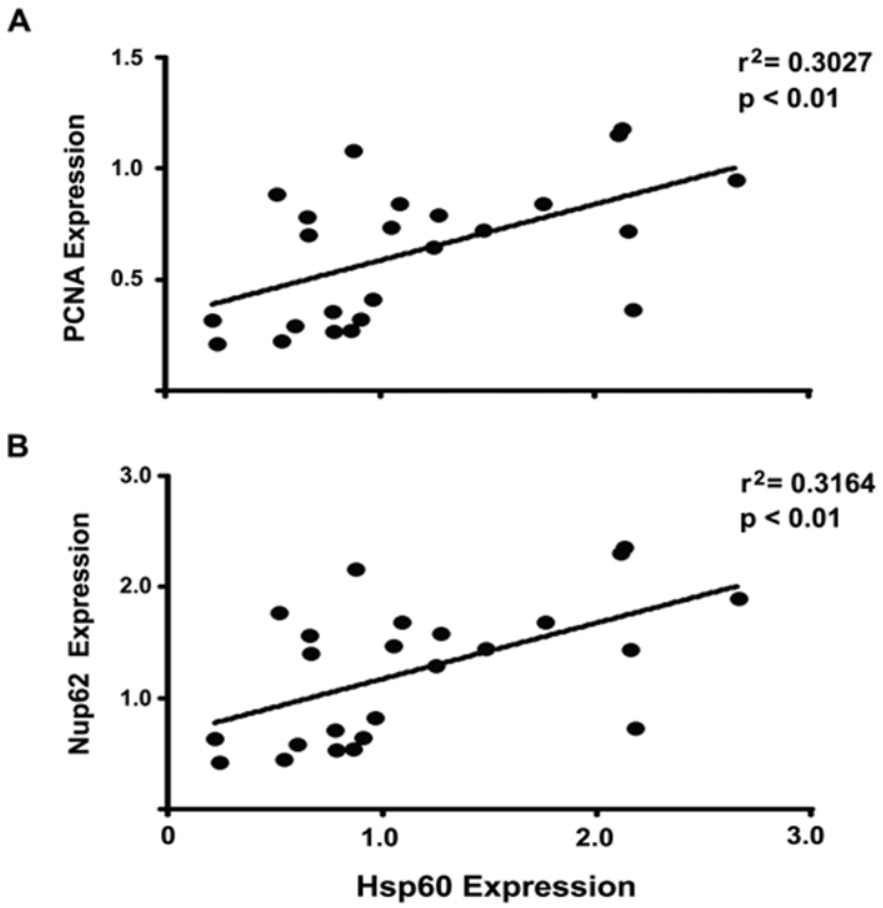

Figure 28. Correlations of aortic Hsp60 levels with Nup62 and PCNA levels

Relationship between Hsp60 and PCNA (A), and between Hsp60 and Nup62 (B) in rabbit aortic tissue. Re-used with permission from Deniset, JF. *The Role of Chlamydia Pneumoniae Infection and Stress Responses in Vascular Remodelling.* 2013, University of Manitoba.

CHAPTER VI: DISCUSSION

1. Involvement of Hsp60 in the modulation of NPI during stress-induced VSMC proliferation

Under baseline conditions endogenous Hsp60 is distributed between the mitochondria and the cytosol, with the majority (80-85%) functioning in the mitochondria[168–170]. When cells are exposed to stress stimuli, Hsp60 localizes to the cytoplasm[171]. We demonstrated that overexpression of cytosolic Hsp60 was sufficient to stimulate VSMC proliferation (Figure 11). One potential mechanism by which cytosolic Hsp60 stimulates VSMC proliferation is through inhibitory interactions with pro-apoptotic mediators[359,360]. Our results showed that in response to a stress stimulus (oxLDL at 25 μg/ml), there was an acute spike in Hsp60 followed by a modest but significant increase in cell number (Figures 6 and 7). Thus, acute elevation of Hsp60 levels in response to stress may allow this protein to promote survival and growth through inhibition of pro-apoptotic mediators.

Alternatively, previous work in our lab showed that increases in NPI are associated increased cellular proliferation[27,29,101,343]. However, it was incompletely understood how stress-related changes in NPI were mediated during VSMC proliferation and if Hsp60 was involved or not. This current study was the first to show that Hsp60 is a positive regulator of NPI. Elevated levels of Hsp60 were sufficient to increase NPI, whereas reduced levels of Hsp60 had no effect on NPI relative to controls (Figures 16 and 17). Therefore, Hsp60 can increase NPI at high intracellular levels but is not required for NPI at baseline.

NPI can be regulated by a number of mechanisms including modulation of the expression levels and localization of NPI-associated proteins[328,336,337,345,347]. During stress conditions, Hsp60 induction coincides with the increased expression of nucleoporins[27,29,101]. This study demonstrated that stress-mediated Hsp60 induction correlated with the increased expression of nucleoporins (i.e. Nup62 and Nup153) and nuclear transport receptors (i.e. Imp-α, Ran) (Figure 7B, Figure 19). Hsp60 can participate in the regulation of cell signalling pathways through post-translational modification[361]. This suggests that Hsp60 plays a signalling role to increase the expression of nucleoporins and nuclear transport receptors.

We also demonstrated that at high intracellular levels, Hsp60 interacted with cytosolic Ran (Figure 23). Hsp60 functions as a molecular chaperone that can mediate intracellular trafficking of its client proteins[362]. Other heat shock proteins have the capacity to shuttle NPI-associated proteins across the nuclear envelope to regulate their localization[363]. This collectively suggests that Hsp60 interacts with cytosolic Ran (i.e. Ran-GDP) to assist with its recycling back to the nucleus and thereby facilitate NPI.

The concept of Ran re-localization to mediate changes in NPI has been previously demonstrated[345]. Czubryt *et al.* showed that NPI was inhibited through re-localization of Ran to the cytosol in hydrogen peroxide-treated VSMCs[345]. As Ran-GTP and Ran-GDP gradients provide energy for NPI[247], redistribution of GTP or GDP-bound forms of Ran can alter nuclear import. More efficient shuttling of Ran-GDP into the nucleus through interactions with Hsp60 would lead to a larger pool of

nuclear Ran-GTP through the action of RanGEF. This would increase the Ran-GTP concentration gradient and thereby increase the capacity of the cell for NPI.

Thus, high levels of Hsp60 can mediate increases in NPI by inducing augmented expression of NPI-associated proteins and through interaction with Ran. Previous studies have suggested that endogenous Hsp60 mediates SMC migration and proliferation through an extracellular mechanism[108,176]. The findings in this study support the contention that endogenous Hsp60 additionally plays an intracellular signalling and chaperoning role to mediate increases in NPI as part of VSMC proliferation.

On a technical note, doses of 25 and 50μg/ml of oxLDL were chosen in the cell titer assay (Figure 6) as previous studies in rabbit VSMCs showed that an oxLDL dose of 50μg/ml increased cell number by approximately 20%, while 25μg/ml increased cell number by approximately 10%[29]. When cell titer was assessed in rat VSMCs, there was a significant rise in VSMC number versus control cells in response to 25μg/ml oxLDL, whereas a concentration of 50μg/ml did not show any significant changes relative to control cells (Figure 6). Specifically, 25μg/ml oxLDL treatment resulted in 10% more VSMCs than control cells, while the VSMC number was 7% higher than control cells with 50μg/ml oxLDL treatment (Figure 6). This is a narrow window for the effect of oxLDL on cell proliferation. Previous *in vitro* work suggests that oxLDL can either cause cell proliferation[26,27,29] or apoptosis[32,364]. Therefore a lower concentration of oxLDL stimulates proliferation, while a higher concentration of oxLDL is toxic and induces apoptosis[365].

2. Expression and relationship of Hsp60, NPI-associated proteins, and PCNA during atherosclerotic development

The role of Hsp60 in modulating components of NPI and cell proliferation during plaque development was investigated. Although various Hsps are considered pro-atherogenic[208], *in vivo* and clinical studies show that Hsp60 is the only Hsp with a direct role in atherosclerosis[209]. Hsp60 is found in VSMCs within atherosclerotic lesions[210], however, it's relation to cell proliferation and NPI parameters *in vivo* is unknown. Thus, expression of Hsp60, NPI-associated proteins, and a cellular proliferation marker was studied in a rabbit model employing a cholesterol withdrawal diet that induced atherosclerotic plaque growth and stabilization (Figure 24). There were elevated levels of PCNA, Hsp60, and NPI-associated proteins (Ran, Imp-β, Nup62) during plaque growth, which returned to baseline during plaque stabilization (Figures 25-27). Furthermore, during plaque growth Hsp60 and Nup62 followed similar expression patterns (Figures 26 and 27). Correlation analysis revealed strong associations between Hsp60 and Nup62 levels (Figure 26B) as well as between Hsp60 and PCNA levels (Figure 26A). Previous *in vitro* work demonstrated this same strong positive correlation between Hsp60 and Nup62 levels as well as Hsp60 and PCNA levels[27].

Other heat shock proteins, Hsp70 and Hsp90, were also measured throughout development of the atherosclerotic plaques. The expression of both these Hsps decreased below baseline levels during plaque growth (Figure 26). This further suggests that changes in NPI parameters and the proliferative status during plaque growth were Hsp60-dependent and did not involve other Hsps. In addition,

the differential expression pattern of Hsp60 compared to Hsp70 and Hsp90 (Figure 26) suggests that Hsf1 did not regulate Hsp60 induction during plaque growth. Normally Hsf1 mediates increases in expression of Hsp60, Hsp70, and Hsp90 in response to various stress stimuli[116].

NFκB, a transcriptional mediator activated by oxLDL during atherosclerosis[38], can stimulate Hsp60 expression[204]. It is possible that NFκB, oxLDL and many other factors *in vivo* may play a role in the alterations in Hsp60, NPI-associated proteins, PCNA and, ultimately, VSMC proliferation. This study provides *in vivo* evidence that Hsp60 is involved in atherosclerotic plaque development through alteration of NPI machinery and proliferative status.

Limitations

Although these experiments demonstrate novel findings on the role of Hsp60 in VSMC proliferation and atherosclerotic development, they must be interpreted with caution. One of the major flaws in the experimental design was the concentration of oxLDL used in the experiments where NPI and the expression of Hsp60, PCNA, and NPI-associated proteins were measured in VSMCs treated with Hsp60 siRNA then oxLDL (Figures 14, 15, 16, 18 and Table 1). In all of these experiments an oxLDL concentration of 50 μg/ml was used. This was the incorrect dose to use because initial experiments showed that oxLDL stimulated cell proliferation, Hsp60 induction, and increased expression of NPI-associated proteins at a concentration of 25μg/ml, but not 50 μg/ml (Figures 6, 7 and 19).

The use of a non-proliferative dose of oxLDL (50 μg/ml) explains the lack of response to oxLDL in the scrambled siRNA + oxLDL treatment groups in the NPI

assay (Figures 16 and 18) and in the measurement of Hsp60 (Figure 14) and NPI-associated protein expression (Table 1). For example, VSMCs treated with scrambled siRNA and then 50μg/ml of oxLDL did not exhibit an increased rate of NPI versus controls (Figures 16 and 18), despite previous work which showed that oxLDL treatment increased NPI[29]. In addition, VSMCs treated with scrambled siRNA followed by 50μg/ml oxLDL treatment did not demonstrate a significant rise in Hsp60 or any of the NPI-associated proteins (Figure 14 and Table 1).

Another limitation was that a MTT assay was used to evaluate cell proliferation (Figures 6 and 11). In this assay, cell number is quantified in response to treatment and differences are noted relative to untreated controls. The difficulty, however, is that this assay measures cell number but not how cells become that number. For example, we assumed that an increased cell number in response to oxLDL treatment meant cell proliferation (Figure 6). An alternative explanation for increased cell number in response to treatment could be less cell death relative to control cells. Hence, to further evaluate cell proliferation, PCNA expression levels were measured in VSMCs.

Interestingly, VSMCs treated with a proliferative dose of oxLDL (25μg/ml) (Figure 6) did not exhibit significantly increased PCNA expression after 6 or 24 hours versus control cells (Figures 7 and 8). Although these results are discordant with previous studies in rabbit VSMCs, which showed that significant increases in cell number corresponded to significant increases in PCNA expression[29], they do show a trend in PCNA expression towards significant elevation. This suggests that

increasing the number of biological repeats in these experiments may yield significant increases in PCNA in response to oxLDL at 25μg/ml.

CHAPTER VII: CONCLUSION AND FUTURE DIRECTIONS

Conclusion

Previous work showed that various atherogenic stimuli (i.e. oxLDL, mechanical stretch, and *Chlamydia pneumoniae*) can induce Hsp60 and/or stimulate NPI to lead to VSMC proliferation[26,27,29,101]. We demonstrated that at high levels Hsp60 stimulated an increased rate of NPI, was correlated with increased nucleoporin and nuclear transport receptor expression, and associated with Ran. Therefore, we conclude that Hsp60 may be directly involved in augmenting NPI as part of the mechanism of stress-induced VSMC proliferation.

Hsp60 has been implicated in the pathogenesis of atherosclerosis[209], however the intracellular mechanism by which Hsp60 influences atherosclerosis is not well characterized. We demonstrated that Hsp60 levels were related to the expression of nucleoporins and a cell proliferation marker during atherosclerotic plaque growth. Hence, we conclude that Hsp60 may be involved in atherosclerotic plaque development through alteration of NPI machinery and proliferative status.

These results suggest that Hsp60 may function as a common downstream regulator of VSMC proliferation during atherosclerotic development. Instead of targeting individual stress stimuli, targeting Hsp60, the regulator of a common cellular process (i.e. NPI), may be an effective therapeutic strategy to regulate pathologic VSMC growth in atherosclerosis.

Future Directions

This study has further elucidated the role of Hsp60 in VSMC proliferation and atherosclerotic development, however additional studies are required to investigate the role of Hsp60 in intracellular trafficking during VSMC proliferation, to understand the role of the Hsp60 co-chaperone Hsp10 in VSMC proliferation, and to determine how Hsp60 is transcriptionally regulated under stress conditions.

Hsp60 can play a role in intracellular protein trafficking362 and this study showed that at high intracellular levels Hsp60 co-immunoprecipitated with Ran as a potential mechanism to increase NPI (Figure 23). A future experiment could investigate whether Hsp60 co-immunoprecipitates with Ran in VSMCs treated with oxLDL at 25 μg/ml for 6 hours. Since previous work has shown that oxLDL stimulates NPI29, this future experiment would investigate whether oxLDL stimulates NPI through the interaction of Hsp60 with Ran.

Hsp10 functions as a co-chaperone with Hsp60366 and there is evidence that Hsp10/Hsp60 complexes have an anti-apoptotic function in vitro367. One study showed that overexpression of Hsp10 was sufficient to protect cardiac muscle cells from apoptosis when they were subjected to ischemia/reperfusion injury368. A future experiment could investigate whether overexpression of Hsp10 and Hsp60 can induce VSMC proliferation and increase NPI. In addition, it may be interesting that to test whether overexpression of solely Hsp10 can stimulate VSMC proliferation and NPI. These experiments would provide further mechanistic insights on how Hsp60 regulates VSMC proliferation.

This study demonstrated that Hsp60 is the sole Hsp induced during atherosclerotic plaque growth (Figure 26). Previous work suggested that Hsp60, 70, and 90 are all activated in response to stress stimuli by the transcriptional regulator Hsf1116. Future experiments could investigate whether Hsp60 expression is increased via a Hsf1-independent mechanism during stress-induced VSMC proliferation. For example, Hsp60 expression could be measured in VSMCs subjected to Hsf1 knockdown followed by oxLDL treatment at 25μg/ml oxLDL for 6 hours.

This work has highlighted NPI as a cellular pathway that regulates cell growth and proliferation. Previous in vitro work in VSMCs has demonstrated that NPI is modulated in response to proliferative stimuli27,29,101. However there are no studies that have investigated NPI in VSMCs in vivo. Previous studies have demonstrated a method of isolating and culturing VSMCs from atherosclerotic plaque samples369,370. A future experiment could use our atherosclerotic rabbit model357 to obtain plaque samples throughout the growth and plateau phases of atherosclerosis. VSMCs could be isolated and cultured from this atherosclerotic tissue and subjected to NPI assays. This would allow investigation of the potential correlation between Hsp60 expression, nucleoporin expression, and NPI during atherosclerotic development.

Lastly, there a number of experiments from this study that require repetition with slightly altered parameters. Repeating the NPI assay and western blotting for nuclear transport receptors, nucleoporins, Hsp60, and PCNA in VSMCs treated with Hsp60 siRNA followed by oxLDL at 25μg/ml for 6 hours would demonstrate how

VSMCs actually respond to a proliferative stimulus with reduced Hsp60 expression. In addition, a cell titer assay in VSMCs with Hsp60 knockdown and oxLDL treatment at 25μg/ml for 6 hours would confirm the effect of oxLDL treatment on VSMC proliferation when Hsp60 is knocked down. It would also be interesting to investigate whether a lower dose of oxLDL could stimulate proliferation and increase Hsp60 expression in rat VSMCs. In rabbit VSMCs, oxLDL treatment at 10μg/ml increased cell number by 10% versus untreated cells, while oxLDL at 25μg/ml increased cell number by 11% compared to control cells29. This similarity in proliferative response between oxLDL doses of 10 and 25μg/ml in rabbit VSMCs merits a cell titer assay with rat VSMCs subjected to oxLDL at 10 or 25μg/ml for 24 hours.

Further work to understand the role of Hsp60 in VSMC proliferation and atherosclerosis is necessary as despite modern medication regimens and interventions, cardiovascular disease remains the number one cause of mortality in the world1.

LITERATURE CITED

1. Naghavi M, Wang H, Lozano R, et al. Global, regional, and national age-sex specific all-cause and cause-specific mortality for 240 causes of death, 1990-2013: a systematic analysis for the Global Burden of Disease Study 2013. *Lancet*. 2015;385(9963):117-171. doi:10.1016/S0140-6736(14)61682-2.Global.
2. Moran A, Roth G, Narula J, Mensah G. 1990-2010 Global Cardiovascular Disease Atlas. *Glob Heart*. 2014;9(1):3-16.
3. Effat MA. Pathophysiology of ischemic heart disease: an overview. *AACN Clin Issues*. 1995;6(3):369-374.
4. Ross R. Atherosclerosis - An Inflammatory Disease. *N Engl J Med*. 1999;340(2):115-126.
5. Kemp CD, Conte JV. The pathophysiology of heart failure. *Cardiovasc Pathol*. 2012;21(5):365-371.
6. Castelli WP. Epidemiology of coronary heart disease: the Framingham Study. *Am J Med*. 1984;76:4-12.
7. Jousilahti P, Vartiainen E, Tuomilehto J, Puska P. Sex, age, cardiovascular risk factors, and coronary heart disease: a prospective follow-up study of 14 786 middle-aged men and women in Finland. *Circulation*. 1999;99(9):1165-1172.
8. Ripatti S, Tikkanen E, Orho-Melander M. A multilocus genetic risk score for coronary heart disease: case-control and prospective cohort analyses. *Lancet*. 2010;376(9750):1393-1400.
9. Kannel WB, Dawber TR, Kagan A, Revotskie N, Stokes J. Factors of risk in the development of coronary heart disease - six year follow-up experience: the Framingham Study. *Ann Intern Med*. 1961;55:33-50.
10. Moore KJ, Tabas I. Macrophages in the pathogenesis of atherosclerosis. *Cell*. 2011;145(3):341-355. doi:10.1016/j.cell.2011.04.005.
11. Ross R. The pathogenesis of atherosclerosis: a perspective for the 1990s. *Nature*. 1993;362:801-809.
12. Libby P, Ridker PM, Hansson GK. Progress and challenges in translating the biology of atherosclerosis. *Nature*. 2011;473(7347):317-325. doi:10.1038/nature10146.
13. Libby P. History of Discovery: Inflammation in Atherosclerosis. *Arterioscler Thromb Vasc Biol*. 2012;32(9):2045-2051.
14. Tabas I, Williams KJ, Boren J. Subendothelial lipoprotein retention as the initiating process in atherosclerosis: update and therapeutic implications. *Circulation*. 2007;116:1832-1844.
15. Steinberg D. Low density lipoprotein oxidation and its pathobiological significance. *J Biol Chem*. 1997;272(34):20963-20966.

16. Han J, Hajjar DP, Febbraio M, Nicholson AC. Native and modified low density lipoproteins increase the functional expression of the macrophage class B scavenger receptor, CD36. *J Biol Chem*. 1997;272(34):21654-21659.

17. Packard RRS, Libby P. Inflammation in atherosclerosis: From vascular biology to biomarker discovery and risk prediction. *Clin Chem*. 2008;54(1):24-38. doi:10.1373/clinchem.2007.097360.

18. Di Pietro N, Formoso G, Pandolfi A. Physiology and pathophysiology of oxLDL uptake by vascular wall cells in atherosclerosis. *Vascul Pharmacol*. 2016;15:30101-30104.

19. De Winther MPJ, Kanters E, Kraal G, Hofker MH. Nuclear factor Kappa Beta signaling in atherogenesis. *Arterioscler Thromb Vasc Biol*. 2005;25(5):904-914. doi:10.1161/01.ATV.0000160340.72641.87.

20. Tabas I. Macrophage death and defective inflammation resolution in atherosclerosis. *Nat Rev Immunol*. 2010;10:36-46.

21. Virmani R, Burke AP, Kolodgie FD, Farb A. Vulnerable plaque: the pathology of unstable coronary lesions. *J Interv Cardiol*. 2002;15(6):439-446.

22. Morgan A, Mooney K, Wilksinson S, Pickles N, Mc Auley M. Cholesterol metabolism: A review of how ageing disrupts the biological mechanisms responsible for its regulation. *Ageing Res Rev*. 2016;27:108-124.

23. Maiolino G, Rossitto G, Caielli P, Bisogni V, Rossi GP, Calo LA. The role of oxidized low-density lipoproteins in atherosclerosis: the myths and the facts. *Mediat Inflamm*. 2013;2013:714653.

24. Berliner JA, Heinecke JW. The role of oxidized lipoproteins in atherogenesis. *Free Radic Biol Med*. 1996;20(5):707-727.

25. Hajjar DP, Haberland ME. Lipoprotein trafficking in vascular cells: molecular Trojan horses and cellular saboteurs. *J Biol Chem*. 1997;272(37):22975-22978.

26. Chahine MN, Deniset J, Dibrov E, et al. Oxidized LDL promotes the mitogenic actions of Chlamydia pneumoniae in vascular smooth muscle cells. *Cardiovasc Res*. 2011;92(3):476-483. doi:10.1093/cvr/cvr251.

27. Chahine MN, Dibrov E, Blackwood DP, Pierce GN. Oxidized LDL enhances stretch-induced smooth muscle cell proliferation through alterations in nuclear protein import. *Can J Physiol Pharmacol*. 2012;90:1559-1568. doi:10.1139/y2012-141 10.1124/pr.108.000620. PMID: 19805478; Chahine, M.N., Blackwood, D.P., Dibrov, E., Richard, M.N., Pierce, G.N., Oxidized LDL affects smooth muscle cell growth through MAPK-mediated actions on nuclear protein import (2009) J. Mol. Cell. Cardiol, 46 (3), pp. 431-441. , doi:10.1016/j.yjmcc.2008.10.009. PMID:19010332; Chahine, M.N., Deniset, J.F., Dibrov, E., Hirono, S., Blackwood, D.P., Austria, J.A., Pierce, G.N., Oxidized LDL promotes the mitogenic actions of Chlamydia pneumonia.

28. Zettler ME, Prociuk M a, Austria JA, Massaeli H, Zhong G, Pierce GN. OxLDL

stimulates cell proliferation through a general induction of cell cycle proteins. *Am J Physiol Heart Circ Physiol*. 2003;284(2):H644-53. doi:10.1152/ajpheart.00494.2001.

29. Chahine MN, Blackwood DP, Dibrov E, Richard MN, Pierce GN. Oxidized LDL affects smooth muscle cell growth through MAPK-mediated actions on nuclear protein import. *J Mol Cell Cardiol*. 2009;46(3):431-441. doi:10.1016/j.yjmcc.2008.10.009.
30. Liu J, Ren Y, Kang L, Zhang L. Oxidized low-density lipoprotein increases the proliferation and migration of human coronary artery smooth muscle cells through the upregulation of osteopontin. *Int J Mol Med*. 2014;33(5):1341-1347. doi:10.3892/ijmm.2014.1681.
31. Kataoka H, Kume N, Miyamoto S, et al. Oxidized LDL modulates Bax/Bcl-2 through the lectinlike Ox-LDL receptor-1 in vascular smooth muscle cells. *Arterioscler Thromb Vasc Biol*. 2001;21(6):955-960. doi:10.1161/01.ATV.21.6.955.
32. Salvayre R, Auge N, Benoist H, Negre-Salvayre A. Oxidized low-density lipoprotein-induced apoptosis. *Biochim Biophys Acta - Mol Cell Biol Lipids*. 2002;1585(2-3):213-221. doi:10.1016/S1388-1981(02)00343-8.
33. Bjokerud B, Bjokerud S. Contrary effects of lightly and strongly oxidized LDL with potent promotion of growth versus apoptosis on arterial smooth muscle cells, macrophages, and fibroblasts. *Arterioscler Thromb Vasc Biol*. 1996;16(3):416-424.
34. Napoli C, Quehenberger O, De Nigris F, Abete P, Glass CK, Palinski W. Mildly oxidized low density lipoprotein activates multiple apoptotic signaling pathways in human coronary cells. *FASEB J*. 2000;14(13):1997-2007.
35. Owens GK. Regulation of differentiation of vascular smooth muscle cells. *Physiol Rev*. 1995;75(3):487-517.
36. Owens GK, Kumar MS, Wamhoff BR. Molecular regulation of vascular smooth muscle cell differentiation in development and disease. *Physiol Rev*. 2004;84:767-801. doi:10.1152/physrev.00041.2003.
37. Perry RL, Rudnick MA. Molecular mechanisms regulating myogenic determination and differentiation. *Front Biosci*. 2000;5:D750-767.
38. Chistiakov DA, Orekhov AN, Bobryshev Y V. Vascular smooth muscle cell in atherosclerosis. *Acta Physiol*. 2015;214(1):33-50. doi:10.1111/apha.12466.
39. Frid MG, Moiseeva EP, Stenmark KR. Multiple phenotypically distinct smooth muscle cell populations exist in the adult and developing bovine pulmonary arterial media in vivo. *Circ Res*. 1994;75(4):669-681.
40. Bennett MR, Sinha S, Owens GK. Vascular Smooth Muscle Cells in Atherosclerosis. *Circ Res*. 2016;118(4):692-702. doi:10.1161/CIRCRESAHA.115.306361.
41. Qiu J, Zheng Y, Hu J, et al. Biomechanical regulation of vascular smooth muscle

cell functions: from in vitro to in vivo understanding. *J R Soc Interface / t*. 2014;11:20130852. doi:10.1098/rsif.2013.0852.

42. Holycross BJ, Blank RS, Thompson MM, Peach MJ, Owens GK. Platelet-derived growth factor-BB-induced suppression of smooth muscle cell differentiation. *Circ Res*. 1992;71:1525-1532.

43. Christen T, Bochaton-Piallat M-L, Neuville P, et al. Cultured Porcine Coronary Artery Smooth Muscle Cells: A New Model With Advanced Differentiation. *Circ Res*. 1999;85(1):99-107. doi:10.1161/01.res.85.1.99.

44. Corjay MH, Thompson MM, Lynch KR, Owens GK. Differential effect of platelet-derived growth factor- versus serum-induced growth on smooth muscle alpha-actin and nonmuscle beta-actin mRNA expression in cultured rat aortic smooth muscle cells. *J Biol Chem*. 1989;264:10501-10506.

45. Blank RS, Owens GK. Platelet derived growth factor regulates actin isoform expression and growth state in cultured rat aortic smooth muscle cells. *J Cell Physiol*. 1990;142:635-642.

46. Regan CP, Adam PJ, Madsen CS, Owens GK. Molecular mechanisms of decreased smooth muscle differentiation marker expression after vascular injury. *J Clin Invest*. 2000;106(9):1139-1147. doi:10.1172/JCI10522.

47. Mosse PR, Campbell GR, Campbell JH. Smooth muscle phenotypic expression in human carotid arteries. II. Atherosclerosis-free diffuse intimal thickenings compared with the media. *Arteriosclerosis*. 1986;6(6):664-669.

48. Aikawa M, Yamaguchi H, Yazaki Y, Nagai R. Smooth muscle phenotypes in developing and atherosclerotic human arteries demonstrated by myosin expression. *J Atheroscler Thromb*. 1995;2(1):14-23. http://www.ncbi.nlm.nih.gov/entrez/query.fcgi?cmd=Retrieve&db=PubMed&dopt=Citation&list_uids=9225203.

49. Shankman LS, Gomez D, Cherepanova OA, et al. KLF4-dependent phenotypic modulation of smooth muscle cells has a key role in atherosclerotic plaque pathogenesis. *Nat Med*. 2015;21(6):628-637.

50. Feil S, Fehrenbacher B, Lukowski R, et al. Transdifferentiation of vascular smooth muscle cells to macrophage-like cells during atherogenesis. *Circ Res*. 2014;115(7):662-667.

51. Albarran-Juarez J, Kaur H, Grimm M, Offermanns S, Wettschureck N. Lineage tracing of cells involved in atherosclerosis. *Atherosclerosis*. 2016;16:30257-X.

52. Iwata H, Manabe I, Nagai R. Lineage of bone marrow-derived cells in atherosclerosis. *Circ Res*. 2013;112(12):1634-1647.

53. Sata M, Saiura A, Kunisato A, et al. Hematopoietic stem cells differentiate into vascular cells that participate in the pathogenesis of atherosclerosis. *Nat Med*. 2002;8(4):403-409.

54. Caplice NM, Bunch TJ, Stalboerger PG, et al. Smooth muscle cells in human coronary atherosclerosis can originate from cells administered at marrow

transplantation. *Proc Natl Acad Sci U S A*. 2003;100(8):4754-4759. doi:10.1073/pnas.0730743100.

55. Bentzon J, Sondergaard C, Kassem M, Falk E. Smooth muscle cells healing atherosclerotic plaque disruptions are of local, not blood, origin in apolipoprotein E knockout mice. *Circulation*. 2007;116:2053-2061.

56. Iwata H, Manabe I, Fujiu K, et al. Bone marrow-derived cells contribute to vascular inflammation but do not differentiate into smooth muscle cell lineages. *Circulation*. 2010;122(20):2048-2057.

57. Allahverdian S, Chehroudi AC, McManus BM, Abraham T, Francis GA. Contribution of intimal smooth muscle cells to cholesterol accumulation and macrophage-like cells in human atherosclerosis. *Circulation*. 2014;129(15):1551-1559. doi:10.1161/CIRCULATIONAHA.113.005015.

58. Johnson JL. Matrix metalloproteinases: influence on smooth muscle cells and atherosclerotic plaque stability. *Expert Rev Cardiovasc Ther*. 2007;5(2):265-282.

59. Ketelhuth DF, Back M. The role of matrix metalloproteinases in atherothrombosis. *Curr Atheroscler Rep*. 2011;13:162-169.

60. Hansson GK, Libby P, Tabas I. Inflammation and plaque vulnerability. *J Intern Med*. 2015;278(5):483-493. doi:10.1111/joim.12406.

61. Alexander MR, Owens GK. Epigenetic control of smooth muscle cell differentiation and phenotypic switching in vascular development. *Annu Rev Physiol*. 2012;74:13-40.

62. Gomez D, Owens GK. Smooth muscle cell phenotypic switching in atherosclerosis. *Cardiovasc Res*. 2012;95(2):156-164. doi:10.1093/cvr/cvs115.

63. Davis-Dusenbery BN, Wu C, Hata A. Micromanaging vascular smooth muscle cell differentiation and phenotypic modulation. *Arterioscler Thromb Vasc Biol*. 2011;31(11):2370-2377. doi:10.1161/ATVBAHA.111.226670.

64. Ackers-Johnson M, Talasila A, Sage A, et al. Myocardin regulates vascular smooth muscle cell inflammatory activation and disease. *Arterioscler Thromb Vasc Biol*. 2015;35(4):817-828.

65. McDonald OG, Wamhoff BR, Hoofnagle MH, Owens GK. Control of SRF binding to CArG box chromatin regulates smooth muscle gene expression in vivo. *J Clin Invest*. 2006;116:36-48.

66. Yoshida T, Sinha S, Dandre F, Wamhoff BR, Hoofnagle MH. Myocardin is a key regulator of CArG-dependent transcription of multiple smooth muscle marker genes. *Circ Res*. 2003;92:856-862.

67. Cherepanova OA, Pidkovka NA, Sarmento OF, et al. Oxidized phospholipids induce type VIII collagen expression and vascular smooth muscle cell migration. *Circ Res*. 2009;104(5):609-618.

68. Pidkovka NA, Cherepanova OA, Yoshida T, et al. Oxidized phosholipids induce

phenotypic switching of vascular smooth muscle cells in vivo and in vitro. *Circ Res*. 2007;101(8):792-801.

69. Thomas JA, Deaton RA, Hastings NE, et al. PDGF-DD, a novel mediator of smooth muscle cell phenotypic modulation, is upregulated in endothelial cells exposed to atherosclerosis-prone flow patterns. *Am J Physiol Hear Circ Physiol*. 2009;296(2):H442-452.

70. Yoshida T, Gan Q, Owens GK. Kruppel-like factor 4, Elk-1, and histone deactylases cooperatively suppress smooth muscle cell differentiation markers in response to oxidized phospholipids. *Am J Physiol Cell Physiol*. 2008;101:792-801.

71. Salmon M, Gomez D, Greene E, Shankman LS, Owens GK. Cooperative binding of KLF4, pELK-1, and HDAC2 to a G/C repressor element in the SM22alpha promoter mediates transcriptional silencing of SMC phenotypic switching in vivo. *Circ Res*. 2012;111(6):685-696.

72. Yu X, Li Z. MicroRNAs regulate vascular smooth muscle cell functions in atherosclerosis (review). *Int J Mol Med*. 2014;34(4):923-933.

73. Cordes KR, Sheehy NT, White MP, et al. miR-145 and miR-143 regulate smooth muscle cell fate and plasticity. *Nature*. 2009;460(7265):705-710.

74. Rangrez AY, Massy ZA, Metzinger-Le Meuth V, Metzinger L. miR-143 and miR-145: molecular keys to switch the phenotype of vascular smooth muscle cells. *Circ Cardiovasc Genet*. 2011;4:197-205.

75. Boettger T, Beetz N, Kostin S, et al. Acquisition of the contractile phenotype by murine arterial smooth muscle cells depends on the Mi143/145 gene cluster. *J Clin Invest*. 2009;119:2634-2647.

76. Davis BN, Hilyard AC, Lagna G, Hata A. SMAD proteins control DROSHA-mediated microRNA maturation. *Nature*. 2008;454:56-61.

77. Chen J, Yin H, Jiang Y, et al. Induction of microRNA-1 by myocardin in smooth muscle cells inhibits cell proliferation. *Arterioscler Thromb Vasc Biol*. 2011;31:368-375.

78. Davis BN, Hilyard AC, Nguyen PH, Lagna G, Hata A. Induction of microRNA-221 by platelet-derived growth factor signaling is critical for modulation of vascular smooth muscle cell phenotype. *J Biol Chem*. 2009;284:3728-3738.

79. Sun SG, Zheng B, Han M, et al. miR-146a and Kruppel-like factor 4 form a feedback loop to participate in vascular smooth muscle cell proliferation. *EMBO Rep*. 2011;12:56-62.

80. Ferns GA, Raines EW, Sprugel KH, Motani AS, Reidy MA, Ross R. Inhibition of neointimal smooth muscle accumulation after angioplasty by an antibody to PDGF. *Science (80-)*. 1991;253:1129-1132.

81. Jaiwen A, Bowen-Pope DF, Lindner V, Schwartz SM, Clowes AW. Platelet-derived growth factor promotes smooth muscle migration and intimal thickening in a rat model of balloon angioplasty. *J Clin Invest*. 1992;89:507-

511.

82. ten Dijke P, Arthur HM. Extracellular control of TGFbeta signalling in vascular development and disease. *Nat Rev Mol Cell Biol*. 2007;8(11):857-869.

83. Lagna G, Ku MN, Nguyen PH, Neuman NA, Davis BN, Hata A. Control of phenotypic plasticity of smooth muscle cells by bone morphogenetic protein signaling through the myocardin-related transcription factors. *J Biol Chem*. 2007;282:37244-37255.

84. Stegemann JP, Hong H, Nerem RM, Jan P. Mechanical, biochemical, and extracellular matrix effects on vascular smooth muscle cell phenotype. *J App Physiol*. 2005;98(6):2321-2327. doi:10.1152/japplphysiol.01114.2004.

85. Newby AC. Dual Role of Matrix Metalloproteinases (Matrixins) in Intimal Thickening and Atherosclerotic Plaque Rupture. *Physiol Rev*. 2005;85:1-31. doi:10.1152/physrev.00048.2003.

86. Li DY, Brooke B, Davis EC, et al. Elastin is an essential determinant of arterial morphogenesis. *Nature*. 1998;393(May):276-280. doi:10.1038/30522.

87. Koyama H, Raines EW, Bornfeldt KE, Roberts JM, Ross R. Fibrillar collagen inhibits arterial smooth muscle proliferation through regulation of Cdk2 inhibitors. *Cell*. 1996;87(6):1069-1078. doi:10.1016/S0092-8674(00)81801-2.

88. Fukumoto Y, Deguchi JO, Libby P, et al. Genetically determined resistance to collagenase action augments interstitial collagen accumulation in atherosclerotic plaques. *Circulation*. 2004;110(14):1953-1959. doi:10.1161/01.CIR.0000143174.41810.10.

89. Xiao Q, Zhang F, Grassia G, et al. Matrix metalloproteinase-8 promotes vascular smooth muscle cell proliferation and neointima formation. *Arterioscler Thromb Vasc Biol*. 2014;34(1):90-98. doi:10.1161/ATVBAHA.113.301418.

90. Austin KM, Nguyen N, Golrokh J, Covic L, Kuliopulos A. Noncanonical Matrix Metalloprotease-1-Protease-activated Receptor-1 Signaling Triggers Vascular Smooth Muscle Cell Dedifferentitation and Arterial Stenosis. *J Biol Chem*. 2014;288(32):23105-23115.

91. Wang M, Kim SH, Monticone RE, Lakatta EG. Matrix metalloproteinases promote arterial remodeling in aging, hypertension, and atherosclerosis. *Hypertension*. 2015;65(4):698-703. doi:10.1016/bs.mcb.2015.01.016.Observing.

92. Qi Y, Jiang J, Jiang X, et al. PDGF-BB and TGF-β1 on cross-talk between endothelial and smooth muscle cells in vascular remodeling induced by low shear stress. *Pnas*. 2011;108:1908-1913. doi:10.1073/pnas.1019219108/-/DCSupplemental.www.pnas.org/cgi/doi/10.1073/pnas.1019219108.

93. Buga G, Gold M, Fukuto J, Ignarro L. Shear stress-induced release of nitric oxide from endothelial cells grown on beads. *Hypertension*. 1991;17(2):187-

193. doi:10.1161/01.HYP.17.2.187.

94. Berceli SA, Davies MG, Kenagy RD, Clowes AW. Flow-induced neointimal regression in baboon polytetrafluoroethylene grafts is associated with decreased cell proliferation and increased apoptosis. *J Vasc Surg*. 2002;36(6):1248-1255. doi:10.1067/mva.2002.128295.

95. Hergenreider E, Heydt S, Tréguer K, et al. Atheroprotective communication between endothelial cells and smooth muscle cells through miRNAs. *Nat Cell Biol*. 2012;14(3):249-256. doi:10.1038/ncb2441.

96. Chen LJ, Chuang L, Huang YH, et al. MicroRNA mediation of endothelial inflammatory response to smooth muscle cells and its inhibition by atheroprotective shear stress. *Circ Res*. 2015;116(7):1157-1169. doi:10.1161/CIRCRESAHA.116.305987.

97. Ueba J, Kawakami M, Yaginuma T. Shear stress as an inhibitor of vascular smooth muscle cell proliferation. Role of transforming growth factor-beta 1 and tissue-type plasminogen activator. *Arterioscler Thromb Vasc Biol*. 1997;17(8):1512-1516.

98. Ono O, Ando J, Kamiya a, Kuboki Y, Yasuda H. Flow effects on cultured vascular endothelial and smooth muscle cell functions. *Cell Struct Funct*. 1991;16(5):365-374. http://www.ncbi.nlm.nih.gov/pubmed/1769069.

99. Wara AK, Mitsumata M, Yamane T, Kusumi Y, Yoshida Y. Gene expression in endothelial cells and intimal smooth muscle cells in atherosclerosis-prone or atherosclerosis-resistant regions of the human aorta. *J Vasc Res*. 2008;45(4):303-313.

100. Wilson E, Mai Q, Sudhir K, Weiss RH, Ives HE. Mechanical strain induces growth of vascular smooth muscle cells via autocrine action of PDGF. *J Cell Biol*. 1993;123(3):741-747. doi:10.1083/jcb.123.3.741.

101. Richard MN, Deniset JF, Kneesh AL, Blackwood D, Pierce AN. Mechanical stretching stimulates smooth muscle cell growth, nuclear protein import, and nuclear pore expression through mitogen-activated protein kinase activation. *J Biol Chem*. 2007;282(32):23081-23088. doi:10.1074/jbc.M703602200.

102. Lee RM, Triggle CR, Cheung DW, Coughlin MD. Structural and functional consequence of neonatal sympathectomy on the blood vessels of spontaneously hypertensive rats. *Hypertension*. 1987;10:328-338.

103. Owens GK, Schwartz SM. Alterations in vascular smooth muscle mass in the spontaneously hypertensive rat. *Circ Res*. 1982;51:280-289.

104. Fan L, Karino T. Effect of a disturbed flow on proliferation of the cells of a hybrid vascular graft. *Biorheology*. 2010;47(1):31-38.

105. Cooper AL, Beasley D. Hypoxia stimulates proliferation and interleukin-1alpha production in human vascular smooth muscle cells. *Am J Physiol Hear Circ Physiol*. 1999;277(4):H1326-1337. http://ajpheart.physiology.org.ezp-prod1.hul.harvard.edu/content/277/4/H1326.long.

106. Baas AS, Berk BC. Differential activation of mitogen-activated protein kinases by H2O2 and O2- in vascular smooth muscle cells. *Circ Res*. 1995;77:29-36.

107. Rao GN, Berk BC. Active Oxygen Species Stimulate Vascular Smooth Muscle Cell Growth and Proto-oncogene Expression. *Circ Res*. 1992;70:593-599.

108. de Graaf R, Kloppenburg G, Kitslaar PJHM, Bruggeman CA, Stassen F. Human heat shock protein 60 stimulates vascular smooth muscle cell proliferation through Toll-like receptors 2 and 4. *Microbes Infect*. 2006;8(7):1859-1865. doi:10.1016/j.micinf.2006.02.024.

109. Kültz D. Evolution of the cellular stress proteome: from monophyletic origin to ubiquitous function. *J Exp Biol*. 2003;206(Pt 18):3119-3124. doi:10.1242/jeb.00549.

110. Fulda S, Gorman AM, Hori O, Samali A. Cellular stress responses: cell survival and cell death. *Int J Cell Biol*. 2010;2010:214074. doi:10.1155/2010/214074.

111. Craig EA. The heat shock response. *CRC Crit Rev Biochem*. 1985;18(3):239-280.

112. Ritossa F. A new puffing pattern induced by temperature shock and DNP in Drosophila. *Experientia*. 1962;18:571-573.

113. Tissieres A, Mitchell HK, Tracy UM. Protein Synthesis in Salivary Glands of Drosophila melanogaster: Relation to Chromosome Puffs. *J Mol Biol*. 1974;84:389-398.

114. Ashburner M, Bonnert JJ. The Induction of Gene Activity Drosophila by Heat Shock in Review. *Cell*. 1979;17:241-254.

115. Samali A, Orrenius S. Heat shock proteins regulate stress response and apoptosis 1998.pdf. *Cell Stress Chaperones*. 1998;3(4):228-236.

116. Anckar J, Sistonen L. Regulation of HSF1 Function in the Heat Stress Response: Implications in Aging and Disease. *Annu Rev Biochem*. 2011;80:1089-1115. doi:10.1146/annurev-biochem-060809-095203.

117. Beere HM. "The stress of dying": the role of heat shock proteins in the regulation of apoptosis. *J Cell Sci*. 2004;117(Pt 13):2641-2651. doi:10.1242/jcs.01284.

118. Radons J. The human HSP70 family of chaperones: where do we stand? *Cell Stress Chaperones*. 2016;21(3):379-404. doi:10.1007/s12192-016-0676-6.

119. Parcellier A, Brunet M, Schmitt E, et al. HSP27 favors ubiquitination and proteasomal degradation of p27Kip1 and helps S-phase re-entry in stressed cells. *FASEB J*. 2006;20(8):1179-1181. doi:10.1096/fj.05-4184fje.

120. Zhang H, Rajasekaran NS, Orosz A, Xiao X, Rechsteiner M, Benjamin IJ. Selective degradation of aggregate-prone CryAB mutants by HSPB1 is mediated by ubiquitin-proteasome pathways. *J Mol Cell Cardiol*. 2010;49(6):918-930. doi:10.1016/j.yjmcc.2010.09.004.

121. Pearl LH, Prodromou C. STRUCTURE, FUNCTION, AND MECHANISM OF THE

Hsp90 MOLECULAR CHAPERONE. *Adv Protein Chem*. 2002;59:157-186.

122. Burrows F, Zhang H, Kamal A. Hsp90 activation and cell cycle regulation. *Cell Cycle*. 2004;3(12):1530-1536. doi:http://dx.doi.org/10.4161/cc.3.12.1277.

123. Ryan MT, Pfanner N. Hsp70 proteins in protein translocation. *Adv Protein Chem*. 2001;59(1986):223-242. http://www.ncbi.nlm.nih.gov/pubmed/11868273.

124. Neupert W, Brunner M. The protein import motor of mitochondria. *Nat Rev Mol Cell Biol*. 2002;3(8):555-565. doi:10.1038/nrm878.

125. Didelot C, Schmitt E, Brunet M, Maingret L, Parcellier A, Garrido C. Heat shock proteins: endogenous modulators of apoptotic cell death. *Handb Exp Pharmacol*. 2006;172:171-198.

126. Kampinga HH, Hageman J, Vos MJ, et al. Guidelines for the nomenclature of the human heat shock proteins. *Cell Stress Chaperones*. 2009;14(1):105-111. doi:10.1007/s12192-008-0068-7.

127. Verma S, Goyal S, Jamal S, Singh A, Grover A. Hsp90: Friends, clients and natural foes. *Biochimie*. 2016;127:227-240. doi:10.1016/j.biochi.2016.05.018.

128. Langer T, Rosmus S, Fasold H. Intracellular localization of 90kDa heat shock protein (HSP90alpha) determined by expression of a EGFP-HSP90alpha-fusion protein in unstressed and heat stressed 3T3 cells. *Cell Biol Int*. 2003;27:47-52.

129. Felts SJ, Owen BA, Nguyen P, Trepel J, Donner DB, Toft DO. The hsp90-related protein TRAP1 is a mitochondrial protein with distinct functional properties. *J Biol Chem*. 2000;275:3305-3312.

130. Mazzarella RA, Green M. ERp99, an abundant, conserved glycoprotein of the endoplasmic reticulum, is homologous to the 90kDa heat shock protein (hsp90) and the 94kDa glucose regulated protein (GRP94). *J Biol Chem*. 1987;262:8875-8883.

131. Hartl FU, Hayer-Hartl M. Molecular chaperones in the cytosol: from nascent chain to folded protein. *Science (80-)*. 2002;295:1852-1858.

132. Ben-Zvi AP, Goloubinoff P. Review: mechanisms of disaggregation and refolding of stable protein aggregates by molecular chaperones. *J Struct Biol*. 2001;135:84-93.

133. Pratt WB, Morishima Y, Peng H-M, Osawa Y. Proposal for a role of the Hsp90/Hsp70-based chaperone machinery in making triage decisions when proteins undergo oxidative and toxic damage. *Exp Biol Med*. 2010;235:278-289.

134. Whittier JE, Xiong Y, Rechsteiner MC, Squier TC. Hsp90 enhances degradation of oxidized calmodulin by the 20 S proteasome. *J Biol Chem*. 2004;279:46135-46142.

135. Young JC, Hoogenraad NJ, Hartl FU. Molecular chaperones Hsp90 and Hsp70 deliver preproteins to the mitochondrial import receptor Tom70. *Cell*.

2003;112:41-50.

136. Flaherty KM, Deluca-Flaherty C, McKay DB. Three-dimensional structure of the ATPase fragment of a 70K heat-shock cognate protein. *Nature*. 1990;346(6285):623-628. doi:10.1016/0021-9797(80)90501-9.

137. Prodromou C, Roe SM, Piper PW, Pearl LH. A molecular clamp in the crystal structure of the N-terminal domain of the yeast Hsp90 chaperone. *Nat Struct Mol Biol*. 1997;4:477-482.

138. Meyer P, Prodromou C, Hu B, et al. Structural and functional analysis of the middle segment of hsp90: implications for ATP hydrolysis and client protein and co-chaperone interactions. *Mol Cell*. 2003;11:647-658.

139. Li J, Buchner J. Structure, function and regulation of the hsp90 machinery. *Biomed J*. 2012;36(3):106-117. doi:10.4103/2319-4170.113230.

140. Hessling M, Richter K, Buchner J. Dissection of the ATP-induced conformational cycle of the molecular chaperone Hsp90. *Nat Struct Mol Biol*. 2009;16(3):287-293. doi:10.1038/nsmb.1565.

141. Young JC. Mechanisms of the Hsp70 chaperone system. *Biochem Cell Biol*. 2010;88(2):291-300.

142. Chen S, Smith DF. Hop as an adaptor in the heat shock protein 70 (Hsp70) and Hsp90 chaperone machinery. *J Biol Chem*. 1998;273(52):35194-35200. doi:10.1074/jbc.273.52.35194.

143. Mollapour M, Neckers L. Post-translational modifications of Hsp90 and their contributions to chaperone regulation. *Biochim Biophys Acta - Mol Cell Res*. 2012;1823(3):648-655. doi:10.1016/j.bbamcr.2011.07.018.

144. Mattoo RUH, Sharma SK, Priya S, Finka A, Goloubinoff P. Hsp110 is a bona fide chaperone using ATP to unfold stable misfolded polypeptides and reciprocally collaborate with Hsp70 to solubilize protein aggregates. *J Biol Chem*. 2013;288(29):21399-21411. doi:10.1074/jbc.M113.479253.

145. Franck E, Madsen O, Van Rheede T, Ricard G, Huynen MA, De Jong WW. Evolutionary diversity of vertebrate small heat shock proteins. *J Mol Evol*. 2004;59(6):792-805. doi:10.1007/s00239-004-0013-z.

146. Vos MJ, Carra S, Kanon B, et al. Specific protein homeostatic functions of small heat-shock proteins increase lifespan. *Aging Cell*. 2016;15(2):217-226. doi:10.1111/acel.12422.

147. Concannon CG, Gorman AM, Samali A. On the role of Hsp27 in regulating apoptosis. *Apoptosis*. 2003;8(1):61-70.

148. Mymrikov E V, Seit-Nebi AS, Gusev NB. Large Potentials of Small Heat Shock Proteins. *Physiol Rev*. 2011;91(4):1123-1159. doi:10.1152/physrev.00023.2010.

149. Treweek TM, Meehan S, Ecroyd H, Carver JA. Small heat-shock proteins: Important players in regulating cellular proteostasis. *Cell Mol Life Sci*. 2015;72(3):429-451. doi:10.1007/s00018-014-1754-5.

150. Carra S, Rusmini P, Crippa V, et al. Different anti-aggregation and pro-degradative functions of the members of the mammalian sHSP family in neurological disorders. *Philos Trans R Soc Lond B Biol Sci*. 2013;368(1617):20110409. doi:10.1098/rstb.2011.0409.

151. Samali A, Cotter TG. Heat shock proteins increase resistance to apoptosis. *Exp Cell Res*. 1996;223(1):163-170. doi:10.1006/excr.1996.0070.

152. Samali A, Robertson JD, Peterson E, et al. Hsp27 protects mitochondria of thermotolerant cells against apoptotic stimuli. *Cell Stress Chaperones*. 2001;6(1):49-58. doi:10.1379/1466-1268(2001)006<0049:HPMOTC>2.0.CO;2.

153. Concannon CG, Orrenius S, Samali A. Hsp27 inhibits cytochrome c-mediated caspase activation by sequestering both pro-caspase-3 and cytochrome c. *Gene Expr*. 2001;9(4-5):195-201.

154. Lee GJ, Roseman AM, Saibil HR, Vierling E. A small heat shock protein stably binds heat-denatured model substrates and can maintain a substrate in a folding-competent state. *EMBO J*. 1997;16(3):659-671. doi:10.1093/emboj/16.3.659.

155. Mogk A, Schlieker C, Friedrich KL, Schönfeld HJ, Vierling E, Bukau B. Refolding of substrates bound to small Hsps relies on a disaggregation reaction mediated most efficiently by ClpB/DnaK. *J Biol Chem*. 2003;278(33):31033-31042. doi:10.1074/jbc.M303587200.

156. Cashikar AG, Duennwald M, Lindquist SL. A chaperone pathway in protein disaggregation: Hsp26 alters the nature of protein aggregates to facilitate reactivation by Hsp104. *J Biol Chem*. 2005;280(25):23869-23875. doi:10.1097/MPG.0b013e3181a15ae8.Screening.

157. Bryantsev AL, Kurchashova SY, Golyshev SA, et al. Regulation of stress-induced intracellular sorting and chaperone function of Hsp27 (HspB1) in mammalian cells. *Biochem J*. 2007;407(3):407-417. doi:10.1042/BJ20070195.

158. Lelj-Garolla B, Mauk AG. Self-association and chaperone activity of Hsp27 are thermally activated. *J Biol Chem*. 2006;281:8169-8174.

159. Chernik IS, Panasenko OO, Li Y, Marston SB, Gusev NB. pH-induced changes of the structure of small heat shock proteins with molecular mass 24/27kDa (HspB1). *Biochem Biophys Res Commun*. 2004;324:1199-1203.

160. Maguire M, Coates ARM, Henderson B. Chaperonin 60 unfolds its secrets of cellular communication. *Cell Stress Chaperones*. 2002;7(4):317-329. doi:10.1379/1466-1268(2002)007<0317:CUISOC>2.0.CO;2.

161. Amberger A, Maczek C, Jürgens G, et al. Co-expression of ICAM-1, VCAM-1, ELAM-1 and Hsp60 in human arterial and venous endothelial cells in response to cytokines and oxidized low-density lipoproteins. *Cell Stress Chaperones*. 1997;2(2):94-103. doi:10.1379/1466-1268(1997)002<0094:CEOIVE>2.3.CO;2.

162. Hirono S, Dibrov E, Hurtado C, Kostenuk a, Ducas R, Pierce GN. Chlamydia pneumoniae Stimulates Proliferation of Vascular Smooth Muscle Cells Through Induction of Endogenous Heat Shock Protein 60. *Circ Res*. 2003;93:710-716. doi:10.1161/01.RES.0000095720.46043.F2.

163. Martin J, Langer T, Boteva R, Schramel a, Horwich a L, Hartl FU. Chaperonin-mediated protein folding at the surface of groEL through a "molten globule"-like intermediate. *Nature*. 1991;352(6330):36-42. doi:10.1038/352036a0.

164. Zwickl P, Pfeifer G, Lottspeich F, Kopp F, Dahlmann B, Baumeister W. Electron microscopy and image analysis reveal common principles of organization in two large protein complexes: groEL-Type proteins and proteasomes. *J Struct Biol*. 1990;103(3):197-203. doi:10.1016/1047-8477(90)90037-D.

165. Viitanen P V, Lubben TH, Reed J, Goloubinoff P, O'Keefe DP, Lorimer GH. Chaperonin-facilitated refolding of ribulosebisphosphate carboxylase and ATP hydrolysis by chaperonin 60 (groEL) are K+ dependent. *Biochemistry*. 1990;29(24):5665-5671. doi:10.1021/bi00476a003.

166. Langer T, Pfeifer G, Martin J, Baumeister W, Hartl FU. Chaperonin-mediated protein folding: GroES binds to one end of the GroEL cylinder, which accommodates the protein substrate within its central cavity. *EMBO J*. 1992;11(13):4757-4765.

167. Clare DK, Vasishtan D, Stagg S, et al. ATP-triggered conformational changes delineate substrate-binding and -folding mechanics of the GroEL chaperonin. *Cell*. 2012;149(1):113-123. doi:10.1016/j.cell.2012.02.047.

168. Soltys BJ, Gupta RS. Cell surface localization of the 60 kDa heat shock chaperonin protein (hsp60) in mammalian cells. *Cell Biol Int*. 1997;21(5):315-320. doi:10.1006/cbir.1997.0144.

169. Soltys BJ, Gupta RS. Immunoelectron microscopic localization of the 60-kDa heat shock chaperonin protein (Hsp60) in mammalian cells. *Exp Cell Res*. 1996;222(1):16-27. doi:10.1006/excr.1996.0003.

170. Cechetto JD, Soltys BJ, Gupta RS. Localization of mitochondrial 60-kD heat shock chaperonin protein (Hsp60) in pituitary growth hormone secretory granules and pancreatic zymogen granules. *JHistochemCytochem*. 2000;48(0022-1554):45-56.

171. Chandra D, Choy G, Tang DG. Cytosolic accumulation of HSP60 during apoptosis with or without apparent mitochondrial release: Evidence that its pro-apoptotic or pro-survival functions involve differential interactions with caspase-3. *J Biol Chem*. 2007;282(43):31289-31301. doi:10.1074/jbc.M702777200.

172. Gupta S, Knowlton AA. HSP60 trafficking in adult cardiac myocytes: role of the exosomal pathway. *Am J Physiol - Hear Circ Physiol*. 2007;292(6):H3052-H3056. doi:10.1152/ajpheart.01355.2006.

173. Merendino AM, Bucchieri F, Campanella C, et al. Hsp60 is actively secreted by human tumor cells. *PLoS One*. 2010;5(2). doi:10.1371/journal.pone.0009247.

174. Kim S, Stice J, Chen L, Jung J. Extracellular heat shock protein 60, cardiac myocytes, and apoptosis. *Circulation*. 2009;105(12):1186-1195. doi:10.1161/CIRCRESAHA.109.209643.Extracellular.

175. Tian J, Guo X, Liu XM, et al. Extracellular HSP60 induces inflammation through activating and up-regulating TLRs in cardiomyocytes. *Cardiovasc Res*. 2013;98(3):391-401. doi:10.1093/cvr/cvt047.

176. Zhao Y, Zhang C, Wei X, et al. Heat shock protein-60 stimulates the migration of vascular smooth muscle cells via Toll-like receptor 4 and ERK MAPK activation. *Sci Rep*. 2015;5:15352.

177. Zhang L, Pelech SL, Mayrand D, Grenier D, Heino J, Uitto VJ. Bacterial heat shock protein-60 increases epithelial cell proliferation through the ERK1/2 MAP kinases. *Exp Cell Res*. 2001;266:11-20. doi:10.1006/excr.2001.5199.

178. Sasu S, LaVerda D, Qureshi N, Golenbock DT, Beasley D. Chlamydia pneumoniae and chlamydial heat shock protein 60 stimulate proliferation of human vascular smooth muscle cells via toll-like receptor 4 and p44/p42 mitogen-activated protein kinase activation. *Circ Res*. 2001;89(3):244-250. http://www.ncbi.nlm.nih.gov/entrez/query.fcgi?cmd=Retrieve&db=PubMed&dopt=Citation&list_uids=11485974.

179. Kirchhoff SR, Gupta S, Knowlton AA. Cytosolic heat shock protein 60, apoptosis, and myocardial injury. *Circulation*. 2002;105(24):2899-2904. doi:10.1161/01.CIR.0000019403.35847.23.

180. Pirkkala L, Nykänen P, Sistonen L. Roles of the heat shock transcription factors in regulation of the heat shock response and beyond. *FASEB J*. 2001;15(7):1118-1131. doi:10.1096/fj00-0294rev.

181. Anckar J, Sistonen L. Heat Shock Factor 1 as a Coordinator of Stress and Developmental Pathways. *Adv Exp Med Biol*. 2007;594:78-88.

182. Perisic O, Xiao H, Lis JT. Stable binding of Drosophila heat shock factor to head-to-head and tail-to-tail repeats of a conserved 5 bp recognition unit. *Cell*. 1989;59:797-806.

183. Pelham HR. A regulatory upstream promoter element in Drosophila hsp 70 heat-shock gene. *Cell*. 1982;30(2):517-528.

184. Akerfelt M, Morimoto RI, Sistonen L. Heat shock factors: integrators of cell stress, development and lifespan. *Nat Rev Mol Cell Biol*. 2010;11(8):545-555. doi:10.1038/nrm2938.

185. Nakai A. New aspects in the vertebrate heat shock factor system: Hsf3 and Hsf4. *Cell Stress Chaperones*. 1999;4(2):86-93. doi:10.1379/1466-1268(1999)004<0086:NAITVH>2.3.CO;2.

186. McMillan D., Xiao X, Shao L, Graves K, Benjamin IJ. Targeted disruption of heat shock transcription factor 1 abolishes thermotolerance and protection agaisnt heat-inducible apoptosis. *J Biol Chem*. 1998;273(13):7523-7528. doi:10.1074/jbc.273.13.7523.

187. Östling P, Björk JK, Roos-Mattjus P, Mezger V, Sistonen L. Heat Shock Factor 2 (HSF2) contributes to inducible expression of hsp genes through interplay with HSF1. *J Biol Chem*. 2007;282(10):7077-7086. doi:10.1074/jbc.M607556200.

188. Inouye S, Izu H, Takaki E, et al. Impaired IgG production in mice deficient for heat shock transcription factor 1. *J Biol Chem*. 2004;279(37):38701-38709. doi:10.1074/jbc.M405986200.

189. Hahn J, Hu Z, Thiele DJ, Iyer VR. Genome-Wide Analysis of the Biology of Stress Responses through Heat Shock Transcription Factor. *Society*. 2004;24(12):5249-5256. doi:10.1128/MCB.24.12.5249.

190. Mahat DB, Salamanca HH, Duarte FM, Danko CG, Lis JT. Mammalian Heat Shock Response and Mechanisms Underlying Its Genome-wide Transcriptional Regulation. *Mol Cell*. 2016;62(1):63-78. doi:10.1016/j.molcel.2016.02.025.

191. Voellmy R, Boellmann F. Chaperone regulation of the heat shock protein response. *Adv Exp Med Biol*. 2007;594:89-99.

192. Zou J, Guo Y, Guettouche T, Smith DF, Voellmy R. Repression of heat shock transcription factor HSF1 activation by HSP90 (HSP90 complex) that forms a stress-sensitive complex with HSF1. *Cell*. 1998;94(4):471-480. doi:10.1016/S0092-8674(00)81588-3.

193. Ali A, Bharadwaj S, O'Carroll R, Ovsenek N. HSP90 interacts with and regulates the activity of heat shock factor 1 in Xenopus oocytes. *Mol Cell Biol*. 1998;18(9):4949-4960. http://www.pubmedcentral.nih.gov/articlerender.fcgi?artid=109079&tool=pmcentrez&rendertype=abstract.

194. Morimoto RI. Dynamic remodeling of transcription complexes by molecular chaperones. *Cell*. 2002;110(3):281-284. doi:10.1016/S0092-8674(02)00860-7.

195. Zhong M, Orosz a, Wu C. Direct sensing of heat and oxidation by Drosophila heat shock transcription factor. *Mol Cell*. 1998;2(1):101-108. doi:10.1016/S1097-2765(00)80118-5.

196. Ahn S, Thiele D. Redox regulation of mammalian heat shock factor 1 is essential for Hsp gene activation and protection from stress. *Genes Dev*. 2003:516-528. doi:10.1101/gad.1044503.ors.

197. Guettouche T, Boellmann F, Lane WS, Voellmy R. Analysis of phosphorylation of human heat shock factor 1 in cells experiencing a stress. *BMC Biochem*. 2005;6(1):4. doi:10.1186/1471-2091-6-4.

198. Boellmann F, Guettouche T, Guo Y, Fenna M, Mnayer L, Voellmy R. DAXX interacts with heat shock factor 1 during stress activation and enhances its transcriptional activity. *Proc Natl Acad Sci U S A*. 2004;101(12):4100-4105. doi:10.1073/pnas.0304768101.

199. Holmberg CI, Hietakangas V, Mikhailov A, et al. Phosphorylation of serine 230 promotes inducible transcriptional activity of heat shock factor 1. *EMBO J*. 2001;20(14):3800-3810. doi:10.1093/emboj/20.14.3800.

200. Chu B, Soncin F, Price BD, Stevenson MA, Calderwood SK. Sequential Phosphorylation by Mitogen-activated Protein Kinase and Glycogen Synthase Kinase 3Represses Transcriptional Activation by Heat Shock Factor-1. *J Biol Chem*. 1996;271(48):30847-30857. doi:10.1074/jbc.271.48.30847.

201. He B, Meng Y, Mivechi N. Extracellular Signal-Regulated Kinase Inactivate Heat Shock Transcription Factor 1 By Facilitating the Disappearance of Transcriptionally Active Granules After Heat Shock. *Mol Cell Biol*. 1998;18(11):6624-6633. http://mcb.asm.org/content/18/11/6624.short.

202. Guo Y, Guettouche T, Fenna M, et al. Evidence for a Mechanism of Repression of Heat Shock Factor 1 Transcriptional Activity by a Multichaperone Complex. *J Biol Chem*. 2001;276(49):45791-45799. doi:10.1074/jbc.M105931200.

203. Shi Y, Mosser DD, Morimoto RI. Molecular chaperones as HSF1-specific transcriptional repressors. *Genes Dev*. 1998;12(5):654-666. doi:10.1101/gad.12.5.654.

204. Wang Y, Chen L, Hagiwara N, Knowlton AA. Regulation of heat shock protein 60 and 72 expression in the failing heart. *J Mol Cell Cardiol*. 2010;48(2):360-377. doi:10.1097/MPG.0b013e3181a15ae8.Screening.

205. Stephanou A, Isenberg DA, Nakajima K, Latchman DS. Signal transducer and activator of transcription-1 and heat shock factor-1 interact and activate the transcription of Hsp-70 and Hsp-90beta gene promoters. *J Biol Chem*. 1999;274:1723-1728.

206. Stephanou A, Isenberg DA, Akira S, Kishimoto T, Latchman DS. The nuclear factor interleukin-6 (NF-IL6) and signal transducer and activator of transcription-3 (STAT3) signalling pathways co-operate to mediate the activation of the hsp90 beta gene by interleukin-6 but have opposite effects on its inducibility by heat. *Biochem J*. 1998;330(Pt 1):189-195.

207. Sasi BK, Sonawane PJ, Gupta V, Sahu BS, Mahapatra NR. Coordinated transcriptional regulation of hspa1a gene by multiple transcription factors: Crucial roles for HSF-1, NF-Y, NF-kB, and CREB. *J Mol Biol*. 2014;426(1):116-135. doi:10.1016/j.jmb.2013.09.008.

208. Deniset JF, Pierce GN. Heat Shock Proteins: Mediators of Atherosclerotic Development. *Curr Drug Targets*. 2015;16(8):816-826.

209. Wick G, Jakic B, Buszko M, Wick MC, Grundtman C. The role of heat shock proteins in atherosclerosis. *Nat Rev Cardiol*. 2014;11(9):516-529. doi:10.1038/nrcardio.2014.91.

210. Kleindienst R, Xu Q, Willeit J, Waldenberger FR, Weimann S, Wick G. Immunology of atherosclerosis. Demonstration of heat shock protein 60 expression and T lymphocytes bearing alpha/beta or gamma/delta receptor in human atherosclerotic lesions. *Am J Pathol*. 1993;142(6):1927-1937.

http://www.ncbi.nlm.nih.gov/pubmed/8099471.

211. Hochleitner BW, Hochleitner EO, Obrist P, et al. Fluid shear stress induces heat shock protein 60 expression in endothelial cells in vitro and in vivo. *Arterioscler Thromb Vasc Biol*. 2000;20:617-623. doi:10.1161/01.ATV.20.3.617.

212. Kanwar RK, Kanwar JR, Wang D, Ormrod DJ, Krissansen GW. Temporal expression of heat shock proteins 60 and 70 at lesion-prone sites during atherogenesis in ApoE-deficient mice. *Arterioscler Thromb Vasc Biol*. 2001;21(12):1991-1997. doi:10.1161/hq1201.100263.

213. Wick G, Xu Q. Autoimmunity to heat shock proteins in atherosclerosis. *Atherosclerosis*. 1997;134:289-289.

214. Kreutmayer SB, Messner B, Knoflach M, et al. Dynamics of heat shock protein 60 in endothelial cells exposed to cigarette smoke extract. *J Mol Cell Cardiol*. 2011;51(5):777-780.

215. Henderson B, Pockley a G. Molecular chaperones and protein-folding catalysts as intercellular signaling regulators in immunity and inflammation. *J Leukoc Biol*. 2010;88(3):445-462. doi:10.1189/jlb.1209779.

216. Henderson B, Graham Pockley A. Proteotoxic stress and circulating cell stress proteins in the cardiovascular diseases. *Cell Stress Chaperones*. 2012;17(3):303-311. doi:10.1007/s12192-011-0318-y.

217. Ohashi K, Burkart V, Flohe S, Kolb H. Cutting Edge: Heat Shock Protein 60 Is a Putative Endogenous Ligand of the Toll-Like Receptor-4 Complex. *J Immunol*. 2000;164(2):558-561. doi:10.4049/jimmunol.164.2.558.

218. Kol A, Bourcier T, Lichtman AH, Libby P. Chlamydial and human heat shock protein 60s activate human vascular endothelium, smooth muscle cells, and macrophages. *J Clin Invest*. 1999;103(4):571-577. doi:10.1172/JCI5310.

219. Pockley AG, Wu R, Lemne C, Kiessling R, de Faire U, Frostegard J. Circulating heat shock protein 60 is associated with early cardiovascular disease. *Hypertension*. 2000;36:303-307. doi:10.1161/01.ATV.0000038493.65177.94.

220. Xiao Q, Mandal K, Schett G, et al. Association of serum-soluble heat shock protein 60 with carotid atherosclerosis: Clinical significance determined in a follow-up study. *Stroke*. 2005;36(12):2571-2576. doi:10.1161/01.STR.0000189632.98944.ab.

221. Zhang X, He M, Cheng L, et al. Elevated Heat Shock Protein 60 Levels Are Associated With Higher Risk of Coronary Heart Disease in Chinese. *Circulation*. 2008;118:2687-2693. doi:10.1161/CIRCULATIONAHA.108.781856.

222. Xu Q, Schett G, Perschinka H, et al. Serum Soluble Heat Shock Protein 60 Is Elevated in Subjects With Atherosclerosis in a General Population. *Circulation*. 2000;102(1):14-20.

223. Xu Q, Schett G, Seitz CS, Hu Y, Gupta RS, Wick G. Surface staining and cytotoxic

activity of heat-shock protein 60 antibody in stressed aortic endothelial cells. *Circ Res*. 1994;75(6):1078-1085. doi:10.1161/01.RES.75.6.1078.

224. Seitz CS, Kleindienst R, Xu Q, Wick G. Coexpression of heat-shock protein 60 and intercellular-adhesion molecule-1 is related to increased adhesion of monocytes and T cells to aortic endothelium of rats in response to endotoxin. *Lab Invest*. 1996;74(1):241-252.

225. Kreutmayer S, Csordas A, Kern J, et al. Chlamydia pneumoniae infection acts as an endothelial stressor with the potential to initiate the earliest heat shock protein 60-dependent inflammatory stage of atherosclerosis. *Cell Stress Chaperones*. 2013;18(3):259-268. doi:10.1007/s12192-012-0378-7.

226. Schett G, Xu Q, Amberger A, et al. Autoantibodies against heat shock protein 60 mediate endothelial cytotoxicity. *J Clin Invest*. 1995;96(6):2569-2577. doi:10.1172/JCI118320.

227. Schett G, Metzler B, Mayr M, et al. Macrophage-lysis mediated by autoantibodies to heat shock protein 65/60. *Atherosclerosis*. 1997;128(1):27-38. doi:10.1016/S0021-9150(96)05975-8.

228. Foteinos G, Afzal AR, Mandal K, Jahangiri M, Xu Q. Anti-heat shock protein 60 autoantibodies induce atherosclerosis in apolipoprotein E-deficient mice via endothelial damage. *Circulation*. 2005;112(8):1206-1213. doi:10.1161/CIRCULATIONAHA.105.547414.

229. Grundtman C, Kreutmayer SB, Almanzar G, Wick MC. Heat Shock Protein 60 and Immune Inflammatory Responses in Atherosclerosis. *Arterioscler Thromb*. 2011;31(5):960-968. doi:10.1161/ATVBAHA.110.217877.Heat.

230. Perschinka H, Mayr M, Millonig G, et al. Cross-reactive B-cell epitopes of microbial and human heat shock protein 60/65 in atherosclerosis. *Arterioscler Thromb Vasc Biol*. 2003;23(6):1060-1065. doi:10.1161/01.ATV.0000071701.62486.49.

231. Wick C. Tolerization against atherosclerosis using heat shock protein 60. *Cell Stress Chaperones*. 2016;21(2):201-211. doi:10.1007/s12192-015-0659-z.

232. Andrié RP, Bauriedel G, Braun P, Höpp HW, Nickenig G, Skowasch D. Prevalence of intimal heat shock protein 60 homologues in unstable angina and correlation with anti-heat shock protein antibody titers. *Basic Res Cardiol*. 2011;106(4):657-665. doi:10.1007/s00395-011-0171-2.

233. Xu Q, Luef G, Weimann S, Gupta RS, Wolf H, Wick G. Staining of endothelial cells and macrophages in atherosclerotic lesions with human heat-shock protein-reactive antisera. *Arterioscler Thromb Vasc Biol*. 1993;13(12):1763-1769.

234. Hoppichler F, Koch T, Dzien A, Gschwandtner G, Lechleitner M. Prognostic value of antibody titre to heat-shock protein 65 on cardiovascular events. *Cardiology*. 2000;94(4):220-223.

235. Almanzar G, Öllinger R, Leuenberger J, et al. Autoreactive HSP60 epitope-

specific T-cells in early human atherosclerotic lesions. *J Autoimmun*. 2012;39(4):441-450. doi:10.1016/j.jaut.2012.07.006.

236. Xu Q, Kleindienst R, Waitz W, Dietrich H, Wick G. Increased expression of heat shock protein 65 coincides with a population of infiltrating T lymphocytes in atherosclerotic lesions of rabbits specifically responding to heat shock protein 65. *J Clin Invest*. 1993;91(6):2693-2702. doi:10.1172/JCI116508.

237. De Kleer IM, Kamphuis SM, Rijkers GT, et al. The spontaneous remission of juvenile idiopathic arthritis is characterized by CD30+ T cells directed to human heat-shock protein 60 capable of producing the regulatory cytokine interleukin-10. *Arthritis Rheum*. 2003;48(7):2001-2010. doi:10.1002/art.11174.

238. Wieten L, Broere F, van der Zee R, Koerkamp EK, Wagenaar J, van Eden W. Cell stress induced HSP are targets of regulatory T cells: A role for HSP inducing compounds as anti-inflammatory immuno-modulators? *FEBS Lett*. 2007;581(19):3716-3722. doi:10.1016/j.febslet.2007.04.082.

239. Zanin-Zhorov A, Cahalon L, Tal G, Margalit R, Lider O, Cohen IR. Heat shock protein 60 enhances CD4+CD25+ regulatory T cell function via innate TLR2 signaling. *J Clin Invest*. 2006;116(7):2022-2032.

240. Van Puijvelde GHM, Van Es T, Van Wanrooij EJA, et al. Induction of oral tolerance to HSP60 or an HSP60-peptide activates t cell regulation and reduces atherosclerosis. *Arterioscler Thromb Vasc Biol*. 2007;27(12):2677-2683. doi:10.1161/ATVBAHA.107.151274.

241. Zhong Y, Tang H, Wang X, et al. Intranasal immunization with heat shock protein 60 induces CD4+ CD25+ GARP+ and type 1 regulatory T cells and inhibits early atherosclerosis. *Clin Exp Immunol*. 2016;183(3):452-468. doi:10.1111/cei.12726.

242. Maron R, Sukhova G, Faria AM, et al. Mucosal administration of heat shock protein-65 decreases atherosclerosis and inflammation in aortic arch of low-density lipoprotein receptor-deficient mice. *Circulation*. 2002;106(13):1708-1715. doi:10.1161/01.CIR.0000029750.99462.30.

243. Harats D, Yacov N, Gilburd B, Shoenfeld Y, George J. Oral tolerance with heat shock protein 65 attenuates Mycobacterium tuberculosis-induced and high-fat-diet-driven atherosclerotic lesions. *J Am Coll Cardiol*. 2002;40(7):1333-1338. doi:10.1016/S0735-1097(02)02135-6.

244. Klingenberg R, Ketelhuth DFJ, Strodthoff D, Gregori S, Hansson GK. Subcutaneous immunization with heat shock protein-65 reduces atherosclerosis in Apoe -/- mice. *Immunobiology*. 2012;217(5):540-547. doi:10.1016/j.imbio.2011.06.006.

245. Dingwall C, Laskey RA. The nuclear membrane. *Science (80-)*. 1992;258(5084):942-947.

246. Faustino RS, Pierce GN. Nucleocytoplasmic Trafficking. *Curr Res Cardiol*. 2016;3(2):43-52.

247. Gorlich D, Kutay U. Transport between the cell nucleus and the cytoplasm. *Annu Rev Cell Dev Biol*. 1999;15:607-660.

248. Jans DA, Hübner S. Regulation of protein transport to the nucleus: central role of phosphorylation. *Physiol Rev*. 1996;76(3):651-685. http://www.ncbi.nlm.nih.gov/pubmed/8757785.

249. Ryan KJ, Wente SR. The nuclear pore complex: A protein machine bridging the nucleus and cytoplasm. *Curr Opin Cell Biol*. 2000;12(3):361-371. doi:10.1016/S0955-0674(00)00101-0.

250. Rout MP, Aitchison JD, Suprapto A, Hjertaas K, Zhao Y, Chait BT. The yeast nuclear pore complex: Composition, architecture, transport mechanism. *J Cell Biol*. 2000;148(4):635-651. doi:10.1083/jcb.148.4.635.

251. Wente SR, Rout MP. The nuclear pore complex and nuclear transport. *Cold Spring Harb Perspect Biol*. 2010;2(10):1-19. doi:10.1101/cshperspect.a000562.

252. Cronshaw JM, Krutchinsky A, Zhang W, Chait B, Matunis M. Proteomic analysis of the mammalian nuclear pore complex. *J Cell Biol*. 2002;158(5):915-927. doi:10.1083/jcb.200206106.

253. Danker T, Oberleithner H. Nuclear pore function viewed with atomic force microscopy. *Plfugers Arch*. 2000;439:671-681.

254. Pante N, Kann M. Nuclear Pore Complex Is Able to Transport Macromolecules with Diameters of 39 nm. *Mol Biol Cell*. 2002;13(February):425-434. doi:10.1091/mbc01.

255. Hoelz A, Debler EW, Blobel G. The structure of the nuclear pore complex. *Annu Rev Biochem*. 2011;80:613-643. doi:10.1146/annurev-biochem-060109-151030.

256. Shahin V, Danker T, Enss K, Ossig R, Oberleithner H. Evidence for Ca2+- and ATP-sensitive peripheral channels in nuclear pore complexes. *Faseb J*. 2001;15(11):1895-1901. doi:10.1096/fj.00-0838com.

257. Hinshaw JE, Carragher BO, Milligan R a. Architecture and design of the nuclear pore complex. *Cell*. 1992;69(7):1133-1141. doi:10.1016/0092-8674(92)90635-P.

258. Wu J, Matunis MJ, Kraemer D, Blobel G, Coutavas E. Nup358, a cytoplasmically exposed nucleoporin with peptide repeats, Ran-GTP binding sites, zinc fingers, a cyclophilin A homologous domain, and a leucine-rich region. *J Biol Chem*. 1995;270(23):14209-14213. doi:10.1074/jbc.270.23.14209.

259. Yaseen NR, Blobel G. Two distinct classes of Ran-binding sites on the nucleoporin Nup-358. *Proc Natl Acad Sci U S A*. 1999;96(10):5516-5521. doi:10.1073/pnas.96.10.5516.

260. Goldberg MW, Allen TD. High resolution scanning electron microscopy of the nuclear envelope: Demonstration of a new, regular, fibrous lattice attached to the baskets of the nucleoplasmic face of the nuclear pores. *J Cell Biol*.

1992;119(6):1429-1440. doi:10.1083/jcb.119.6.1429.

261. Stoffler D, Feja B, Fahrenkrog B, Walz J, Typke D, Aebi U. Cryo-electron tomography provides novel insights into nuclear pore architecture: Implications for nucleocytoplasmic transport. *J Mol Biol*. 2003;328(1):119-130. doi:10.1016/S0022-2836(03)00266-3.

262. Daigle N, Beaudouin J, Hartnell L, et al. Nuclear pore complexes form immobile networks and have a very low turnover in live mammalian cells. *J Cell Biol*. 2001;154(1):71-84. doi:10.1083/jcb.200101089.

263. Fahrenkrog B, Maco B, Fager AM, et al. Domain-specific antibodies reveal multiple-site topology of Nup153 within the nuclear pore complex. *J Struct Biol*. 2002;140(1-3):254-267. doi:10.1016/S1047-8477(02)00524-5.

264. Stoffler D, Fahrenkrog B, Aebi U. The nuclear pore complex: From molecular architecture to functional dynamics. *Curr Opin Cell Biol*. 1999;11(3):391-401. doi:10.1016/S0955-0674(99)80055-6.

265. Ibarra A, Hetzer MW. Nuclear pore proteins and the control of genome functions. *Genes Dev*. 2015;29(4):337-349. doi:10.1101/gad.256495.114.

266. Capelson M, Liang Y, Schulte R, Mair W, Wagner U, Hetzer MW. Chromatin-bound nuclear pore components regulate gene expression in higher eukaryotes. *Cell*. 2010;140(3):372-383. doi:10.1016/j.cell.2009.12.054.Chromatin-bound.

267. Liang Y, Franks TM, Marchetto MC, Gage FH, Hetzer MW. Dynamic Association of NUP98 with the Human Genome. *PLoS Genet*. 2013;9(2). doi:10.1371/journal.pgen.1003308.

268. Lenz-böhme B, Wismar J, Fuchs S, et al. Insertional Mutation of the Drosophila Nuclear Lamin Dm0 Gene Results in Defective Nuclear Envelopes, Clustering of Nuclear Pore Complexes, and Accumulation of Annulate Lamellae. *Cell*. 1997;137(5):1001-1016.

269. Pemberton LF, Rout MP, Blobel G. Disruption of the nucleoporin gene NUP133 results in clustering of nuclear pore complexes. *Proc Natl Acad Sci U S A*. 1995;92(4):1187-1191. doi:10.1073/pnas.92.4.1187.

270. Heath C V., Copeland CS, Amberg DC, Del Priore V, Snyder M, Cole CN. Nuclear pore complex clustering and nuclear accumulation of poly(A)+ RNA associated with mutation of the Saccharomyces cerevisiae RAT2/NUP120 gene. *J Cell Biol*. 1995;131(6 Pt. 2):1677-1697. doi:10.1083/jcb.131.6.1677.

271. Christie M, Chang C-W, Róna G, et al. Structural biology and regulation of protein import into the nucleus. *J Mol Biol*. 2016;428(2015):2060-2090. doi:10.1016/j.jmb.2015.10.023.

272. Lange A, Mills RE, Lange CJ, Stewart M, Devine SE, Corbett AH. Classical nuclear localization signals: Definition, function, and interaction with importin alpha. *J Biol Chem*. 2007;282(8):5101-5105. doi:10.1074/jbc.R600026200.

273. Marfori M, Mynott A, Ellis JJ, et al. Molecular basis for specificity of nuclear import and prediction of nuclear localization. *Biochim Biophys Acta - Mol Cell Res*. 2011;1813(9):1562-1577. doi:10.1016/j.bbamcr.2010.10.013.

274. Moore MS. Ran and nuclear transport. *J Biol Chem*. 1998;273(36):22857-22860. doi:10.1074/jbc.273.36.22857.

275. Ben-Efraim I, Gerace L. Gradient of increasing affinity of importin beta for nucleoporins along the pathway of nuclear import. *J Cell Biol*. 2001;152(2):411-417.

276. Kutay U, Bischoff R, Kostka S, Kraft R, Gorlich D. Export of importin alpha from the nucleus is mediated by a specific nuclear transport factor. *Cell*. 1997;90(6):1061-1071.

277. Ribbeck K, Lipowsky G, Kent HM, Stewart M, Görlich D. NTF2 mediates nuclear import of Ran. *EMBO J*. 1998;17(22):6587-6598. doi:10.1093/emboj/17.22.6587.

278. Kalderon D, Richardson WD, Markham AF, Smith AE. Sequence requirements for nuclear location of simian virus 40 large-T antigen. *Nature*. 1984;311:33-38.

279. Robbins J, Dilworth SM, Laskey RA, Dingwall C. Two interdependent basic domains in nucleoplasmin nuclear targeting sequence: Identification of a class of bipartite nuclear targeting sequence. *Cell*. 1991;64:615-623.

280. Conti E, Uy M, Leighton L, Blobel G, Kuriyan J. Crystallographic analysis of the recognition of a nuclear localization signal by the nuclear import factor karyopherin α. *Cell*. 1998;94(2):193-204. doi:10.1016/S0092-8674(00)81419-1.

281. Fontes MR, Teh T, Kobe B. Structural basis of recognition of monopartite and bipartite nuclear localization sequences by mammalian importin-alpha. *J Mol Biol*. 2000;297(5):1183-1194. doi:10.1006/jmbi.2000.3642.

282. Cingolani G, Petosa C, Weis K, Müller CW. Structure of importin-beta bound to the IBB domain of importin-alpha. *Nature*. 1999;399:221-229. doi:10.1038/20367.

283. Cingolani G, Lashuel HA, Gerace L, M??ller CW. Nuclear import factors importin alpha and importin beta undergo mutually induced conformational changes upon association. *FEBS Lett*. 2000;484(3):291-298. doi:10.1016/S0014-5793(00)02154-2.

284. Bayliss R, Littlewood T, Stewart M. Structural basis for the interaction between FxFG nucleoporin repeats and importin-beta in nuclear trafficking. *Cell*. 2000;102(1):99-108. doi:10.1016/S0092-8674(00)00014-3.

285. Bayliss R, Littlewood T, Strawn LA, Wente SR, Stewart M. GLFG and FxFG nucleoporins bind to overlapping sites on importin-β. *J Biol Chem*. 2002;277(52):50597-50606. doi:10.1074/jbc.M209037200.

286. Kalab P, Weis K, Heald R. Visualization of a Ran-GTP gradient in interphase

and mitotic Xenopus egg extracts. *Science (80-)*. 2002;295:2452-2456.

287. Moroianu J, Blobel G, Radu a. Nuclear protein import: Ran-GTP dissociates the karyopherin alphabeta heterodimer by displacing alpha from an overlapping binding site on beta. *Proc Natl Acad Sci U S A*. 1996;93(14):7059-7062. doi:10.1073/pnas.93.14.7059.

288. Gorlich D, Pante N, Kutay U, Aebi U, Bischoff FR. Identification of different roles for RanGDP and RanGTP in nuclear protein import. *EMBO J*. 1996;15(5584-5594).

289. Matsuura Y, Lange A, Harreman MT, Corbett AH, Stewart M. Structural basis for Nup2p function in cargo release and karyopherin recycling in nuclear import. *EMBO J*. 2003;22(20):5358-5369. doi:10.1093/emboj/cdg538.

290. Matsuura Y, Stewart M. Nup50/Npap60 function in nuclear protein import complex disassembly and importin recycling. *EMBO J*. 2005;24(21):3681-3689. doi:10.1038/sj.emboj.7600843.

291. Harreman MT, Hodel MR, Fanara P, Hodel AE, Corbett AH. The auto-inhibitory function of importin-alpha is essential in vivo. *J Biol Chem*. 2003;278(8):5854-5863. doi:10.1074/jbc.M210951200.

292. Richards S a, Carey KL, Macara IG. Requirement of guanosine triphosphate-bound ran for signal-mediated nuclear protein export. *Science (80-)*. 1997;276(5320):1842-1844. doi:10.1126/science.276.5320.1842.

293. Izaurralde E, Kutay U, Von Kobbe C, Mattaj LW, Görlich D. The asymmetric distribution of the constituents of the Ran system is essential for transport into and out of the nucleus. *EMBO J*. 1997;16(21):6535-6547. doi:10.1093/emboj/16.21.6535.

294. Geyer M, Assheuer R, Klebe C, et al. Conformational states of the nuclear GTP-binding protein ran and its complexes with the exchange factor RCC1 and the effector protein RanBP1. *Biochemistry*. 1999;38(35):11250-11260. doi:10.1021/bi9904306.

295. Bischoff FR, Görlich D. RanBP1 is crucial for the release of RanGTP from importin β-related nuclear transport factors. *FEBS Lett*. 1997;419(2-3):249-254. doi:10.1016/S0014-5793(97)01467-1.

296. Bischoff FR, Klebe C, Kretschmer J, Wittinghofer A, Ponstingl H. RanGAP1 induces GTPase activity of nuclear Ras-related Ran. *Proc Natl Acad Sci U S A*. 1994;91(7):2587-2591. doi:10.1073/pnas.91.7.2587.

297. Lounsbury KM, Macara LG. Ran-binding protein 1 (RanBP1) forms a ternary complex with ran and karyopherin-beta and reduces ran GTPase-activating protein (RanGAP) inhibition by karyopherin-beta. *J Biol Chem*. 1997;272(1):551-555. doi:10.1074/jbc.272.1.551.

298. Nehrbass U, Blobel G. Role of the nuclear transport factor p10 in nuclear import. *Science (80-)*. 1996;272(5258):120-122.

299. Bayliss R, Ribbeck K, Akin D, et al. Interaction between NTF2 and xFxFG-

containing nucleoporins is required to mediate nuclear import of RanGDP. *J Mol Biol*. 1999;293(3):579-593. doi:10.1006/jmbi.1999.3166.

300. Steggerda SM, Black BE, Paschal BM. Monoclonal antibodies to NTF2 inhibit nuclear protein import by preventing nuclear translocation of the GTPase Ran. *Mol Biol Cell*. 2000;11(2):703-719. http://www.pubmedcentral.nih.gov/articlerender.fcgi?artid=14804&tool=pmcentrez&rendertype=abstract.
301. Klebe C, Bischoff FR, Ponstingl H, Wittinghofer a. Interaction of the nuclear GTP-binding protein Ran with its regulatory proteins RCC1 and RanGAP1. *Biochemistry*. 1995;34(2):639-647. doi:10.1021/bi00002a031.
302. Poon IKH, Jans D a. Regulation of nuclear transport: central role in development and transformation? *Traffic*. 2005;6:173-186. doi:10.1111/j.1600-0854.2005.00268.x.
303. Jans DA. Phosphorylation-mediated regulation of signal-dependent nuclear protein transport-the "CcN motif." *Membr Protein Transp*. 1995;2:161-199.
304. Zhu J, Shibasaki F, Price R, et al. Intramolecular masking of nuclear import signal on NF-AT4 by casein kinase I and MEKK1. *Cell*. 1998;93(5):851-861. doi:10.1016/S0092-8674(00)81445-2.
305. Okamura H, Aramburu J, García-Rodríguez C, et al. Concerted Dephosphorylation of the Transcription Factor NFAT1 Induces a Conformational Switch that Regulates Transcriptional Activity. *Mol Cell*. 2000;6(3):539-550. doi:10.1016/S1097-2765(00)00053-8.
306. Jans DA, Ackermann MJ, Bischoff JR, Beach DH, Peters R. p34cdc2-mediated phosphorylation at T124 inhibits nuclear import of SV-40 T antigen proteins. *J Cell Biol*. 1991;115(5):1203-1212. doi:10.1083/jcb.115.5.1203.
307. Jans DA, Moll T, Nasmyth K, Jans P. Cyclin-dependent Kinase Site-regulated Signal-dependent Nuclear Localization of the SW15 Yeast Transcription Factor in Mammalian Cells. *J Biol Chem*. 1995;270(29):17064-17067.
308. Hay RT, Vuillard L, Desterro JM, Rodriguez MS. Control of NF-kappa B transcriptional activation by signal induced proteolysis of I kappa B alpha. *Philos Trans R Soc Lond B Biol Sci*. 1999;354(1389):1601-1609. doi:10.1098/rstb.1999.0504.
309. Fulcher AJ, Roth DM, Fatima S, Alvisi G, Jans DA. The BRCA-1 binding protein BRAP2 is a novel, negative regulator of viral proteins, dependent on phosphorylation flanking the nuclear localization signal. *FASEB J*. 2010;24:1454-1466.
310. Huxford T, Huang DB, Malek S, Ghosh G. The crystal structure of the IkappaBalpha/NF-kappaB complex reveals mechanisms of NF-kappaB inactivation. *Cell*. 1998;95(6):759-770. doi:S0092-8674(00)81699-2 [pii].
311. Beg AA, Ruben SM, Scheinman RI, Haskill S, Rosen CA, Baldwin ASJ. IkappaB Interacts With the Nuclear Localization Signal of the Subunits of NF-kappaB: a

mechanism for cytoplasmic retention. *Genes Dev*. 1992;6:1899-1913.

312. Henkel T, Machleidt T, Alkalay M, Kronke M, Ben-Neriah Y, Baeuerle PA. Rapid proteolysis of I kappa B-alpha is necessary for activation of transcription factor NF-kappa B. *Nature*. 1993;365:182-185.

313. Rona G, Palinkas HL, Borsos M, et al. NLS copy-number variation governs efficiency of nuclear import - Case study on dUTPases. *FEBS J*. 2014;281(24):5463-5478. doi:10.1111/febs.13086.

314. Rihs HP, Jans D a, Fan H, Peters R. The rate of nuclear cytoplasmic protein transport is determined by the casein kinase II site flanking the nuclear localization sequence of the SV40 T-antigen. *EMBO J*. 1991;10(3):633-639.

315. Xiao CY, Hübner S, Jans DA. SV40 large tumor antigen nuclear import is regulated by the double- stranded DNA-dependent protein kinase site (Serine 120) flanking the nuclear localization sequence. *J Biol Chem*. 1997;272(35):22191-22198. doi:10.1074/jbc.272.35.22191.

316. Rona G, Marfoni M, Borsos M, et al. Phosphorylation adjacent to the nuclear localization signal of human dUTPase abolishes nuclear import: Structural and mechanistic insights. *Acta Cryst*. 2013;69:2495-2505.

317. Hübner S, Xiao CY, Jans DA. The protein kinase CK2 site (Ser 111/112) enhances recognition of the simian virus 40 large T-antigen nuclear localization sequence by importin. *J Biol Chem*. 1997;272(27):17191-17195. doi:10.1074/jbc.272.27.17191.

318. Lubert EJ, Sarge KD. Interaction between protein phosphatase 2A and members of the importin-beta superfamily. *Biochem Biophys Res Commun*. 2003;303(3):908-913. doi:10.1016/S0006-291X(03)00434-0.

319. Wang W, Yang X, Kawai T, et al. AMP-activated protein kinase-regulated phosphorylation and acetylation of importin ??1: Involvement in the nuclear import of RNA-binding protein HuR. *J Biol Chem*. 2004;279(46):48376-48388. doi:10.1074/jbc.M409014200.

320. Kosako H, Yamaguchi N, Aranami C, et al. Phosphoproteomics reveals new ERK MAP kinase targets and links ERK to nucleoporin-mediated nuclear transport. *Nat Struct Mol Biol*. 2009;16(10):1026-1035. doi:10.1038/nsmb.1656.

321. Faustino RS, Maddaford TG, Pierce GN. Mitogen activated protein kinase at the nuclear pore complex. *J Cell Mol Med*. 2011;15(4):928-937. doi:10.1111/j.1582-4934.2010.01093.x.

322. Picard D, Salser SJ, Yamamoto KR. A movable and regulable inactivation function within the steroid binding domain of the glucocorticoid receptor. *Cell*. 1988;54(7):1073-1080. doi:10.1016/0092-8674(88)90122-5.

323. Pines J, Hunter T. The differential localization of human cyclins A and B is due to a cytoplasmic retention signal in cyclin B. *EMBO J*. 1994;13(16):3772-3781. http://www.pubmedcentral.nih.gov/articlerender.fcgi?artid=395290&tool=p

mcentrez&rendertype=abstract.

324. Tago K, Tsukahara F, Naruse M, Yoshioka T, Takano K. Regulation of nuclear retention of glucocorticoid receptor by nuclear Hsp90. *Mol Cell Endocrinol*. 2004;213(2):131-138.

325. Shi Y, Thomas JO. The transport of proteins into the nucleus requires the 70-kilodalton heat shock protein or its cytosolic cognate. *Mol Cell Biol*. 1992;12(5):2186-2192. doi:10.1128/MCB.12.5.2186.Updated.

326. Lam MHC, Thomas RJ, Loveland KL, et al. Nuclear transport of parathyroid hormone (PTH)-related protein is dependent on microtubules. *Mol Endocrinol*. 2002;16(2):390-401. doi:10.1210/me.16.2.390.

327. Roth DM, Moseley GW, Pouton CW, Jans DA. Mechanism of microtubule-facilitated "fast track" nuclear import. *J Biol Chem*. 2011;286(16):14335-14351. doi:10.1074/jbc.M110.210302.

328. Furuta M, Kose S, Koike M, et al. Heat-shock induced nuclear retention and recycling inhibition of importin alpha. *Genes to Cells*. 2004;9(5):429-441. doi:10.1111/j.1356-9597.2004.00734.x.

329. Jans D a., Xiao C-Y, Lam MHC. Nuclear targeting signal recognition: a key control point in nuclear transport? *BioEssays*. 2000;22(6):532-544. doi:10.1002/(SICI)1521-1878(200006)22:6<532::AID-BIES6>3.0.CO;2-O.

330. Fang X, Chen T, Tran K, Parker CS. Developmental regulation of the heat shock response by nuclear transport factor karyopherin-a3. *Development*. 2001;128:3349-3358.

331. Köhler M, Ansieau S, Prehn S, Leutz A, Haller H, Hartmann E. Cloning of two novel human importin-α subunits and analysis of the expression pattern of the importin-α protein family. *FEBS Lett*. 1997;417(1):104-108. doi:10.1016/S0014-5793(97)01265-9.

332. Nachury M V, Ryder UW, Lamond AI, Weis K. Cloning and characterization of hSRP1 gamma, a tissue-specific nuclear transport factor. *Proc Natl Acad Sci U S A*. 1998;95(2):582-587. doi:10.1073/pnas.95.2.582.

333. Fan F, Liu CP, Korobova O, et al. cDNA cloning and characterization of Npap60: a novel rat nuclear pore-associated protein with an unusual subcellular localization during male germ cell differentiation. *Genomics*. 1997;40(3):444-453. doi:10.1006/geno.1996.4557.

334. Allen NPC, Huang L, Burlingame A, Rexach M. Proteomic Analysis of Nucleoporin Interacting Proteins. *J Biol Chem*. 2001;276(31):29268-29274. doi:10.1074/jbc.M102629200.

335. Wu X, Kasper LH, Mantcheva RT, Mantchev GT, Springett MJ, van Deursen JM. Disruption of the FG nucleoporin NUP98 causes selective changes in nuclear pore complex stoichiometry and function. *Proc Natl Acad Sci U S A*. 2001;98(6):3191-3196. doi:10.1073/pnas.051631598.

336. Yang W, Musser SM. Nuclear import time and transport efficiency depend on

importin beta concentration. *J Cell Biol*. 2006;174(7):951-961. doi:10.1083/jcb.200605053.

337. Riddick G, Macara IG. A systems analysis of importin-alpha-beta mediated nuclear protein import. *J Cell Biol*. 2005;168(7):1027-1038. doi:10.1083/jcb.200409024.

338. McLane LM, Corbett AH. Nuclear localization signals and human disease. *IUBMB Life*. 2009;61(7):697-706. doi:10.1002/iub.194.

339. Chahine MN, Pierce GN. Therapeutic targeting of nuclear protein import in pathological cell conditions. *Pharmacol Rev*. 2009;61(3):358-372. doi:10.1124/pr.108.000620.

340. Terry LJ, Shows EB, Wente SR. Crossing the nuclear envelope: hierarchical regulation of nucleocytoplasmic transport. *Science (80-)*. 2007;318(5855):1412-1416. doi:10.1126/science.1142204.

341. Chai Y-C, Howe PH, DiCorleto PE, Chisolm GM. Oxidized Low Density Lipoprotein and Lysophosphatidylcholine Stimulate Cell Cycle Entry in Vascular Smooth Muscle Cells: EVIDENCE FOR RELEASE OF FIBROBLAST GROWTH FACTOR-2. *J Biol Chem*. 1996;271(30):17791-17797. doi:10.1074/jbc.271.30.17791.

342. Yamakawa T, Eguchl S, Yamakawa Y, et al. Lysophosphatidylcholine Stirnulates MAP Kinase in Rat Vascular Srnooth Muscle Cells. *Hypertension*. 1998;31(1 Pt 2):248-253.

343. Faustino RS, Stronger LNW, Richard MN, et al. RanGAP-Mediated Nuclear Protein Import in Vascular Smooth Muscle Cells Is Augmented by Lysophosphatidylcholine. *Mol Pharmacol*. 2007;71(2):438-445. doi:10.1124/mol.105.021667.lian.

344. Jacobs D, Glossip D, Xing H, Muslin AJ, Kornfeld K. Multiple docking sites on substrate proteins form a modular system that mediates recognition by ERK MAP Kinase. *Genes Dev*. 1999;13(2):163-175.

345. Czubryt MP, Austria J a, Pierce GN. Hydrogen peroxide inhibition of nuclear protein import is mediated by the mitogen-activated protein kinase, ERK2. *J Cell Biol*. 2000;148(1):7-16. doi:10.1083/jcb.148.1.7.

346. Kodiha M, Chu a, Matusiewicz N, Stochaj U. Multiple mechanisms promote the inhibition of classical nuclear import upon exposure to severe oxidative stress. *Cell Death Differ*. 2004;11:862-874. doi:10.1038/sj.cdd.4401432.

347. Faustino RS, Cheung P, Richard MN, et al. Ceramide regulation of nuclear protein import. *J Lipid Res*. 2008;49(3):654-662. doi:10.1194/jlr.M700464-JLR200.

348. Johns DG, Webb RC, Charpie JR. Impaired ceramide signalling in spontaneously hypertensive rat vascular smooth muscle: a possible mechanism for augmented cell proliferation. *J Hypertens*. 2001;19(1):63-70.

349. Vorpahl M, Schonhofer-Merl S, Michaelis C, Flotho A, Melchior F, Wessely R.

The ran GTPase-activating protein (RanGAP1) is critically involved in smooth muscle cell differentiation, proliferation and migration following vascular injury: Implications for neointima formation and restenosis. *PLoS One*. 2014;9(7):e101519. doi:10.1371/journal.pone.0101519.

350. Saward L, Zahradka P. Coronary artery smooth muscle in culture: migration of heterogeneous cell populations from vessel wall. *Mol Cell Biochem*. 1997;176(1-2):53-59.

351. Massaeli H, Austria JA, Pierce GN. Chronic exposure of smooth muscle cells to minimally oxidized LDL results in depressed inositol 1,4,5-trisphosphate receptor density and Ca(2+) transients. *Circ Res*. 1999;85(6):515-523. doi:10.1161/01.RES.85.6.515.

352. Zettler ME, Prociuk M a., Austria JA, Zhong G, Pierce GN. Oxidized Low-Density Lipoprotein Retards the Growth of Proliferating Cells by Inhibiting Nuclear Translocation of Cell Cycle Proteins. *Arterioscler Thromb Vasc Biol*. 2004;24(4):727-732. doi:10.1161/01.ATV.0000120373.95552.aa.

353. Taylor SC, Berkelman T, Yadav G, Hammond M. A Defined Methodology for Reliable Quantification of Western Blot Data. *Mol Biotechnol*. 2013;55(3):217-226. doi:10.1007/s12033-013-9672-6.

354. Short R, Posch a. Stain-Free Approach for Western Blotting. *Genet Eng ….* 2011;31(20):5-7. http://scholar.google.com/scholar?hl=en&btnG=Search&q=intitle:Stain-Free+Approach+for+Western+Blotting#1.

355. Taylor SC, Posch A. The design of a quantitative western blot experiment. *Biomed Res Int*. 2014;2014:361590. doi:10.1155/2014/361590.

356. Gürtler A, Kunz N, Gomolka M, et al. Stain-Free technology as a normalization tool in Western blot analysis. *Anal Biochem*. 2013;433(2):105-111. doi:10.1016/j.ab.2012.10.010.

357. Francis A a, Deniset JF, Austria J a, et al. Effects of dietary flaxseed on atherosclerotic plaque regression. *Am J Physiol Heart Circ Physiol*. 2013;304(12):H1743-51. doi:10.1152/ajpheart.00606.2012.

358. Dupasquier CM, Weber AM, Ander BP, et al. Effects of dietary flaxseed on vascular contractile function and atherosclerosis during prolonged hypercholesterolemia in rabbits. *Am J Physiol Hear Circ Physiol*. 2006;291(6):H2987-2996.

359. Gupta S, Knowlton a a. HSP60, Bax, apoptosis and the heart. *J Cell Mol Med*. 2005;9(1):51-58. doi:10.1111/j.1582-4934.2005.tb00336.x.

360. Chang AYW, Chan JYH, Chou JLJ, Li FCH, Dai K-Y, Chan SHH. Heat shock protein 60 in rostral ventrolateral medulla reduces cardiovascular fatality during endotoxaemia in the rat. *J Physiol*. 2006;574(Pt 2):547-564. doi:10.1113/jphysiol.2006.110890.

361. Shan YX, Yang TL, Mestril R, Wang PH. Hsp10 and Hsp60 suppress

ubiquitination of insulin-like growth factor-1 receptor and augment insulin-like growth factor-1 receptor signaling in cardiac muscle: Implications on decreased myocardial protection in diabetic cardiomyopathy. *J Biol Chem*. 2003;278(46):45492-45498. doi:10.1074/jbc.M304498200.

362. Deocaris CC, Kaul SC, Wadhwa R. On the brotherhood of the mitochondrial chaperones mortalin and heat shock protein 60. *Cell Stress Chaperones*. 2006;11(2):116-128. doi:10.1379/CSC-144R.1.

363. Kose S, Furata M, Koike M, Yoneda Y, Imamoto N. The 70-kD heat shock cognate protein (hsc70) facilitates the nuclear export of the import receptors. *J Cell Biol*. 2005;171:19-25.

364. Kataoka H, Kume N, Miyamoto S, Minami M, Morimoto M, Hayashida K HNAKT. Oxidized LDL Modulates Bax / Bcl-2 Through the Lectinlike Ox-LDL Receptor-1 in Vascular Smooth Muscle Cells. *Arterioscler Thromb Vasc Biol*. 2001;21:955-960. doi:10.1161/01.ATV.21.6.955.

365. Nègre-Salvayre A, Augé N, Camaré C, Bacchetti T, Ferretti G, Salvayre R. Dual signaling evoked by oxidized LDLs in vascular cells. *Free Radic Biol Med*. 2017;106(October 2016):118-133. doi:10.1016/j.freeradbiomed.2017.02.006.

366. Nielsen KL, Cowan NJ. A single ring is sufficient for productive chaperonin-mediated folding in vivo. *Mol Cell*. 1998;2(1):93-99. doi:10.1016/S1097-2765(00)80117-3.

367. Shan YX, Liu TJ, Su HF, Samsamshariat A, Mestril R, Wang PH. Hsp10 and Hsp60 modulate Bcl-2 family and mitochondria apoptosis signaling induced by doxorubicin in cardiac muscle cells. *J Mol Cell Cardiol*. 2003;35(9):1135-1143. doi:10.1016/S0022-2828(03)00229-3.

368. Lin KM, Lin B, Lian IY, Mestril R, Scheffler IE, Dillmann WH. Combined and individual mitochondrial HSP60 and HSP10 expression in cardiac myocytes protects mitochondrial function and prevents apoptotic cell deaths Induced by simulated ischemia-reoxygenation. *Circulation*. 2001;103(3):1787-1792. doi:10.1161/01.CIR.103.13.1787.

369. Dartsch P, Voisard R, Bauriedel G, Hofling B, Betz E. Growth characteristics and cytoskeletal organization of cultured smooth muscle cells from human primary stenosing and restenosing lesions. *Arteriosclerosis*. 1990;10(1):62-75. doi:10.1161/01.ATV.10.1.62.

370. Dartsch P, Voisard R, Betz E. In vitro growth characteristics of human atherosclerotic plaque cells: comparison of cells from primary stenosing and restenosing lesions of peripheral and coronary arteries. *Res Exp Med*. 1990;190(2):77-87.